

Hadronic Form Factor Models and Spectroscopy Within the Gauge/Gravity Correspondence

Guy F. de Téramond^{a 1} and Stanley J. Brodsky,^{b 2}

^a*Universidad de Costa Rica, San José, Costa Rica*

^b*SLAC National Accelerator Laboratory, Stanford University, Stanford, CA 94309, USA*

Abstract

We show that the nonperturbative light-front dynamics of relativistic hadronic bound states has a dual semiclassical gravity description on a higher dimensional warped AdS space in the limit of zero quark masses. This mapping of AdS gravity theory to the boundary quantum field theory, quantized at fixed light-front time, allows one to establish a precise relation between holographic wave functions in AdS space and the light-front wavefunctions describing the internal structure of hadrons. The resulting AdS/QCD model gives a remarkably good accounting of the spectrum, elastic and transition form factors of the light-quark hadrons in terms of one parameter, the QCD gap scale. The light-front holographic approach described here thus provides a frame-independent first approximation to the light-front Hamiltonian problem for QCD. This article is based on lectures at the Niccolò Cabeo International School of Hadronic Physics, Ferrara, Italy, May 2011.

¹E-mail: gdt@asterix.crnet.cr

²E-mail: sjbth@slac.stanford.edu

Contents

1	Introduction	3
2	Light-front bound-state Hamiltonian equation of motion and light-front holography	7
2.1	Light-front quantization of QCD	8
2.2	A semiclassical approximation to QCD	9
2.3	Higher spin hadronic modes in AdS space	12
2.3.1	Non-conformal warped metrics	14
2.3.2	Effective confining potentials in AdS	15
2.4	Light-front holographic mapping	16
3	Mesons in light-front holography	18
3.1	A hard-wall model for mesons	18
3.2	A soft-wall model for mesons	21
4	Meson form factors	24
4.1	Meson electromagnetic form factor	24
4.2	Elastic form factor with a dressed current	27
4.3	Effective wave function from holographic mapping of a confined current . .	29
4.4	Some caveats computing matrix elements in AdS/QCD	30
4.5	Meson transition form factors	33
5	Baryons in light-front holography	37
5.1	A hard-wall model for baryons	39
5.2	A soft-wall model for baryons	43
6	Nucleon form factors	48
6.1	Computing nucleon elastic form factors in light-front holographic QCD . . .	50
6.2	Computing nucleon transition form factors in light-front holographic QCD .	53
7	Higher Fock components in light-front holographic QCD	55
8	Conclusions	56
A	AdS boundary conditions and interpolating operators	59

1 Introduction

One of the most challenging problems in particle physics is to understand hadron dynamics and spectroscopy in terms of the confined quark and gluon quanta of quantum chromodynamics, the fundamental theory of the strong interactions. A central goal is to compute detailed hadronic properties, such as moments, structure functions, distribution amplitudes, transversity distributions, elastic and transition form factors, and the excitation dynamics of hadron resonances from first principles; *i.e.*, directly from the QCD Lagrangian. The most successful theoretical approach thus far has been to quantize QCD on discrete lattices in Euclidean space-time [1]. Lattice numerical results follow from the computation of frame-dependent moments of distributions in Euclidean space; however, dynamical observables in Minkowski space-time, such as the time-like hadronic form factors, are not obtained directly from Euclidean-space lattice computations. Dyson-Schwinger methods have led to many important insights, such as the infrared fixed-point behavior of the strong coupling constant [2]; however, in practice, these analyses are limited to ladder approximation in Landau gauge.

In principle, one could calculate hadronic spectroscopy and wavefunctions by solving for the eigenvalues and eigenfunctions of the QCD Hamiltonian: $H|\Psi\rangle = E|\Psi\rangle$ at fixed time t . However, this traditional method – called the “instant form” by Dirac [3], is plagued by complex vacuum and relativistic effects. In contrast, quantization at fixed light-front (LF) time $\tau = t + z/c$ – the “front-form” of Dirac [3] – provides a powerful boost-invariant nonperturbative method for solving QCD and constitutes the ideal framework to describe the structure of hadrons in terms of their quark and gluon degrees of freedom. The simple structure of the light-front vacuum allows an unambiguous definition of the partonic content of a hadron in QCD and of hadronic light-front wavefunctions (LFWFs), the underlying link between large distance hadronic states and the constituent degrees of freedom at short distances. Thus, one can also solve QCD by diagonalizing the light-front QCD Hamiltonian H_{LF} . The spectrum and light-front Fock-state wavefunctions are obtained from the eigenvalues and eigensolutions of the Heisenberg problem $H_{LF}|\psi\rangle = M^2|\psi\rangle$, which becomes an infinite set of coupled integral equations for the light-front components $\psi_n = \langle n|\psi\rangle$ in the Fock expansion [4, 5]. This nonperturbative method has the advantage that it is frame-independent, operates in physical Minkowski space-time, and has no fermion-doubling problem [4]. It has been applied successfully in lower space-time dimensions. In practice, however, the resulting large matrix diagonalization problem in $3 + 1$ space-time has proven to be a daunting task, so alternative methods and approximations are necessary.

The AdS/CFT correspondence between gravity or string theory on a higher-dimensional

anti-de Sitter (AdS) space and conformal field theories (CFT) in physical space-time [6], has led to a semiclassical approximation for strongly-coupled quantum field theories which provides physical insights into its nonperturbative dynamics. The correspondence is holographic in the sense that it determines a duality between theories in different number of space-time dimensions. In practice, the duality provides an effective gravity description in a $(d+1)$ -dimensional AdS space-time in terms of a flat d -dimensional conformally-invariant quantum field theory defined at the AdS asymptotic boundary [7, 8]. Thus, in principle, one can compute physical observables in a strongly coupled gauge theory in terms of a classical gravity theory.

Anti-de Sitter AdS_5 space is the maximally symmetric space-time with negative curvature and a four-dimensional space-time boundary. The most general group of transformations that leave the AdS_{d+1} differential line element

$$ds^2 = \frac{R^2}{z^2} (\eta_{\mu\nu} dx^\mu dx^\nu - dz^2), \quad (1)$$

invariant, the isometry group, has dimensions $(d+1)(d+2)/2$ (R is the AdS radius). Five-dimensional anti-de Sitter space AdS_5 has 15 isometries, in agreement with the number of generators of the conformal group in four dimensions. Since the AdS metric (1) is invariant under a dilatation of all coordinates $x^\mu \rightarrow \lambda x^\mu$ and $z \rightarrow \lambda z$, it follows that the additional dimension, the holographic variable z , acts as a scaling variable in Minkowski space: different values of z correspond to different energy scales at which the hadron is examined. As a result, a short space-like or time-like invariant interval near the light-cone, $x_\mu x^\mu \rightarrow 0$ maps to the conformal AdS boundary near $z \rightarrow 0$. This also corresponds to the $Q \rightarrow \infty$ ultraviolet (UV) zero separation distance. On the other hand, a large invariant four-dimensional interval of confinement dimensions $x_\mu x^\mu \sim 1/\Lambda_{\text{QCD}}^2$ maps to the large infrared (IR) region of AdS space $z \sim 1/\Lambda_{\text{QCD}}$.

QCD is fundamentally different from conformal theories since its scale invariance is broken by quantum effects. A gravity dual to QCD is not known, but the mechanisms of confinement can be incorporated in the gauge/gravity correspondence by modifying the AdS geometry in the large IR domain $z \sim 1/\Lambda_{\text{QCD}}$, which also sets the scale of the strong interactions [9]. In this simplified approach, we consider the propagation of hadronic modes in a fixed effective gravitational background asymptotic to AdS space, which encodes salient properties of the QCD dual theory, such as the UV conformal limit at the AdS boundary, as well as modifications of the background geometry in the large- z IR region to describe confinement.

The physical states in AdS space are represented by normalizable modes $\Phi_P(x, z) =$

$e^{-iP \cdot x} \Phi(z)$, with plane waves along Minkowski coordinates x^μ and a profile function $\Phi(z)$ along the holographic coordinate z . The hadronic invariant mass states $P_\mu P^\mu = \mathcal{M}^2$ are found by solving the eigenvalue problem for the AdS wave equation. The modified theory generates the point-like hard behavior expected from QCD, instead of the soft behavior characteristic of extended objects [9]. It is rather remarkable that the QCD dimensional counting rules [10, 11] are also a key feature of nonperturbative models [9] based on the gauge/gravity duality. Although the mechanisms are different, both the perturbative QCD and the AdS/QCD approaches depend on the leading-twist (dimension minus spin) interpolating operators of the hadrons and their structure at short distances.

The gauge/gravity duality leads to a simple analytical and phenomenologically compelling nonperturbative frame-independent first approximation to the light-front Hamiltonian problem for QCD – “Light-Front Holography” [12]. Incorporating the AdS/CFT correspondence [6] as a useful guide, light-front holographic methods were originally introduced [13, 14] by mapping the Polchinski-Strassler formula for the electromagnetic (EM) form factors in AdS space [15] to the corresponding Drell-Yan-West expression at fixed light-front time in physical space-time [16, 17]. It was also shown that one obtains identical light-front holographic mapping for the gravitational form factor [18] – the matrix elements of the energy-momentum tensor, by perturbing the AdS metric (1) around its static solution [19]. In the usual “bottom-up” approach to the gauge/gravity duality [20, 21], fields in the bulk geometry are introduced to match the chiral symmetries of QCD and axial and vector currents become the primary entities as in effective chiral theory. In contrast, in light-front holography a direct connection with the internal constituent structure of hadrons is established using light-front quantization [12, 13, 14, 18, 22].

The identification of higher dimensional AdS space with partonic physics in physical space-time is specific to the light front: the Polchinski-Strassler formula for computing transition matrix elements is a simple overlap of AdS amplitudes, which maps to a convolution of frame-independent light-front wavefunctions. This AdS convolution formula cannot be mapped to current matrix elements at ordinary fixed time t , since the instant-time wavefunctions must be boosted away from the hadron’s rest frame – an intractable dynamical problem. In fact, the boost of a composite system at fixed time t is only known at weak binding. Moreover, the form factors in instant time also require computing the contributions of currents which arise from the vacuum in the initial state and which connect to the hadron in the final state. Thus instant form wavefunctions alone are not sufficient to compute covariant current matrix elements in the instant form. There is no analog of such contributions in AdS. In contrast, there are no vacuum contributions in the light-front formulae for current

matrix elements – in agreement with the AdS formulae.

Unlike ordinary instant-time quantization, the Hamiltonian equation of motion in the light-front is frame independent and has a structure similar to eigenmode equations in AdS space. This makes a direct connection of QCD with AdS/CFT methods possible. In fact, one can also study the AdS/CFT duality and its modifications starting from the LF Hamiltonian equation of motion for a relativistic bound-state system $H_{LF}|\psi\rangle = \mathcal{M}^2|\psi\rangle$ in physical space-time [12], where the QCD light-front Hamiltonian $H_{LF} \equiv P_\mu P^\mu = P^+ P^- - \mathbf{P}_\perp^2$, $P^\pm = P^0 \pm P^3$, is constructed from the QCD Lagrangian using the standard methods of quantum field theory [4]. To a first semiclassical approximation, where quantum loops and quark masses are not included, LF holography leads to a LF Hamiltonian equation which describes the bound-state dynamics of light hadrons in terms of an invariant impact kinematical variable ζ which measures the separation of the partons within the hadron at equal light-front time $\tau = x^+ = x^0 + x^3$. The transverse coordinate ζ is closely related to the invariant mass squared of the constituents in the LFWF and its off-shellness in the LF kinetic energy, and it is thus the natural variable to characterize the hadronic wavefunction. In fact ζ is the only variable to appear in the relativistic light-front Schrödinger equations predicted from holographic QCD in the limit of zero quark masses. The coordinate z in AdS space is thus uniquely identified with a Lorentz-invariant coordinate ζ which measures the separation of the constituents within a hadron at equal light-front time. The AdS/CFT correspondence shows that the holographic coordinate z in AdS space is related inversely to the internal relative momentum. In fact, light-front holography makes this identification precise.

Remarkably, the unmodified AdS equations correspond to the kinetic energy terms of the partons inside a hadron, whereas the interaction terms in the QCD Lagrangian build confinement and correspond to the truncation of AdS space in an effective dual gravity approximation [12]. Thus, all the complexities of the strong interaction dynamics are hidden in an effective potential $U(\zeta)$, and the central question – how to derive the effective color-confining potential $U(\zeta)$ directly from QCD, remains open. To circumvent this obstacle, the effective confinement potential can be introduced either with a sharp cut-off in the infrared region of AdS space, as in the “hard-wall” model [9], or, more successfully, using a “dilaton” background in the holographic coordinate to produce a smooth cutoff at large distances as in the “soft-wall” model [23]. Furthermore, one can impose from the onset a correct phenomenological confining structure to determine the effective IR warping of AdS space, for example, by adjusting the dilaton background to reproduce the observed linear Regge behavior of the hadronic mass spectrum \mathcal{M}^2 as a function of the excitation quantum

numbers [23, 24]³. By using light-front holographic mapping techniques, one also obtains a connection between the mass parameter μR of the AdS theory with the orbital angular momentum of the constituents in the light-front bound-state Hamiltonian equation [12]. The identification of orbital angular momentum of the constituents is a key element in our description of the internal structure of hadrons using holographic principles, since hadrons with the same quark content, but different orbital angular momenta, have different masses.

In our approach, the holographic mapping is carried out in the strongly coupled regime where QCD is almost conformal, corresponding to an infrared fixed-point. A QCD infrared fixed point arises since the propagators of the confined quarks and gluons in the loop integrals contributing to the β -function have a maximal wavelength [14, 26]; thus, an infrared fixed point appears as a natural consequence of confinement. The decoupling of quantum loops in the infrared is analogous to QED dynamics where vacuum polarization corrections to the photon propagator decouple at $Q^2 \rightarrow 0$. Since there is a window where the QCD coupling is large and approximately constant, QCD resembles a conformal theory for massless quarks. One then uses the isometries of AdS_5 to represent scale transformations within the conformal window. We thus begin with a conformal approximation to QCD to model an effective dual gravity description in AdS space. The large-distance non-conformal effects are taken into account with the introduction of an effective confinement potential as described above.

Early attempts to derive effective one-body equations in light-front QCD are described in reference [27]. We should also mention previous work by 't Hooft, who obtained the spectrum of two-dimensional QCD in the large N_C limit in terms of a Schrödinger equation as a function of the parton x -variable [28]. In the scale-invariant limit, this equation is equivalent to the equation of motion for a scalar field in AdS_3 space [29]. In this case, there is a mapping between the variable x and the radial coordinate in AdS_3 .

2 Light-front bound-state Hamiltonian equation of motion and light-front holography

A key step in the analysis of an atomic system, such as positronium, is the introduction of the spherical coordinates r, θ, ϕ which separates the dynamics of Coulomb binding from the kinematical effects of the quantized orbital angular momentum L . The essential dynamics of the atom is specified by the radial Schrödinger equation whose eigensolutions $\psi_{n,L}(r)$

³Using a mean-field mechanism, an effective harmonic confinement interaction was obtained in Ref. [25] in a constituent quark model.

determine the bound-state wavefunction and eigenspectrum. In our recent work, we have shown that there is an analogous invariant light-front coordinate ζ which allows one to separate the essential dynamics of quark and gluon binding from the kinematical physics of constituent spin and internal orbital angular momentum. The result is a single-variable light-front Schrödinger equation for QCD which determines the eigenspectrum and the light-front wavefunctions of hadrons for general spin and orbital angular momentum [12], thus providing a description of the internal dynamics of hadronic states in terms of their massless constituents at the same LF time $\tau = x^+ = x^0 + x^3$, the time marked by the front of a light wave [3], instead of the ordinary instant time $t = x^0$.

2.1 Light-front quantization of QCD

Our starting point is the $SU(3)_C$ invariant Lagrangian of QCD

$$\mathcal{L}_{\text{QCD}} = \bar{\psi} (i\gamma^\mu D_\mu - m) \psi - \frac{1}{4} G_{\mu\nu}^a G^{a\mu\nu}, \quad (2)$$

where $D_\mu = \partial_\mu - ig_s A_\mu^a T^a$ and $G_{\mu\nu}^a = \partial_\mu A_\nu^a - \partial_\nu A_\mu^a + g_s c^{abc} A_\mu^b A_\nu^c$, with $[T^a, T^b] = ic^{abc} T^c$ and a, b, c are $SU(3)_C$ color indices.

One can express the hadron four-momentum generator $P = (P^+, P^-, \mathbf{P}_\perp)$, $P^\pm = P^0 \pm P^3$, in terms of the dynamical fields, the Dirac field ψ_+ , where $\psi_\pm = \Lambda_\pm \psi$, $\Lambda_\pm = \gamma^0 \gamma^\pm$, and the transverse field \mathbf{A}_\perp in the $A^+ = 0$ gauge [4] quantized on the light-front at fixed light-cone time x^+ , $x^\pm = x^0 \pm x^3$

$$P^- = \frac{1}{2} \int dx^- d^2 \mathbf{x}_\perp \bar{\psi}_+ \gamma^+ \frac{(i\nabla_\perp)^2 + m^2}{i\partial^+} \psi_+ + (\text{interactions}), \quad (3)$$

$$P^+ = \int dx^- d^2 \mathbf{x}_\perp \bar{\psi}_+ \gamma^+ i\partial^+ \psi_+, \quad (4)$$

$$\mathbf{P}_\perp = \frac{1}{2} \int dx^- d^2 \mathbf{x}_\perp \bar{\psi}_+ \gamma^+ i\nabla_\perp \psi_+, \quad (5)$$

where the integrals are over the null plane $\tau = x^+ = 0$, the hyper-plane tangent to the light cone. This is the initial-value surface for the fields where the commutation relations are fixed. The LF Hamiltonian P^- generates LF time translations

$$[\psi_+(x), P^-] = i \frac{\partial}{\partial x^+} \psi_+(x), \quad (6)$$

to evolve the initial conditions to all space-time, whereas the LF longitudinal P^+ and transverse momentum \mathbf{P}_\perp are kinematical generators. For simplicity we have omitted from (3-5) the contributions from the gluon field \mathbf{A}_\perp .

According to Dirac's classification of the forms of relativistic dynamics [3], the fundamental generators of the Poincaré group can be separated into kinematical and dynamical generators. The kinematical generators act along the initial surface and leave the light-front plane invariant: they are thus independent of the dynamics and therefore contain no interactions. The dynamical generators change the light-front position and depend consequently on the interactions. In addition to P^+ and \mathbf{P}_\perp , the kinematical generators in the light-front frame are the z -component of the angular momentum J^z and the boost operator \mathbf{K} . In addition to the Hamiltonian P^- , J^z and J^y are also dynamical generators. The light-front frame has the maximal number of kinematical generators.

2.2 A semiclassical approximation to QCD

A physical hadron in four-dimensional Minkowski space has four-momentum P_μ and invariant hadronic mass states $P_\mu P^\mu = \mathcal{M}^2$ determined by the Lorentz-invariant Hamiltonian equation for the relativistic bound-state system

$$H_{LF}|\psi(P)\rangle = \mathcal{M}^2|\psi(P)\rangle, \quad (7)$$

with $H_{LF} \equiv P_\mu P^\mu = P^- P^+ - \mathbf{P}_\perp^2$, where the hadronic state $|\psi\rangle$ is an expansion in multi-particle Fock eigenstates $|n\rangle$ of the free light-front Hamiltonian: $|\psi\rangle = \sum_n \psi_n |\psi\rangle$. The state $|\psi(P^+, \mathbf{P}_\perp, J^z)\rangle$ is an eigenstate of the total momentum P^+ and \mathbf{P}_\perp and the total spin J^z . Quark and gluons appear from the light-front quantization of the excitations of the dynamical fields ψ_+ and \mathbf{A}_\perp , expanded in terms of creation and annihilation operators at fixed LF time τ . The Fock components $\psi_n(x_i, \mathbf{k}_{\perp i}, \lambda_i)$ are independent of P^+ and \mathbf{P}_\perp and depend only on relative partonic coordinates: the momentum fraction $x_i = k_i^+/P^+$, the transverse momentum $\mathbf{k}_{\perp i}$ and spin component λ_i^z . Momentum conservation requires $\sum_{i=1}^n x_i = 1$ and $\sum_{i=1}^n \mathbf{k}_{\perp i} = 0$. The LFWFs ψ_n provide a *frame-independent* representation of a hadron which relates its quark and gluon degrees of freedom to their asymptotic hadronic state. Since for each constituent $k_i^+ = \sqrt{\mathbf{k}_i^2 + m_i^2} + k_i^z > 0$ there are no contributions from the vacuum. Thus, apart from possible zero modes, the light-front QCD vacuum is the trivial vacuum. The constituent spin and orbital angular momentum properties of the hadrons are also encoded in the LFWFs. Actually, the definition of quark and gluon angular momentum is unambiguous in Dirac's front form in light-cone gauge $A^+ = 0$, and the gluons have physical polarization $S_g^z = \pm 1$.

One can also derive light-front holography using a first semiclassical approximation to transform the fixed light-front time bound-state Hamiltonian equation of motion in QCD (7) to a corresponding wave equation in AdS space [12]. To this end we expand the initial

and final hadronic states in terms of its Fock components. The computation is simplified in the frame $P = (P^+, \mathcal{M}^2/P^+, \vec{0}_\perp)$ where $P^2 = P^+P^-$. We find

$$\mathcal{M}^2 = \sum_n \int [dx_i] [d^2\mathbf{k}_{\perp i}] \sum_q \left(\frac{\mathbf{k}_{\perp q}^2 + m_q^2}{x_q} \right) |\psi_n(x_i, \mathbf{k}_{\perp i})|^2 + (\text{interactions}), \quad (8)$$

plus similar terms for antiquarks and gluons ($m_g = 0$). The integrals in (8) are over the internal coordinates of the n constituents for each Fock state

$$\int [dx_i] \equiv \prod_{i=1}^n \int dx_i \delta\left(1 - \sum_{j=1}^n x_j\right), \quad \int [d^2\mathbf{k}_{\perp i}] \equiv \prod_{i=1}^n \int \frac{d^2\mathbf{k}_{\perp i}}{2(2\pi)^3} 16\pi^3 \delta^{(2)}\left(\sum_{j=1}^n \mathbf{k}_{\perp j}\right), \quad (9)$$

with phase space normalization

$$\sum_n \int [dx_i] [d^2\mathbf{k}_{\perp i}] |\psi_n(x_i, \mathbf{k}_{\perp i})|^2 = 1. \quad (10)$$

Each constituent of the light-front wavefunction $\psi_n(x_i, \mathbf{k}_{\perp i}, \lambda_i)$ of a hadron is on its respective mass shell $k_i^2 = k_i^+ k_i^- - \mathbf{k}_{\perp i}^2 = m_i^2$, $i = 1, 2, \dots, n$. Thus $k_i^- = (\mathbf{k}_{\perp i}^2 + m_i^2)/x_i P^+$. However, the light-front wavefunction represents a state which is off the light-front energy shell: $P^- - \sum_i k_i^- < 0$, for a stable hadron. Scaling out $P^+ = \sum_i k_i^+$, the invariant mass of the constituents \mathcal{M}_n is

$$\mathcal{M}_n^2 = \left(\sum_{i=1}^n k_i^\mu \right)^2 = \sum_i \frac{\mathbf{k}_{\perp i}^2 + m_i^2}{x_i}. \quad (11)$$

The functional dependence for a given Fock state is expressed in terms of the invariant mass, the measure of the off-energy shell of the bound state of the n -parton LFWF: $\mathcal{M}^2 - \mathcal{M}_n^2$.

The LFWF $\psi_n(x_i, \mathbf{k}_{\perp i}, \lambda_i)$ can be expanded in terms of $n-1$ independent position coordinates $\mathbf{b}_{\perp j}$, $j = 1, 2, \dots, n-1$, conjugate to the relative coordinates $\mathbf{k}_{\perp i}$, with $\sum_{i=1}^n \mathbf{b}_{\perp i} = 0$. We can also express Eq. (8) in terms of the internal impact coordinates $\mathbf{b}_{\perp j}$ with the result

$$\mathcal{M}^2 = \sum_n \prod_{j=1}^{n-1} \int dx_j d^2\mathbf{b}_{\perp j} \psi_n^*(x_j, \mathbf{b}_{\perp j}) \sum_q \left(\frac{-\nabla_{\mathbf{b}_{\perp q}}^2 + m_q^2}{x_q} \right) \psi_n(x_j, \mathbf{b}_{\perp j}) + (\text{interactions}). \quad (12)$$

The normalization is defined by

$$\sum_n \prod_{j=1}^{n-1} \int dx_j d^2\mathbf{b}_{\perp j} |\psi_n(x_j, \mathbf{b}_{\perp j})|^2 = 1. \quad (13)$$

If we want to simplify further the description of the multiple parton system and reduce its dynamics to a single variable problem, we must take the limit of quark masses to zero.

Indeed, the underlying classical QCD Lagrangian with massless quarks is scale and conformal invariant [30], and consequently only in this limit it is possible to map the equations of motion and transition matrix elements to their correspondent conformal AdS expressions.

To simplify the discussion we will consider a two-parton hadronic bound state. In the limit of zero quark mass $m_q \rightarrow 0$

$$\mathcal{M}^2 = \int_0^1 \frac{dx}{x(1-x)} \int d^2\mathbf{b}_\perp \psi^*(x, \mathbf{b}_\perp) (-\nabla_{\mathbf{b}_\perp}^2) \psi(x, \mathbf{b}_\perp) + (\text{interactions}). \quad (14)$$

For $n = 2$, the invariant mass is $\mathcal{M}_{n=2}^2 = \frac{\mathbf{k}_\perp^2}{x(1-x)}$. Similarly, in impact space the relevant variable for a two-parton state is $\zeta^2 = x(1-x)\mathbf{b}_\perp^2$. Thus, to first approximation LF dynamics depend only on the boost invariant variable \mathcal{M}_n or ζ , and hadronic properties are encoded in the hadronic mode $\phi(\zeta)$ from the relation

$$\psi(x, \zeta, \varphi) = e^{iL\varphi} X(x) \frac{\phi(\zeta)}{\sqrt{2\pi\zeta}}, \quad (15)$$

thus factoring out the angular dependence φ and the longitudinal, $X(x)$, and transverse mode $\phi(\zeta)$. This is a natural factorization in the light front since the corresponding canonical generators, the longitudinal and transverse generators P^+ and \mathbf{P}_\perp and the z -component of the orbital angular momentum J^z are kinematical generators which commute with the LF Hamiltonian generator P^- . We choose the normalization $\langle \phi | \phi \rangle = \int d\zeta |\langle \zeta | \phi \rangle|^2 = P_{q\bar{q}}$, where $P_{q\bar{q}}$ is the probability of finding the $q\bar{q}$ component in the pion light-front wavefunction. The longitudinal mode is thus normalized as $\int_0^1 \frac{X^2(x)}{x(1-x)} = 1$.

We can write the Laplacian operator in (14) in circular cylindrical coordinates (ζ, φ)

$$\nabla_\zeta^2 = \frac{1}{\zeta} \frac{d}{d\zeta} \left(\zeta \frac{d}{d\zeta} \right) + \frac{1}{\zeta^2} \frac{\partial^2}{\partial \varphi^2}, \quad (16)$$

and factor out the angular dependence of the modes in terms of the $SO(2)$ Casimir representation L^2 of orbital angular momentum in the transverse plane. Using (15) we find [12]

$$\mathcal{M}^2 = \int d\zeta \phi^*(\zeta) \sqrt{\zeta} \left(-\frac{d^2}{d\zeta^2} - \frac{1}{\zeta} \frac{d}{d\zeta} + \frac{L^2}{\zeta^2} \right) \frac{\phi(\zeta)}{\sqrt{\zeta}} + \int d\zeta \phi^*(\zeta) U(\zeta) \phi(\zeta), \quad (17)$$

where $L = |L^z|$. In writing the above equation we have summed the complexity of the interaction terms in the QCD Lagrangian by the introduction of the effective potential $U(\zeta)$, which is modeled to enforce confinement at some IR scale. The LF eigenvalue equation $P_\mu P^\mu |\phi\rangle = \mathcal{M}^2 |\phi\rangle$ is thus a light-front wave equation for ϕ

$$\left(-\frac{d^2}{d\zeta^2} - \frac{1 - 4L^2}{4\zeta^2} + U(\zeta) \right) \phi(\zeta) = \mathcal{M}^2 \phi(\zeta), \quad (18)$$

a relativistic single-variable LF Schrödinger equation. Its eigenmodes $\phi(\zeta)$ determine the hadronic mass spectrum and represent the probability amplitude to find n -partons at transverse impact separation ζ , the invariant separation between pointlike constituents within the hadron [13] at equal LF time. Thus the effective interaction potential is instantaneous in LF time τ , not instantaneous in ordinary time t . The LF potential thus satisfies causality, unlike the instantaneous Coulomb interaction. Extension of the results to arbitrary n follows from the x -weighted definition of the transverse impact variable of the $n - 1$ spectator system [13]

$$\zeta = \sqrt{\frac{x}{1-x}} \left| \sum_{j=1}^{n-1} x_j \mathbf{b}_{\perp j} \right|, \quad (19)$$

where $x = x_n$ is the longitudinal momentum fraction of the active quark. One can also generalize the equations to allow for the kinetic energy of massive quarks using Eqs. (8) or (12) [31]. In this case, however, the longitudinal mode $X(x)$ does not decouple from the effective LF bound-state equations.

2.3 Higher spin hadronic modes in AdS space

We now turn to the formulation of bound-state equations for mesons of arbitrary spin J in AdS space⁴. As we shall show in the next section, there is a remarkable correspondence between the equations of motion in AdS space and the Hamiltonian equation for the relativistic bound-state system for the corresponding angular momentum in light-front theory.

The description of higher spin modes in AdS space is a notoriously difficult problem [34, 35, 36]. A spin- J field in AdS_{d+1} is represented by a rank J tensor field $\Phi(x^A)_{M_1 \dots M_J}$, which is totally symmetric in all its indices. Such a tensor contains also lower spins, which can be eliminated by imposing gauge conditions. The action for a spin- J field in AdS_{d+1} space-time in presence of a dilaton background field $\varphi(z)$ (the string frame) is given by

$$S = \frac{1}{2} \int d^d x dz \sqrt{g} e^{\varphi(z)} \left(g^{NN'} g^{M_1 M'_1} \dots g^{M_J M'_J} D_N \Phi_{M_1 \dots M_J} D_{N'} \Phi_{M'_1 \dots M'_J} \right. \\ \left. - \mu^2 g^{M_1 M'_1} \dots g^{M_J M'_J} \Phi_{M_1 \dots M_J} \Phi_{M'_1 \dots M'_J} + \dots \right), \quad (20)$$

where $M, N = 1, \dots, d+1$, $\sqrt{g} = (R/z)^{d+1}$ and D_M is the covariant derivative which includes parallel transport. The omitted terms in (20) refer to terms with different contractions. The

⁴This section is based on our collaboration with Hans Guenter Dosch. A detailed discussion of higher integer and half-integer spin wave equations in modified AdS spaces will be given in Ref. [32]. See also the discussion in Ref. [33].

coordinates of AdS are the Minkowski coordinates x^μ and the holographic variable z labeled $x^M = (x^\mu, z)$. The $d + 1$ dimensional mass μ is not a physical observable and is *a priori* an arbitrary parameter. The dilaton background field $\varphi(z)$ in (20) introduces an energy scale in the five-dimensional AdS action, thus breaking its conformal invariance. It is a function of the holographic coordinate z which vanishes in the conformal ultraviolet limit $z \rightarrow 0$. In the hard wall model $\varphi = 0$ and the conformality is broken by the IR boundary conditions at $z = z_0 \sim 1/\Lambda_{\text{QCD}}$.

A physical hadron has plane-wave solutions and polarization indices M along the $3 + 1$ physical coordinates

$$\Phi_P(x, z)_{\mu_1 \dots \mu_J} = e^{-iP \cdot x} \Phi(z)_{\mu_1 \dots \mu_J}, \quad (21)$$

with four-momentum P_μ and invariant hadronic mass $P_\mu P^\mu = \mathcal{M}^2$. All other components vanish identically: $\Phi_{z\mu_2 \dots \mu_J} = \Phi_{\mu_1 z \dots \mu_J} = \dots = \Phi_{\mu_1 \mu_2 \dots z} = 0$. One can then construct an effective action in terms of high spin modes $\Phi_J = \Phi_{\mu_1 \mu_2 \dots \mu_J}$, with only physical degrees of freedom [23]. In this case the system of coupled differential equations which follow from (20) reduce to a homogeneous equation in terms of the physical field Φ_J .

In terms of fields with tangent indices

$$\hat{\Phi}_{A_1 A_2 \dots A_J} = e_{A_1}^{M_1} e_{A_2}^{M_2} \dots e_{A_J}^{M_J} \Phi_{M_1 M_2 \dots M_J} = \left(\frac{z}{R}\right)^J \Phi_{A_1 A_2 \dots A_J}, \quad (22)$$

we find the effective action [32] ($\hat{\Phi}_J \equiv \hat{\Phi}_{\mu_1 \dots \mu_J}$)

$$S = \frac{1}{2} \int d^d x dz \sqrt{g} e^{\varphi(z)} \left(g^{NN'} \partial_N \hat{\Phi}_J \partial_{N'} \hat{\Phi}_J - \mu^2 \hat{\Phi}_J^2 \right), \quad (23)$$

containing only the physical degrees of freedom and usual derivatives. Thus, the effect of the covariant derivatives in the effective action for spin- J fields with polarization components along the physical coordinates is a shift in the AdS mass μ . The vielbein e_M^A is defined by $g_{MN} = e_M^A e_N^B \eta_{AB}$, where $A, B = 1, \dots, d + 1$ are tangent AdS space indices and η_{AB} has diagonal components $(1, -1, \dots, -1)$. In AdS the vielbein is $e_M^A = (R/z) \delta_M^A$.

In terms of the AdS field $\Phi_J \equiv \Phi_{\mu_1 \dots \mu_J}$ we can express the effective action (23)

$$S = \frac{1}{2} \int d^d x dz \sqrt{g_J} e^{\varphi(z)} \left(g^{NN'} \partial_N \Phi_J \partial_{N'} \Phi_J - \mu^2 \Phi_J^2 \right), \quad (24)$$

where we have defined an effective metric determinant

$$\sqrt{g_J} = (R/z)^{d+1-2J}, \quad (25)$$

and rescaled the AdS mass μ in (23). Variation of the higher-dimensional action (24) gives the AdS wave equation for the spin- J mode Φ_J

$$\left[-\frac{z^{d-1-2J}}{e^{\varphi(z)}} \partial_z \left(\frac{e^{\varphi(z)}}{z^{d-1-2J}} \partial_z \right) + \left(\frac{\mu R}{z} \right)^2 \right] \Phi(z)_J = \mathcal{M}^2 \Phi(z)_J, \quad (26)$$

where the eigenmode Φ_J is normalized according to

$$R^{d-1-2J} \int_0^\infty \frac{dz}{z^{d-1-2J}} e^{\varphi(z)} \Phi_J^2(z) = 1. \quad (27)$$

The AdS mass is μ obeys the relation

$$(\mu R)^2 = (\tau - J)(\tau - d + J), \quad (28)$$

which follows from the scaling behavior of the tangent AdS field near $z \rightarrow 0$, $\hat{\Phi}_J \sim z^\tau$.

We can also derive (26) by shifting dimensions for a J -spin mode [12, 37]. To this end, we start with the scalar wave equation which follows from the variation of (20) for $J = 0$. This case is particularly simple as the covariant derivative of a scalar field is the usual derivative. We obtain the eigenvalue equation

$$\left[-\frac{z^{d-1}}{e^{\varphi(z)}} \partial_z \left(\frac{e^{\varphi(z)}}{z^{d-1}} \partial_z \right) + \left(\frac{\mu R}{z} \right)^2 \right] \Phi = \mathcal{M}^2 \Phi. \quad (29)$$

A physical spin- J mode $\Phi_{\mu_1 \dots \mu_J}$ with all indices along 3+1 is constructed by shifting dimensions $\Phi_J(z) = (z/R)^{-J} \Phi(z)$. It is simple to show that the shifted field $\Phi_{\mu_1 \mu_2 \dots \mu_J}$ obeys the wave equation (26) which follows from (29) upon mass rescaling $(\mu R)^2 \rightarrow (\mu R)^2 - J(d - J) + Jz\varphi'(z)$.

2.3.1 Non-conformal warped metrics

In the Einstein frame conformal invariance is broken by the introduction of an additional warp factor in the AdS metric in order to include confinement forces

$$\begin{aligned} ds^2 &= (g_E)_{MN} dx^M dx^N \\ &= \frac{R^2}{z^2} e^{\lambda(z)} (\eta_{\mu\nu} dx^\mu dx^\nu - dz^2). \end{aligned} \quad (30)$$

The action is

$$\begin{aligned} S = \frac{1}{2} \int d^d x dz \sqrt{g_E} & \left(g_E^{NN'} g_E^{M_1 M'_1} \dots g_E^{M_J M'_J} D_N \Phi_{M_1 \dots M_J} D_{N'} \Phi_{M'_1 \dots M'_J} \right. \\ & \left. - \mu^2 g_E^{M_1 M'_1} \dots g_E^{M_J M'_J} \Phi_{M_1 \dots M_J} \Phi_{M'_1 \dots M'_J} + \dots \right), \end{aligned} \quad (31)$$

where $g_E^{MN} \equiv (g_E)^{MN}$ and $(g_E)_{MN} = \frac{R^2}{z^2} e^{\lambda(z)} \eta_{MN}$. The flat metric η_{MN} has diagonal components $(1, -1, \dots, -1)$.

The use of warped metrics is useful to visualize the overall confinement behavior as we follow an object in warped AdS space as it falls to the infrared region by the effects of gravity. The gravitational potential energy for an object of mass m in general relativity is given in terms of the time-time component of the metric tensor g_{00}

$$V = mc^2 \sqrt{(g_E)_{00}} = mc^2 R \frac{e^{\lambda(z)/2}}{z}, \quad (32)$$

thus we may expect a potential that has a minimum at the hadronic scale z_0 and grows fast for larger values of z to confine effectively a particle in a hadron within distances $z \sim z_0$. In fact, according to Sonnenschein [38] a background dual to a confining theory should satisfy the conditions for the metric component g_{00}

$$\partial_z(g_{00})|_{z=z_0} = 0, \quad g_{00}|_{z=z_0} \neq 0, \quad (33)$$

to display the Wilson loop area law for confinement of strings.

To relate the results in the Einstein frame where hadronic modes propagate in the non-conformal warped metrics (30) to the results in the String-Jordan frame (20), we scale away the dilaton profile by a redefinition of the fields in the action. This corresponds to the multiplication of the metric determinant $\sqrt{g_E} = \left(\frac{R}{z}\right)^{d+1} e^{(d+1)\lambda(z)/2}$ by the contravariant tensor $(g_E)^{MN}$. Thus the result [32] $\varphi(z) \rightarrow \frac{d-1}{2}\lambda(z)$, or $\varphi \rightarrow \frac{3}{2}\lambda$ for AdS_5 .

2.3.2 Effective confining potentials in AdS

For some applications it is convenient to scale away the dilaton factor in the action by a field redefinition [39]. For example, for a scalar field we can shift $\Phi \rightarrow e^{-\varphi/2}\Phi$, and the bilinear component in the action is transformed into the equivalent problem of a free kinetic part plus an effective confining potential $V(z)$ which breaks the conformal invariance.⁵ For the spin- J effective action (24) we find upon the field redefinition $\Phi_J \rightarrow e^{-\varphi/2}\Phi_J$

$$S = \frac{1}{2} \int d^d x dz \sqrt{g_J} \left(g^{NN'} \partial_N \Phi_J \partial_{N'} \Phi_J - \mu^2 \Phi_J^2 - V(z) \Phi_J^2 \right) - \frac{1}{4} \lim_{\epsilon \rightarrow 0} \int d^d x \left(\frac{R}{z} \right)^{d-1-2J} \varphi'(z) \Phi_J^2 \Big|_{\epsilon}^{\infty}, \quad (34)$$

⁵In fact, for fermions the conformality cannot be broken by the introduction of a dilaton background or by explicitly deforming the AdS metric as discussed above, since the additional warp factor is scaled away by a field redefinition. In this case the breaking of the conformal invariance and the generation of the fermion spectrum can only be accomplished by the introduction of an effective potential. This is further discussed in Sec. 5.2.

with effective metric determinant (25) $\sqrt{g_J} = (R/z)^{d+1-2J}$ and effective potential $V(z) = \frac{z^2}{R^2}U(z)$, where

$$U(z) = \frac{1}{2}\varphi''(z) + \frac{1}{4}\varphi'(z)^2 + \frac{2J-d+1}{2z}\varphi'(z). \quad (35)$$

The action (24) is thus equivalent, modulo a surface term, to the action (34) written in terms of the rotated fields $\Phi_J \rightarrow e^{-\varphi/2}\Phi_J$. The result (35) is identical to the result obtained in Ref. [33]. As we will show in the following section, the effective potential (35), for $d = 4$, is precisely the effective light-front potential which appears in Eq. (18), where the LF transverse impact variable ζ is identified with the holographic variable z . A different approach is discussed in Ref. [40] where the infrared physics is introduced by a back-reaction model to the AdS metric. See also Refs. [41, 42, 43, 44].

2.4 Light-front holographic mapping

The structure of the QCD light-front Hamiltonian equation (7) for the state $|\psi(P)\rangle$ is similar to the structure of the wave equation (26) for the J -mode $\Phi_{\mu_1\cdots\mu_J}$ in AdS space; they are both frame-independent and have identical eigenvalues \mathcal{M}^2 , the mass spectrum of the color-singlet states of QCD. This provides the basis for a profound connection between physical QCD formulated in the light-front and the physics of hadronic modes in AdS space. However, important differences are also apparent: Eq. (7) is a linear quantum-mechanical equation of states in Hilbert space, whereas Eq. (26) is a classical gravity equation; its solutions describe spin- J modes propagating in a higher dimensional warped space. Physical hadrons are composite, and thus inexorably endowed of orbital angular momentum. Thus, the identification of orbital angular momentum is of primary interest in establishing a connection between both approaches. In fact, to a first semiclassical approximation, light-front QCD is formally equivalent to the equations of motion on a fixed gravitational background [12] asymptotic to AdS_5 , where the prominent properties of confinement are encoded in a dilaton profile $\varphi(z)$.

As shown in Sect. 2.2, one can indeed systematically reduce the LF Hamiltonian eigenvalue Eq. (7) to an effective relativistic wave equation (18), analogous to the AdS equations, by observing that each n -particle Fock state has an essential dependence on the invariant mass of the system and thus, to a first approximation, LF dynamics depend only on \mathcal{M}_n^2 . In impact space the relevant variable is the boost invariant variable ζ , which measures the separation of quarks and gluons, and which also allows one to separate the bound state dynamics of the constituents from the kinematics of their internal angular momentum.

Upon the substitution $z \rightarrow \zeta$ and

$$\phi_J(\zeta) = (\zeta/R)^{-3/2+J} e^{\varphi(z)/2} \Phi_J(\zeta), \quad (36)$$

in (26), we find for $d = 4$ the QCD light-front wave equation (18) with effective potential [37]

$$U(\zeta) = \frac{1}{2}\varphi''(\zeta) + \frac{1}{4}\varphi'(\zeta)^2 + \frac{2J-3}{2\zeta}\varphi'(\zeta), \quad (37)$$

provided that the fifth dimensional mass μ is related to the internal orbital angular momentum $L = \max|L^z|$ and the total angular momentum $J^z = L^z + S^z$ of the hadron. Light-front holographic mapping thus implies that the fifth dimensional AdS mass μ is not a free parameter but scales as

$$(\mu R)^2 = -(2 - J)^2 + L^2. \quad (38)$$

The angular momentum projections in the light-front \hat{z} direction L^z, S^z and J^z are kinematical generators in the front form, so they are the natural quantum numbers to label the eigenstates of light-front physics. In general, a hadronic eigenstate with spin J^z in the front form corresponds to an eigenstate of $J^2 = j(j+1)$ in the rest frame in the conventional instant form. It thus has $2j+1$ degenerate states with $J^z = -j, -j+1, \dots, j-1, +j$ [4], thus J represents the maximum value of $|J^z|$, $J = \max|J^z|$.

If $L^2 < 0$, the LF Hamiltonian defined in Eq. (7) is unbounded from below $\langle \phi | H_{LF} | \phi \rangle < 0$ and the spectrum contains an infinite number of unphysical negative values of \mathcal{M}^2 which can be arbitrarily large. As \mathcal{M}^2 increases in absolute value, the particle becomes localized within a very small region near $\zeta = 0$, since the effective potential is conformal at small ζ . For $\mathcal{M}^2 \rightarrow -\infty$ the particle is localized at $\zeta = 0$, the particle “falls towards the center” [45]. The critical value $L = 0$ corresponds to the lowest possible stable solution, the ground state of the light-front Hamiltonian. For $J = 0$ the five dimensional mass μ is related to the orbital momentum of the hadronic bound state by $(\mu R)^2 = -4 + L^2$ and thus $(\mu R)^2 \geq -4$. The quantum mechanical stability condition $L^2 \geq 0$ is thus equivalent to the Breitenlohner-Freedman stability bound in AdS [46]. The scaling dimensions are $2 + L$ independent of J , in agreement with the twist-scaling dimension of a two-parton bound state in QCD. It is important to notice that in the light-front the $SO(2)$ Casimir for orbital angular momentum L^2 is a kinematical quantity, in contrast to the usual $SO(3)$ Casimir $L(L+1)$ from non-relativistic physics which is rotational, but not boost invariant. The $SO(2)$ Casimir form L^2 corresponds to the group of rotations in the transverse LF plane. Indeed, the Casimir operator for $SO(N) \sim S^{N-1}$ is $L(L+N-2)$.

3 Mesons in light-front holography

Considerable progress has recently been achieved in the study of the meson excitation spectrum in QCD from discrete lattices which is a first-principles method [47]. In practice, lattice gauge theory computations of eigenvalues beyond the ground-state are very challenging. Furthermore, states at rest are not classified according to total angular momentum J and J_z , but according to the irreducible representation of the lattice, and thus a large basis of interpolating operators is required for the extraction of meaningful data [47]. In contrast, the semiclassical light-front holographic wave equation (18) obtained in the previous section describes relativistic bound states at equal light-front time with a simplicity comparable to the Schrödinger equation of atomic physics at equal instant time. It thus provides a framework for a first-order analytical exploration of the spectrum of mesons. In the limit of zero-quark masses, the light-front wave equation has a geometrical equivalent to the equation of motion in a warped AdS space-time.

3.1 A hard-wall model for mesons

As the simplest example we consider a truncated model where quarks propagate freely in the hadronic interior up to the confinement scale $1/\Lambda_{\text{QCD}}$. The interaction terms in the QCD Lagrangian effectively build confinement, here depicted by a hard wall potential

$$U(\zeta) = \begin{cases} 0 & \text{if } \zeta \leq \frac{1}{\Lambda_{\text{QCD}}}, \\ \infty & \text{if } \zeta > \frac{1}{\Lambda_{\text{QCD}}}. \end{cases} \quad (39)$$

This provides an analog of the MIT bag model [48] where quarks are permanently confined inside a finite region of space. In contrast to bag models, boundary conditions are imposed on the boost-invariant variable ζ , not on the bag radius at fixed time. The wave functions have support for longitudinal momentum fraction $0 < x < 1$. The resulting model is a manifestly Lorentz invariant model with confinement at large distances, while incorporating conformal behavior at small physical separation.

The eigenvalues of the LF wave equation (18) for the potential (39) are determined by the boundary conditions $\phi(z = 1/\Lambda_{\text{QCD}}) = 0$, and are given in terms of the roots of the Bessel functions: $\mathcal{M}_{L,k} = \beta_{L,k} \Lambda_{\text{QCD}}$. Light-front eigenmodes $\phi(\zeta)$ are normalized according to

$$\int_0^{\Lambda_{\text{QCD}}^{-1}} d\zeta \phi^2(\zeta) = 1, \quad (40)$$

and are given by

$$\phi_{L,k}(\zeta) = \frac{\sqrt{2}\Lambda_{QCD}}{J_{1+L}(\beta_{L,k})} \sqrt{\zeta} J_L(\zeta\beta_{L,k}\Lambda_{QCD}). \quad (41)$$

Individual hadron states can be identified by their interpolating operators, which are defined at the $z \rightarrow 0$ asymptotic boundary of AdS space, and couple to the AdS field $\hat{\Phi}(x, z)$ (22) at the boundary limit (See Appendix A). The short-distance behavior of a hadronic state is characterized by its twist (canonical dimension minus spin) $\tau = \Delta - \sigma$, where σ is the sum over the constituent's spin $\sigma = \sum_{i=1}^n \sigma_i$. The twist of a hadron is also equal to the number of its constituent partons n .⁶

Pion interpolating operators are constructed by examining the behavior of bilinear covariants $\bar{\psi}\Gamma\psi$ under charge conjugation and parity transformation. Thus, for example, a pion interpolating operator $\bar{q}\gamma^+\gamma_5 q$ creates a state with quantum numbers $J^{PC} = 0^{-+}$, and a vector meson interpolating operator $\bar{q}\gamma_\mu q$ a state 1^{--} . Likewise the operator $\bar{q}\gamma_\mu\gamma_5 q$ creates a state with 1^{++} quantum numbers, for example the $a_1(1260)$ positive parity meson. If we include orbital excitations, the pion interpolating operator is $\mathcal{O}_{2+L} = \bar{q}\gamma^+\gamma_5 D_{\{\ell_1 \cdots \ell_m\}} q$. This is an operator with total internal orbital momentum $L = \sum_{i=1}^m \ell_i$, twist $\tau = 2 + L$ and canonical dimension $\Delta = 3 + L$. Similarly the vector-meson interpolating operator is given by $\mathcal{O}_{2+L}^\mu = \bar{q}\gamma^\mu D_{\{\ell_1 \cdots \ell_m\}} q$. The scaling of the AdS field $\hat{\Phi}$ (22) near $z \rightarrow 0$, $\hat{\Phi}(z) \sim z^\tau$, is precisely the scaling required to match the scaling dimension of the local meson interpolating operators.

We list in Table 1 the confirmed (4-star and 3-star) isospin $I = 1$ mesons states from the updated Particle Data Group (PDG) [49], with their assigned internal spin, orbital angular momentum and radial quantum numbers. The $I = 1$ mesons have quark content $|u\bar{d}\rangle$, $\frac{1}{\sqrt{2}}|u\bar{u} - d\bar{d}\rangle$ and $|d\bar{u}\rangle$. The $I = 1$ mesons are the π , b , ρ and a mesons. We have not listed in Table 1 the $I = 0$ mesons which are a mix of $u\bar{u}$, $d\bar{d}$ and $s\bar{s}$, thus more complex entities. The light $I = 0$ mesons are η , η' , h , h' , ω , ϕ , f and f' . This list comprises the puzzling $I = 0$ scalar f -mesons, which may be interpreted as a superposition of tetra-quark states with a $q\bar{q}$, $L = 1$, $S = 1$, configuration which couple to a $J = 0$ state [50].⁷

The light $I = 1$ orbital meson spectrum is compared in Fig. 1 with the truncated-space model for $n = 0$. The data is from PDG [49]. The predictions for the lower mass mesons are in better agreement with data as compared with Ref. [51], where naive conformal dimensions were used instead. However the model fails to account for the pion as a chiral $\mathcal{M}_\pi = 0$ state. The hard-wall model for mesons is degenerate with respect to the orbital

⁶To include orbital L -dependence we make the substitution $\tau \rightarrow n + L$.

⁷The interpretation of the $\pi_1(1400)$ is not very clear [50] and is not included in Table 1. Likewise we do not include the $\pi_1(1600)$ in the present analysis.

Table 1: Confirmed $I = 1$ mesons listed by PDG [49]. The labels L , S and n refer to assigned internal orbital angular momentum, internal spin and radial quantum number respectively. For a $q\bar{q}$ state $P = (-1)^{L+1}$, $C = (-1)^{L+S}$.

L	S	n	J^{PC}	Meson State
0	0	0	0^{-+}	$\pi(140)$
0	0	1	0^{-+}	$\pi(1300)$
0	0	2	0^{-+}	$\pi(1800)$
0	1	0	1^{--}	$\rho(770)$
0	1	1	1^{--}	$\rho(1450)$
0	1	2	1^{--}	$\rho(1700)$
1	0	0	1^{+-}	$b_1(1235)$
1	1	0	0^{++}	$a_0(980)$
1	1	1	0^{++}	$a_0(1450)$
1	1	0	1^{++}	$a_1(1260)$
1	1	0	2^{++}	$a_2(1320)$
2	0	0	2^{-+}	$\pi_2(1670)$
2	0	1	2^{-+}	$\pi_2(1880)$
2	1	0	3^{--}	$\rho_3(1690)$
3	1	0	4^{++}	$a_4(2040)$

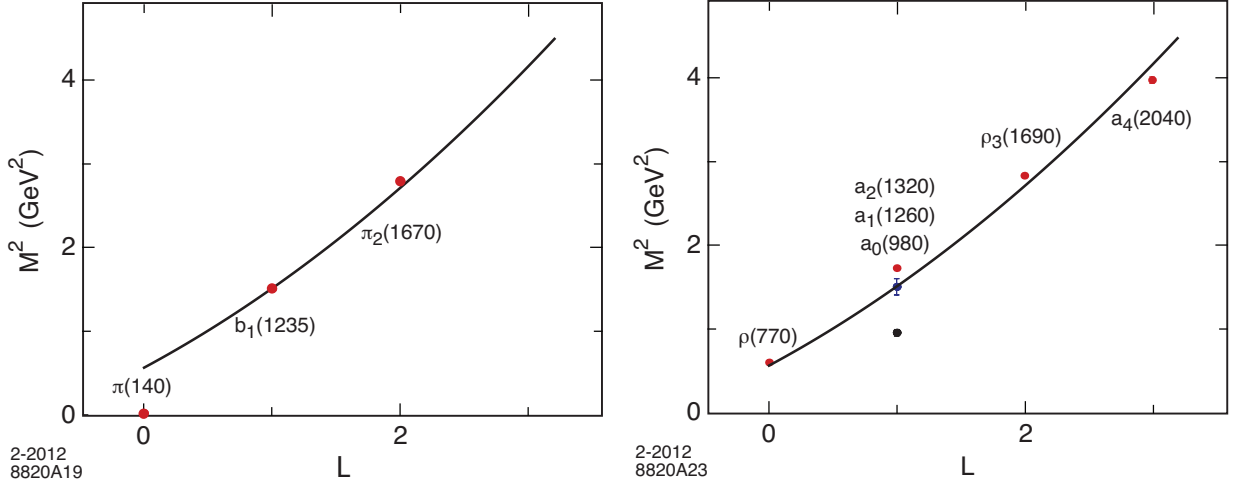


Figure 1: $I = 1$ light-meson orbital states in the hard wall model for $\Lambda_{\text{QCD}} = 0.32$ GeV: pseudoscalar mesons (left) and vector mesons (right).

quantum number L , and thus fails to account for the important $L = |L^z| = 1$ triplet splitting shown in Fig. 1 (right); the $a_0(980)$, $a_1(1260)$ and $a_2(1320)$ states, which corresponds to $J = |J^z| = 0, 1, 2$ respectively. Using the asymptotic expansion of the Bessel function for large arguments we find that $\mathcal{M} \sim 2n + L$, in contrast to the usual Regge dependence $\mathcal{M}^2 \sim n + L$ found experimentally [50]. As a consequence, the radial modes are not well described in the truncated-space model. For example the first radial AdS eigenvalue has a mass 1.77 GeV, which is too high compared to the mass of the observed first radial excitation of the meson, the $\pi(1300)$. The shortcomings of the hard-wall model described in this section are evaded in the soft wall model discussed below, where the sharp cutoff is modified.

3.2 A soft-wall model for mesons

As we discussed in Sec. 2.4, the conformal metric of AdS space can be modified within the gauge/gravity framework to include confinement by the introduction of an additional warp factor or, equivalently, with a dilaton background $\varphi(z)$, which breaks the conformal invariance of the theory. A particularly interesting case is a dilaton profile $\exp(\pm\kappa^2 z^2)$ of either sign, since it leads to linear Regge trajectories [23] and avoids the ambiguities in the choice of boundary conditions at the infrared wall. The corresponding modified metric can be interpreted in the higher dimensional warped AdS space as a gravitational potential in the fifth dimension

$$V(z) = mc^2 \sqrt{g_{00}} = mc^2 R \frac{e^{\pm 3\kappa^2 z^2/4}}{z}. \quad (42)$$

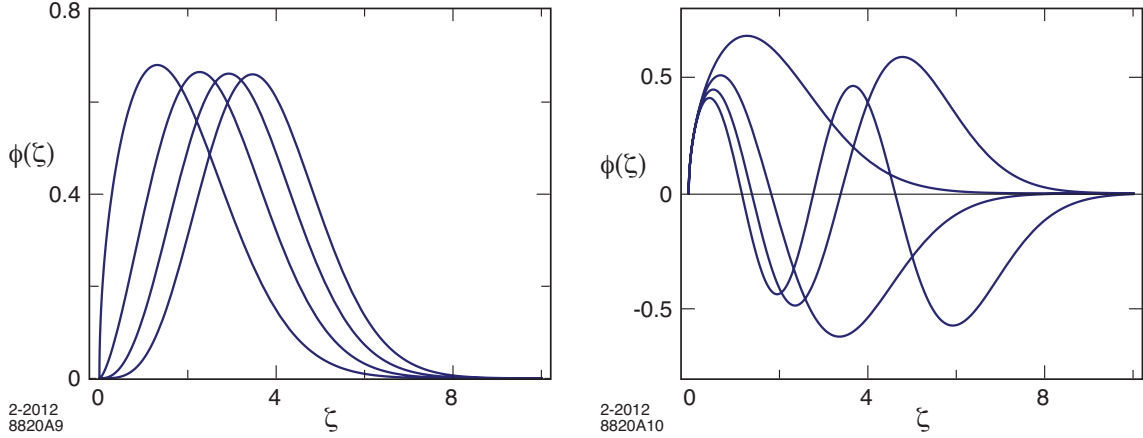


Figure 2: Light-front wavefunctions $\phi_{n,L}(\zeta)$ in physical space-time corresponding to a dilaton profile $\exp(\kappa^2 z^2)$: (left) orbital modes ($n = 0$) and (right) radial modes ($L = 0$).

In the case of the negative solution, the potential decreases monotonically, and thus an object located in the boundary of AdS space will fall to infinitely large values of z . This is illustrated in detail by Klebanov and Maldacena in Ref. [52]. For the positive solution, the potential is nonmonotonic and has an absolute minimum at $z_0 \sim 1/\kappa$. Furthermore, for large values of z the gravitational potential increases exponentially, thus confining any object to distances $\langle z \rangle \sim 1/\kappa$ [53, 54].

From (37) we obtain for the positive sign confining solution $\varphi = \exp(\kappa^2 z^2)$ the effective potential [54]

$$U(\zeta) = \kappa^4 \zeta^2 + 2\kappa^2(J - 1), \quad (43)$$

which corresponds to a transverse oscillator in the light-front. For the effective potential (43) equation (18) has eigenfunctions

$$\phi_{n,L}(\zeta) = \kappa^{1+L} \sqrt{\frac{2n!}{(n+L)!}} \zeta^{1/2+L} e^{-\kappa^2 \zeta^2/2} L_n^L(\kappa^2 \zeta^2), \quad (44)$$

and eigenvalues ⁸

$$\mathcal{M}_{n,J,L}^2 = 4\kappa^2 \left(n + \frac{J+L}{2} \right). \quad (45)$$

The meson spectrum (45) has a string-theory Regge form $\mathcal{M}^2 \sim n + L$: the square of the eigenmasses are linear in both the angular momentum L and radial quantum number n , where n counts the number of nodes of the wavefunction in the radial variable ζ . The

⁸Similar results are found in Ref. [33].

LFWFs (44) for different orbital and radial excitations are depicted in Fig. 2. Constituent quark and antiquark separate from each other as the orbital and radial quantum numbers increase. The number of nodes in the light-front wave function depicted in Fig. 2 (right) correspond to the radial excitation quantum number n .

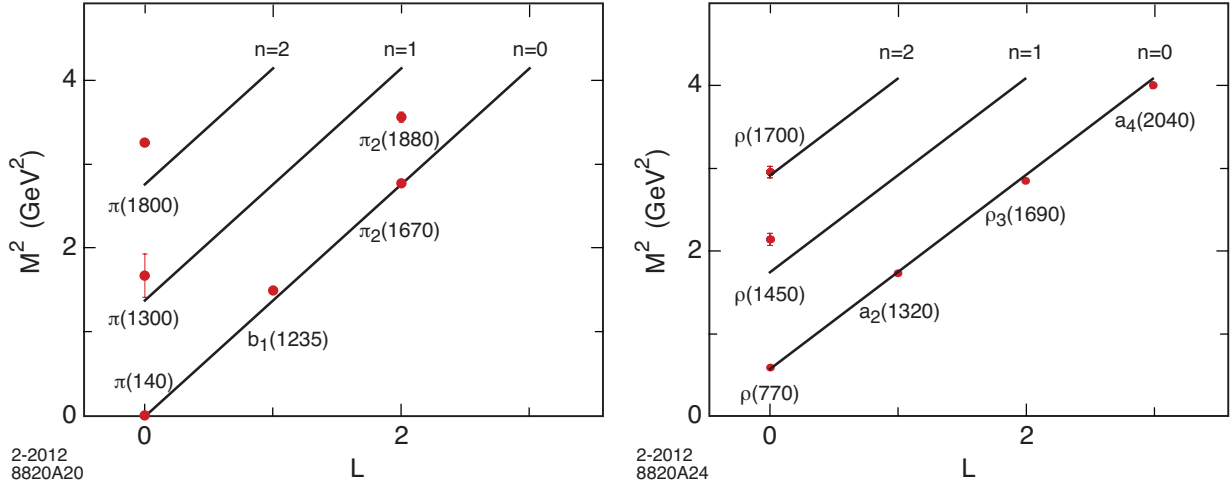


Figure 3: $I=1$ parent and daughter Regge trajectories for the π -meson family (left) with $\kappa = 0.59$ GeV; and the ρ -meson family (right) with $\kappa = 0.54$ GeV.

For the $J = L + S$ meson families Eq. (45) becomes

$$\mathcal{M}_{n,L,S}^2 = 4\kappa^2 \left(n + L + \frac{S}{2} \right). \quad (46)$$

The lowest possible solution for $n = J = 0$ has eigenvalue $\mathcal{M}^2 = 0$. This is a chiral symmetric bound state of two massless quarks with scaling dimension 2 and size $\langle \zeta^2 \rangle \sim 1/\kappa^2$, which we identify with the lowest state, the pion. Thus one can compute the corresponding Regge families by simply adding $4\kappa^2$ for a unit change in the radial quantum number, $4\kappa^2$ for a change in one unit in the orbital quantum number and $2\kappa^2$ for a change of one unit of spin to the ground state value of \mathcal{M}^2 . The spectral predictions for the $J = L + S$ light pseudoscalar and vector meson states, listed in Table. 1, are compared with experimental data in Fig. 3 for the positive sign dilaton model discussed here. The data is from PDG [49].

It is important to notice that in contrast to the hard-wall model, the soft-wall model with positive dilaton accounts for the mass pattern observed in radial excitations, as well as for the triplet splitting for the $L = 1$, $J = 0, 1, 2$, vector meson a -states. Using the spectral formula (45) we find

$$\mathcal{M}_{a_2(1320)} > \mathcal{M}_{a_1(1260)} > \mathcal{M}_{a_0(980)}. \quad (47)$$

The predicted values are 0.76, 1.08 and 1.32 GeV for the masses of the $a_0(980)$, $a_1(1260)$ and $a_2(1320)$ vector mesons, compared with the experimental values 0.98, 1.23 and 1.32 GeV respectively. The prediction for the mass of the $L = 1$, $n = 1$ state $a_0(1450)$ is 1.53 GeV, compared with the observed value 1.47 GeV. For other calculations of the hadronic spectrum in the framework of AdS/QCD, see Refs. [55, 56, 57, 58, 59, 60, 61, 62, 63, 64, 65, 66, 67, 68, 69, 70, 71, 72].⁹

4 Meson form factors

A form factor in QCD is defined by the transition matrix element of a local quark current between hadronic states. The great advantage of the front form – as emphasized by Dirac – is that boost operators are kinematic. Unlike the instant form, the boost operators in the front form have no interaction terms. The calculation of a current matrix element $\langle P + q | J^\mu | P \rangle$ requires boosting the hadronic eigenstate from $|P\rangle$ to $|P + q\rangle$, a task which becomes hopelessly complicated in the instant form. In addition, the virtual photon couples to connected currents which arise from the instant form vacuum.

In AdS space form factors are computed from the overlap integral of normalizable modes with boundary currents which propagate in AdS space. The AdS/CFT duality incorporates the connection between the twist scaling dimension of the QCD boundary interpolating operators to the falloff of the normalizable modes in AdS near its conformal boundary. If both quantities represent the same physical observable for any value of the transferred momentum squared q^2 , a precise correspondence can be established between the string modes Φ in AdS space and the light front wavefunctions of hadrons ψ_n in physical four dimensional space-time [13]. In fact, Light-Front Holography was originally derived by observing the correspondence between matrix elements obtained in AdS/CFT with the corresponding formula using the light-front representation [13]. The same results follow from comparing the relativistic light-front Hamiltonian equation describing bound states in QCD with the wave equations describing the propagation of modes in a warped AdS space, as shown in the previous section [12].

4.1 Meson electromagnetic form factor

In the higher dimensional gravity theory, the hadronic transition matrix element corresponds to the coupling of an external electromagnetic field $A^M(x, z)$, for a photon propagat-

⁹For recent reviews see, for example, Refs. [73, 74].

ing in AdS space, with the extended field $\Phi_P(x, z)$ describing a meson in AdS is [15]

$$\int d^4x dz \sqrt{g} A^M(x, z) \Phi_{P'}^*(x, z) \overleftrightarrow{\partial}_M \Phi_P(x, z) \sim (2\pi)^4 \delta^4(P' - P - q) \epsilon_\mu (P + P')^\mu F_M(q^2). \quad (48)$$

To simplify the discussion we will first describe a model with a wall at $z \sim 1/\Lambda_{\text{QCD}}$ – the hard wall model – which limits the propagation of the string modes in AdS space beyond the IR separation $z \sim 1/\Lambda_{\text{QCD}}$ and also sets the gap scale [9]. We recall from Sec. 2.3 that the coordinates of AdS_5 are the Minkowski coordinates x^μ and z labeled $x^M = (x^\mu, z)$, with $M, N = 1, \dots, 5$, and g is the determinant of the metric tensor. The pion has initial and final four momentum P and P' respectively and q is the four-momentum transferred to the pion by the photon with polarization ϵ_μ . The expression on the right-hand side of (48) represents the space-like QCD electromagnetic transition amplitude in physical space-time

$$\langle P' | J^\mu(0) | P \rangle = (P + P')^\mu F_M(q^2). \quad (49)$$

It is the EM matrix element of the quark current $J^\mu = e_q \bar{q} \gamma^\mu q$, and represents a local coupling to pointlike constituents. Although the expressions for the transition amplitudes look very different, one can show that a precise mapping of the matrix elements can be carried out at fixed light-front time [13, 14].

The form factor is computed in the light front from the matrix elements of the plus-component of the current J^+ in order to avoid coupling to Fock states with different numbers of constituents. Expanding the initial and final meson states $|\psi_M(P^+, \mathbf{P}_\perp)\rangle$ in terms of Fock components, $|\psi_M\rangle = \sum_n \psi_{n/M} |n\rangle$, we obtain the DYW expression [16, 17] upon the phase space integration over the intermediate variables in the $q^+ = 0$ frame:

$$F_M(q^2) = \sum_n \int [dx_i] [d^2\mathbf{k}_{\perp i}] \sum_j e_j \psi_{n/M}^*(x_i, \mathbf{k}'_{\perp i}, \lambda_i) \psi_{n/M}(x_i, \mathbf{k}_{\perp i}, \lambda_i), \quad (50)$$

where the phase space factor $[dx_i] [d^2\mathbf{k}_{\perp i}]$ is given by (9) and the variables of the light cone Fock components in the final-state are given by $\mathbf{k}'_{\perp i} = \mathbf{k}_{\perp i} + (1 - x_i) \mathbf{q}_\perp$ for a struck constituent quark and $\mathbf{k}'_{\perp i} = \mathbf{k}_{\perp i} - x_i \mathbf{q}_\perp$ for each spectator. The formula is exact if the sum is over all Fock states n . The form factor can also be conveniently written in impact space as a sum of overlap of LFWFs of the $j = 1, 2, \dots, n - 1$ spectator constituents [75]

$$F_M(q^2) = \sum_n \prod_{j=1}^{n-1} \int dx_j d^2\mathbf{b}_{\perp j} \exp\left(i\mathbf{q}_\perp \cdot \sum_{j=1}^{n-1} x_j \mathbf{b}_{\perp j}\right) |\psi_{n/M}(x_j, \mathbf{b}_{\perp j})|^2, \quad (51)$$

corresponding to a change of transverse momentum $x_j \mathbf{q}_\perp$ for each of the $n - 1$ spectators with $\sum_{i=1}^n \mathbf{b}_{\perp i} = 0$.

For definiteness we shall consider the π^+ valence Fock state $|u\bar{d}\rangle$ with charges $e_u = \frac{2}{3}$ and $e_{\bar{d}} = \frac{1}{3}$. For $n = 2$, there are two terms which contribute to Eq. (51). Exchanging $x \leftrightarrow 1-x$ in the second integral we find

$$F_{\pi^+}(q^2) = 2\pi \int_0^1 \frac{dx}{x(1-x)} \int \zeta d\zeta J_0\left(\zeta q \sqrt{\frac{1-x}{x}}\right) |\psi_{u\bar{d}/\pi}(x, \zeta)|^2, \quad (52)$$

where $\zeta^2 = x(1-x)\mathbf{b}_\perp^2$ and $F_{\pi^+}(q=0) = 1$.

We now compare this result with the electromagnetic form factor in AdS space-time. The incoming electromagnetic field propagates in AdS according to $A_\mu(x^\mu, z) = \epsilon_\mu(q)e^{-iq \cdot x}V(q^2, z)$ in the gauge $A_z = 0$ (no physical polarizations along the AdS variable z). The bulk-to-boundary propagator $V(q^2, z)$ is the solution of the AdS wave equation for $A_\mu(x^\mu, z)$ given by ($Q^2 = -q^2 > 0$)

$$V(Q^2, z) = zQK_1(zQ), \quad (53)$$

with boundary conditions [15]

$$V(Q^2 = 0, z) = V(Q^2, z = 0) = 1. \quad (54)$$

The propagation of the pion in AdS space is described by a normalizable mode $\Phi_P(x^\mu, z) = e^{-iP \cdot x}\Phi(z)$ with invariant mass $P_\mu P^\mu = \mathcal{M}^2$ and plane waves along Minkowski coordinates x^μ . Extracting the overall factor $(2\pi)^4 \delta^4(P' - P - q)$ from momentum conservation at the vertex which arises from integration over Minkowski variables in (48), we find [15]

$$F(Q^2) = R^3 \int \frac{dz}{z^3} V(Q^2, z) \Phi^2(z), \quad (55)$$

where $F(Q^2 = 0) = 1$. Using the integral representation of $V(Q^2, z)$

$$V(Q^2, z) = \int_0^1 dx J_0\left(zQ \sqrt{\frac{1-x}{x}}\right), \quad (56)$$

we write the AdS electromagnetic form-factor as

$$F(Q^2) = R^3 \int_0^1 dx \int \frac{dz}{z^3} J_0\left(zQ \sqrt{\frac{1-x}{x}}\right) \Phi^2(z). \quad (57)$$

To compare with the light-front QCD form factor expression (52) we use the expression of the LFWF (15) in the transverse LF plane, where we factor out the longitudinal and transverse modes $\phi(\zeta)$ and $X(x)$ respectively. If both expressions for the form factor are to be identical for arbitrary values of Q , we obtain $\phi(\zeta) = (\zeta/R)^{3/2}\Phi(\zeta)$ and $X(x) = \sqrt{x(1-x)}$ [13],

where we identify the transverse impact LF variable ζ with the holographic variable z , $z \rightarrow \zeta = \sqrt{x(1-x)}|\mathbf{b}_\perp|$.¹⁰ Thus, in addition of recovering the expression found in Sec. 2.4 which relates the transverse mode $\phi(\zeta)$ in physical space-time to the field Φ in AdS space, we find a definite expression for the longitudinal LF mode $X(x)$. Identical results follow from mapping the matrix elements of the energy-momentum tensor [18].

4.2 Elastic form factor with a dressed current

The results for the elastic form factor described above correspond to a free current propagating on AdS space. It is dual to the electromagnetic point-like current in the Drell-Yan-West light-front formula [16, 17] for the pion form factor. The DYW formula is an exact expression for the form factor. It is written as an infinite sum of an overlap of LF Fock components with an arbitrary number of constituents. This allows one to map state-by-state to the effective gravity theory in AdS space. However, this mapping has the shortcoming that the multiple pole structure of the time-like form factor does not appear in the time-like region unless an infinite number of Fock states is included. Furthermore, the moments of the form factor at $Q^2 = 0$ diverge term-by-term; for example one obtains an infinite charge radius [76]. This could have been expected, as we are dealing with a massless quark approximation. In fact, infinite slopes also occur in chiral theories when coupling to a massless pion.

Alternatively, one can use a truncated basis of states in the LF Fock expansion with a limited number of constituents and the nonperturbative pole structure can be generated with a dressed EM current as in the Heisenberg picture, *i.e.*, the EM current becomes modified as it propagates in an IR deformed AdS space to simulate confinement. The dressed current is dual to a hadronic EM current which includes any number of virtual $q\bar{q}$ components. The confined EM current also leads to finite moments at $Q^2 = 0$, as illustrated in Fig. 4 for the EM pion form factor.

We describe briefly below how to compute a form factor for a confined current in AdS space using a soft wall example. However, the actual computation of a form factor in AdS has several caveats which we will discuss in Sec. 4.4.

The effective potential corresponding to a dilaton profile $\exp(\pm\kappa^2 z^2)$ has the form of a harmonic oscillator confining potential $\kappa^4 z^2$. The normalizable solution for a meson of twist τ (the number of constituents for a given Fock component) corresponding to the lowest radial

¹⁰Extension of the results to arbitrary n follows from the x -weighted definition of the transverse impact variable of the $n - 1$ spectator system given by Eq. (19). In general the mapping relates the AdS density $\Phi^2(z)$ to an effective LF single particle transverse density [13].

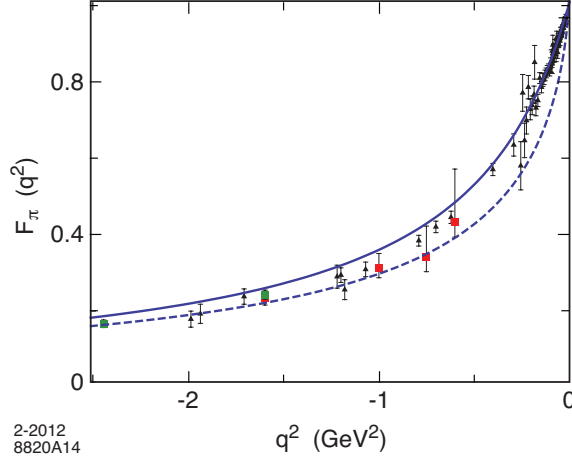


Figure 4: space-like electromagnetic pion form factor $F_\pi(q^2)$. Continuous line: confined current, dashed line free current. Triangles are the data compilation from Baldini [77], boxes are JLAB data [78].

$n = 0$ and orbital $L = 0$ state is given by

$$\Phi^\tau(z) = \sqrt{\frac{2P_\tau}{\Gamma(\tau-1)}} \kappa^{\tau-1} z^\tau e^{-\kappa^2 z^2/2}, \quad (58)$$

with normalization

$$\langle \Phi^\tau | \Phi^\tau \rangle = \int \frac{dz}{z^3} e^{-\kappa^2 z^2} \Phi^\tau(z)^2 = P_\tau, \quad (59)$$

where P_τ is the probability for the twist τ mode (58). This agrees with the fact that the field Φ^τ couples to a local hadronic interpolating operator of twist τ defined at the asymptotic boundary of AdS space (See Appendix A), and thus the scaling dimension of Φ^τ is τ .

In the case of a soft-wall potential the EM bulk-to-boundary propagator is [14, 79]

$$V(Q^2, z) = \Gamma\left(1 + \frac{Q^2}{4\kappa^2}\right) U\left(\frac{Q^2}{4\kappa^2}, 0, \kappa^2 z^2\right), \quad (60)$$

where $U(a, b, c)$ is the Tricomi confluent hypergeometric function

$$\Gamma(a)U(a, b, z) = \int_0^\infty e^{-zt} t^{a-1} (1+t)^{b-a-1} dt. \quad (61)$$

The modified current $V(Q^2, z)$, Eq. (60), has the same boundary conditions (54) as the free current (53), and reduces to (53) in the limit $Q^2 \rightarrow \infty$ [14]. Eq. (60) can be conveniently written in terms of the integral representation [79]

$$V(Q^2, z) = \kappa^2 z^2 \int_0^1 \frac{dx}{(1-x)^2} x^{\frac{Q^2}{4\kappa^2}} e^{-\kappa^2 z^2 x/(1-x)}. \quad (62)$$

Substituting in (55) the expression for the hadronic state (58) with twist τ and the bulk-to-boundary propagator (62), we find that the corresponding elastic form factor for a twist τ Fock component $F_\tau(Q^2)$ ($Q^2 = -q^2 > 0$) [14]

$$F_\tau(Q^2) = \frac{P_\tau}{\left(1 + \frac{Q^2}{\mathcal{M}_\rho^2}\right) \left(1 + \frac{Q^2}{\mathcal{M}_{\rho'}^2}\right) \cdots \left(1 + \frac{Q^2}{\mathcal{M}_{\rho^{\tau-2}}^2}\right)}, \quad (63)$$

which is expressed as a $\tau - 1$ product of poles along the vector meson Regge radial trajectory. For a pion, for example, the lowest Fock state – the valence state – is a twist-2 state, and thus the form factor is the well known monopole form [14]. Thus the mean-square charge radius of the pion $\langle r_\pi^2 \rangle = 6/\mathcal{M}_\rho^2$ in the valence approximation. For $\mathcal{M}_\rho \simeq 770$ MeV we find $\langle r_\pi \rangle \simeq 0.63$ fm, compared with the experimental value $\langle r_\pi \rangle = 0.672 \pm 0.008$ fm [49]. In contrast, the computation with a free current gives the logarithmically divergent result ¹¹.

$$\langle r_\pi^2 \rangle = \frac{3}{2} \ln \left(\frac{4\kappa^2}{Q^2} \right) \Big|_{Q^2 \rightarrow 0}. \quad (64)$$

The remarkable analytical form of (63), expressed in terms of the ρ vector meson mass and its radial excitations, incorporates the correct scaling behavior from the constituent’s hard scattering with the photon and the mass gap from confinement.

4.3 Effective wave function from holographic mapping of a confined current

It is also possible to find a precise mapping of a confined EM current propagating in a warped AdS space to the light-front QCD Drell-Yan-West expression for the form factor. In this case we find an effective LFWF, which corresponds to a superposition of an infinite number of Fock states generated by the “dressed” confined current. For the soft-wall model this mapping can be done analytically.

The form factor in light-front QCD can be expressed in terms of an effective single-particle density [75]

$$F(Q^2) = \int_0^1 dx \rho(x, Q), \quad (65)$$

where

$$\rho(x, Q) = 2\pi \int_0^\infty b db J_0(bQ(1-x)) |\psi(x, b)|^2, \quad (66)$$

¹¹The logarithmically divergent result does not appear in the hard-wall model if one uses Neumann boundary conditions. In this case the EM current is confined and $\langle r_\pi^2 \rangle \sim 1/\Lambda_{\text{QCD}}^2$. A discussion of the pion form factor including chiral symmetry breaking effects in the hard-wall model is given in Refs. [80] and [81].

for a two-parton state ($b = |\mathbf{b}_\perp|$).

We can also compute an effective density on the gravity side corresponding to a twist τ hadronic mode Φ_τ in a modified AdS space. For the soft-wall model the expression is [14]

$$\rho(x, Q) = (\tau - 1) (1 - x)^{\tau - 2} x^{\frac{Q^2}{4\kappa^2}}. \quad (67)$$

To compare (67) with the QCD expression (66) for twist-two we use the integral

$$\int_0^\infty u du J_0(\alpha u) e^{-\beta u^2} = \frac{1}{2\beta} e^{-\alpha^2/4\beta}, \quad (68)$$

and the relation $x^\gamma = e^{\gamma \ln(x)}$. We find the effective two-parton LFWF

$$\psi(x, \mathbf{b}_\perp) = \kappa \frac{(1 - x)}{\sqrt{\pi \ln(\frac{1}{x})}} e^{-\frac{1}{2}\kappa^2 \mathbf{b}_\perp^2 (1-x)^2 / \ln(\frac{1}{x})}, \quad (69)$$

in impact space. The momentum space expression follows from the Fourier transform of (69) and it is given by

$$\psi(x, \mathbf{k}_\perp) = 4\pi \frac{\sqrt{\ln(\frac{1}{x})}}{\kappa(1 - x)} x^{\mathbf{k}_\perp^2 / 2\kappa^2 (1-x)^2} \quad (70)$$

$$= 4\pi \frac{\sqrt{\ln(\frac{1}{x})}}{\kappa(1 - x)} e^{-\mathbf{k}_\perp^2 / 2\kappa^2 (1-x)^2 \ln(\frac{1}{x})}. \quad (71)$$

The effective LFWF encodes nonperturbative dynamical aspects that cannot be learned from a term-by-term holographic mapping, unless one includes an infinite number of terms. Furthermore, it has the right analytical properties to reproduce the bound state vector meson pole in the time-like EM form factor. Unlike the “true” valence LFWF, the effective LFWF, which represents a sum of an infinite number of Fock components, is not symmetric in the longitudinal variables x and $1 - x$ for the active and spectator quarks, respectively.

4.4 Some caveats computing matrix elements in AdS/QCD

The positive dilaton background $\exp(+\kappa^2 z^2)$ used in Sec. 3.2 leads to a successful description of the meson spectrum in terms of the internal quantum numbers n , L and S , and has been preferred for computations in the framework of light-front holography, where the internal structure of hadrons is encoded in the wave function. The positive dilaton background has been discussed in the literature [33, 53, 54, 82, 83] since it has the expected behavior of a model dual to a confining theory [38, 52]. This solution was studied in Ref. [23] but discarded

in the same paper, as it leads to a spurious massless scalar mode in the two-point correlation function for vector mesons [84], and a dilaton field with opposite sign, $\exp(-\kappa^2 z^2)$, was adopted instead [23]. However, using the results of Sec. 2.3.2, one can readily show that the difference in the effective potential $U(z)$ corresponding to positive and negative dilaton factors $\exp(\pm\kappa^2 z^2)$ simply amounts to a z -independent shift in the light-front effective potential U , which in fact vanishes in the vector meson $J = 1$ channel. From (35)

$$\Delta U(z) = U_\varphi(z) - U_{-\varphi}(z) = \varphi''(z) + \frac{2J - d + 1}{z} \varphi'(z), \quad (72)$$

in agreement with the results found in Ref. [33].

For the dilaton profile $\varphi = k^2 z^2$ we find for $d = 4$

$$\Delta U = 4(J - 1)\kappa^2. \quad (73)$$

Therefore, from the point of view of light-front physics, plus and minus dilaton soft-wall solutions are equivalent upon a redefinition of the eigenvalues for $J \neq 1$. For $J = 1$ the effective potential is $U = \kappa^4 z^2$, identical for the plus and minus solutions [39]. Thus, the five-dimensional effective AdS action for a conserved EM current V_M in presence of a confining potential $U = \kappa^4 z^2$ [39]

$$S = \int d^4x dz \sqrt{g} \left(\frac{1}{4} F_{MN} F^{MN} - \frac{\kappa^4 z^4}{2R^2} V_M V^M \right), \quad (74)$$

where $F_{MN} = \partial_M V_N - \partial_N V_M$, only differs by a surface term from the action corresponding to plus or minus dilaton profiles. Equivalently, one can start from the five-dimensional action (74). Upon the field redefinition $V_M \rightarrow e^{\pm\kappa^2 z^2/2} V_M$ one obtains the five-dimensional actions corresponding to plus or minus dilaton solutions, which differ from (74) only by a surface term. Consequently, essential physics cannot depend on the particular choice of the dilaton sign.

Another difficulty found in the holographic approach to QCD is that the vector meson masses obtained from the spin-1 equation of motion do not match the poles of the dressed current when computing a form factor. The discrepancy, in the case of the pion, is an overall factor of $\sqrt{2}$ between the value of the gap scale which follows from the spectrum or from the computation of the pion form factor in the valence state approximation.¹² This

¹²This discrepancy is also present in the gap scale if one computes the spectrum and form factors without recourse to holographic methods, for example using the semi-classical approximation of Ref. [12]. In this case a discrepancy of a factor $\sqrt{2}$ is also found between the spectrum and the computation of space-like form factors.

is quite puzzling, since the same discrepancy is also found, for example, when computing a space-like form factor using the Drell-Yan-West expression, which is an exact expression if all Fock states are included. In AdS conserved currents are not renormalized and correspond to five dimensional massless fields propagating in AdS according to the relation $(\mu R)^2 = (\Delta - p)(\Delta + p - 4)$ for a p form. In the usual AdS/QCD framework [20, 21] this corresponds for $p = 1$ to $\Delta = 3$ or 1, the canonical dimensions of an EM current and the massless gauge field respectively. Normally, one uses a hadronic interpolating operator with minimum twist τ to identify a hadron and to predict the power-law fall-off behavior of its form factors and other hard scattering amplitudes [9]; *e.g.*, for a two-parton bound state $\tau = 2$. However, in the case of a current, one needs to use an effective field operator with dimension $\Delta = 3$. The apparent inconsistency between twist (28) and canonical dimension is removed by noticing that in the light-front one chooses to calculate the matrix element of the twist-3 plus component of the “good” current J^+ [13, 14], in order to avoid coupling to Fock states with different numbers of constituents [16, 17].

As described in Sec. 2.4, light front holography provides a precise relation of the fifth-dimensional mass μ with the total and orbital angular momentum of a hadron in the transverse LF plane $(\mu R)^2 = -(2 - J)^2 + L^2$ (38). Thus the poles computed from the AdS wave equations for a conserved current $\mu R = 0$, correspond to a $J = L = 1$ twist-3 state. Following this, we can compute the mass of the radial excitations of the twist-3 vector family $J = L = 1$ using Eq. (45). The result is

$$\mathcal{M}_{n,J=1,L=1}^2 = 4\kappa^2(n + 1), \quad (75)$$

which is identical with the results obtained in Ref. [23], since, as explained above, the meson spectrum computed with positive or negative dilaton solutions is indistinguishable for $J = 1$.

The twist-3 computation of the space-like form factor, involves the current J^+ , and the poles given by (75) do not correspond to the physical poles of the twist-2 transverse current \mathbf{J}_\perp present in the annihilation channel, namely the $J = 1, L = 0$ state. In this case Eq. (45) gives for the twist-2, $J = 1, L = 0$ vector family the result

$$\mathcal{M}_{n,J=1,L=0}^2 = 4\kappa^2 \left(n + \frac{1}{2} \right). \quad (76)$$

Thus, to compare with physical data one must shift in (63) the twist-2 poles given by (75) to their physical positions (76). When the vector meson masses are shifted to their physical values the agreement of the predictions with observed data is very good [85]. We presume that the problem arises because of the specific truncation used.

4.5 Meson transition form factors

The photon-to-meson transition form factors ¹³ (TFFs) $F_{M\gamma}(Q^2)$ measured in $\gamma\gamma^* \rightarrow M$ reactions have been of intense experimental and theoretical interest. The pion transition form factor between a photon and pion measured in the $e^-e^- \rightarrow e^-e^-\pi^0$ process, with one tagged electron, is the simplest bound-state process in QCD. It can be predicted from first principles in the asymptotic $Q^2 \rightarrow \infty$ limit [88]. More generally, the pion TFF at large Q^2 can be calculated at leading twist as a convolution of a perturbative hard scattering amplitude $T_H(\gamma\gamma^* \rightarrow q\bar{q})$ and a gauge-invariant meson distribution amplitude (DA), which incorporates the nonperturbative dynamics of the QCD bound-state [88].

The BaBar Collaboration has reported measurements of the transition form factors from $\gamma^*\gamma \rightarrow M$ process for the π^0 [89], η , and η' [90, 91] pseudoscalar mesons for a momentum transfer range much larger than previous measurements [92, 93]. Surprisingly, the BaBar data for the π^0 - γ TFF exhibit a rapid growth for $Q^2 > 15 \text{ GeV}^2$, which is unexpected from QCD predictions. In contrast, the data for the η - γ and η' - γ TFFs are in agreement with previous experiments and closer in agreement with theoretical predictions. Many theoretical studies have been devoted to explaining BaBar's experimental results [94, 95, 96, 97, 98, 99, 100, 101, 102, 103, 104, 105, 106, 107, 108, 109, 110].

The pion transition form factor $F_{\pi\gamma}(Q^2)$ can be computed from first principles in QCD. To leading order in $\alpha_s(Q^2)$ and leading twist the result is [88] ($Q^2 = -q^2 > 0$)

$$Q^2 F_{\pi\gamma}(Q^2) = \frac{4}{\sqrt{3}} \int_0^1 dx \frac{\phi(x, \bar{x}Q)}{\bar{x}} \left[1 + O\left(\alpha_s, \frac{m^2}{Q^2}\right) \right], \quad (77)$$

where x is the longitudinal momentum fraction of the quark struck by the virtual photon in the hard scattering process and $\bar{x} = 1 - x$ is the longitudinal momentum fraction of the spectator quark. The pion distribution amplitude $\phi(x, Q)$ in the light-front formalism [88] is the integral of the valence $q\bar{q}$ LFWF in light-cone gauge $A^+ = 0$

$$\phi(x, Q) = \int_0^{Q^2} \frac{d^2\mathbf{k}_\perp}{16\pi^3} \psi_{q\bar{q}/\pi}(x, \mathbf{k}_\perp), \quad (78)$$

and has the asymptotic form [88] $\phi(x, Q \rightarrow \infty) = \sqrt{3}f_\pi x(1-x)$; thus the leading order QCD result for the TFF at the asymptotic limit is obtained [88],

$$Q^2 F_{\pi\gamma}(Q^2 \rightarrow \infty) = 2f_\pi. \quad (79)$$

¹³This section is based on our collaboration with Fu-Guang Cao. Further details are given in [86, 87].

To describe the two-photon processes $\gamma\gamma^* \rightarrow M$, using light-front holographic methods similar to those described in Sec. 4, we need to explore the mathematical structure of higher-dimensional forms in the five dimensional action, since the amplitude (48) can only account for the elastic form factor $F_M(Q^2)$ [87]. For example, in the five-dimensional AdS action there is an additional Chern-Simons (CS) term in addition to the usual Yang-Mills term F^2 [8]. In the case of a $U(1)$ gauge theory the CS action is of the form $\epsilon^{LMNPQ} A_L \partial_M A_N \partial_P A_Q$. The CS action is not gauge invariant: under a gauge transformation it changes by a total derivative which gives a surface term. The CS form is the product of three fields at the same point in five-dimensional space corresponding to a local interaction. Indeed the five-dimensional CS action is responsible for the anomalous coupling of mesons to photons and has been used to describe, for example, the $\omega \rightarrow \pi\gamma$ [111] decay as well as the $\gamma\gamma^* \rightarrow \pi^0$ [112, 113] and $\gamma^*\rho^0 \rightarrow \pi^0$ [114] processes.¹⁴

The hadronic matrix element for the anomalous electromagnetic coupling to mesons in the higher gravity theory is given by the five-dimensional CS amplitude

$$\int d^4x \int dz \epsilon^{LMNPQ} A_L \partial_M A_N \partial_P A_Q \sim (2\pi)^4 \delta^{(4)}(P + q - k) F_{\pi\gamma}(q^2) \epsilon^{\mu\nu\rho\sigma} \epsilon_\mu(q) P_\nu \epsilon_\rho(k) q_\sigma, \quad (80)$$

which includes the pion field as well as the external photon fields by identifying the fifth component of A with the meson mode in AdS space [116]. In the right-hand side of (80) q and k are the momenta of the virtual and on-shell incoming photons respectively with corresponding polarization vectors $\epsilon_\mu(q)$ and $\epsilon_\mu(k)$ for the amplitude $\gamma\gamma^* \rightarrow \pi^0$. The momentum of the outgoing pion is P .

We now compare the QCD expression on the right-hand side of (80) with the AdS transition amplitude on the left-hand side. As for the elastic form factor discussed in Sec. 4.1, the incoming off-shell photon is represented by the propagation of the non-normalizable electromagnetic solution in AdS space, $A_\mu(x^\mu, z) = \epsilon_\mu(q) e^{-iq \cdot x} V(q^2, z)$, where $V(q^2, z)$ is the bulk-to-boundary propagator with boundary conditions (54) $V(q^2 = 0, z) = V(q^2, z = 0) = 1$. Since the incoming photon with momentum k is on its mass shell, $k^2 = 0$, its wave function is $A_\mu(x^\mu, z) = \epsilon_\mu(k) e^{ik \cdot x}$. Likewise, the propagation of the pion in AdS space is described by a normalizable mode $\Phi_P(x^\mu, z) = e^{-iP \cdot x} \Phi_\pi(z)$ with invariant mass $P_\mu P^\mu = \mathcal{M}_\pi^2 = 0$ in the chiral limit for massless quarks. The normalizable mode $\Phi_\pi(z)$ scales as $\Phi_\pi(z) \rightarrow z^2$ in the limit $z \rightarrow 0$, since the leading interpolating operator for the pion has twist two. A simple dimensional analysis implies that $A_z \sim \Phi_\pi(z)/z$, matching the twist scaling dimensions:

¹⁴The anomalous EM couplings to mesons in the Sakai and Sugimoto model is described in Ref. [115].

two for the pion and one for the EM field. Substituting in (80) the expression given above for the pion and the EM fields propagating in AdS, and extracting the overall factor $(2\pi)^4 \delta^4(P' - q - k)$ upon integration over Minkowski variables, we find ($Q^2 = -q^2 > 0$)

$$F_{\pi\gamma}(Q^2) = \frac{1}{2\pi} \int_0^\infty \frac{dz}{z} \Phi_\pi(z) V(Q^2, z), \quad (81)$$

where the normalization is fixed by the asymptotic QCD prediction (79). We have defined our units such that the AdS radius $R = 1$.

Since the LF mapping of (81) to the asymptotic QCD prediction (79) only depends on the asymptotic behavior near the boundary of AdS space, the result is independent of the particular model used to modify the large z IR region of AdS space. At large enough Q , the important contribution to (79) only comes from the region near $z \sim 1/Q$ where $\Phi(z) = 2\pi f_\pi z^2 + \mathcal{O}(z^4)$. Using the integral $\int_0^\infty dx x^\alpha K_1(x) = 2^{\alpha-2} \alpha \left[\Gamma\left(\frac{\alpha}{2}\right) \right]^2$, $\text{Re}(\alpha) > 1$, we recover the asymptotic result (79)

$$Q^2 F_{\pi\gamma}(Q^2 \rightarrow \infty) = 2f_\pi + \mathcal{O}\left(\frac{1}{Q^2}\right), \quad (82)$$

with the pion decay constant f_π [87]

$$f_\pi = \frac{1}{4\pi} \frac{\partial_z \Phi^\pi(z)}{z} \Big|_{z=0}. \quad (83)$$

A simple analytical expression for the pion TFF can be obtained from the “soft-wall” holographic model described in Sec. 4.2. Using (58) to describe the twist-two pion valence wave function in AdS space we find

$$Q^2 F_{\pi\gamma}(Q^2) = \frac{4}{\sqrt{3}} \int_0^1 dx \frac{\phi(x)}{1-x} \left[1 - \exp\left(-\frac{(1-x)P_{q\bar{q}}Q^2}{4\pi^2 f_\pi^2 x}\right) \right], \quad (84)$$

where $\phi(x) = \sqrt{3}f_\pi x(1-x)$ is the asymptotic QCD distribution with f_π the pion decay constant and $P_{q\bar{q}}$ is the probability for the valence state. Remarkably, the holographic result for the pion TFF factor given by (84) for $P_{q\bar{q}} = 1$ is identical to the results for the pion TFF obtained with the exponential light-front wave function model of Musatov and Radyushkin [117] consistent with the leading order QCD result [88]. Since the pion field is identified as the fifth component of A_M , the CS form $\epsilon^{LMNPQ} A_L \partial_M A_N \partial_P A_Q$ is similar in form to an axial current; this correspondence can explain why the resulting pion distribution amplitude has the asymptotic form. ¹⁵

¹⁵In Ref. [112] the pion TFF was studied in the framework of a CS extended hard-wall AdS/QCD model with $A_z \sim \partial_z \Phi(z)$. The expression for the TFF which follows from (80) then vanishes at $Q^2 = 0$, and has to be corrected by the introduction of a surface term at the IR wall [112]. However, this procedure is only possible for a model with a sharp cutoff.

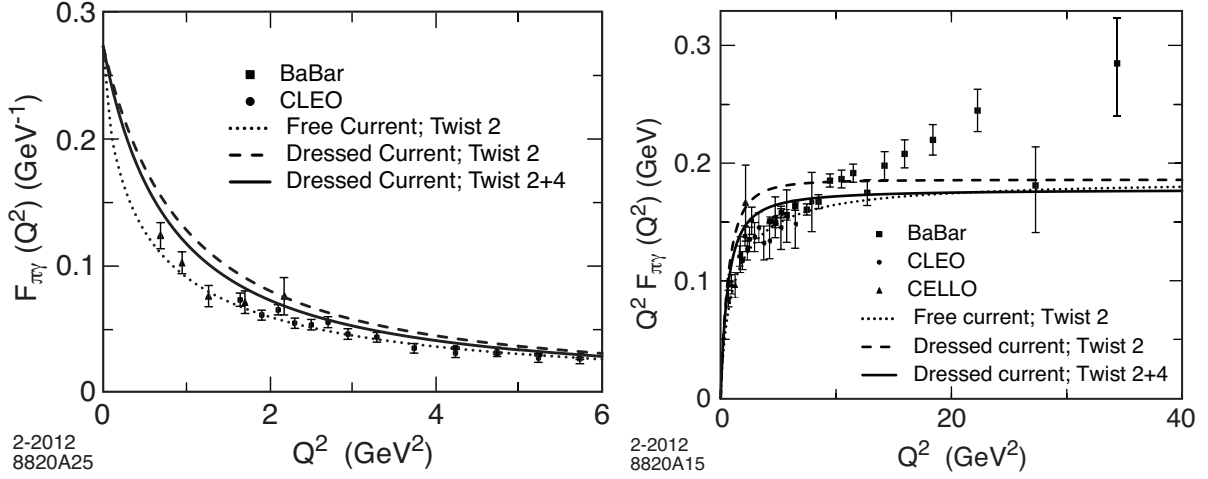


Figure 5: The $\gamma\gamma^* \rightarrow \pi^0$ transition form factor $F_{\pi\gamma}(Q^2)$ (left) and $Q^2 F_{\pi\gamma}(Q^2)$ (right). The dotted curve is the asymptotic result. The dashed and solid curves include the effects of using a confined EM current for twist-two and twist-two plus twist-four respectively. The data are from [89, 92, 93].

Taking $P_{q\bar{q}} = 0.5$ in (84) one obtains a result in agreement with the Adler, Bell and Jackiw anomaly result which agrees within a few percent with the observed value obtained from the decay $\pi^0 \rightarrow \gamma\gamma$. This suggests that the contribution from higher Fock states vanishes at $Q = 0$ in this simple holographic confining model. Thus (84) represents a description of the pion TFF which encompasses the low-energy nonperturbative and the high-energy hard domains, but includes only the asymptotic distribution amplitude of the $q\bar{q}$ component of the pion wave function at all scales. The results from (84) for $P_{q\bar{q}} = 0.5$ are shown in Fig. 5. Also shown in Fig. 5 are the results for the free current approximation (which corresponds to the asymptotic result) with $P_{q\bar{q}} = 0.5$ and a twist-two plus twist-four model [87] with $P_{q\bar{q}} = 0.915$, and $P_{q\bar{q}q\bar{q}} = 0.085$. The calculations [87] agree reasonably well with the experimental data at low- and medium- Q^2 regions ($Q^2 < 10 \text{ GeV}^2$), but disagree with BaBar's large Q^2 data.

The η and η' mesons result from the mixing of the neutral states η_8 and η_1 of the $\text{SU}(3)_F$ quark model. The TFFs for the η and η' mesons have the same expression as the pion transition form factor, except for an overall multiplying factor $c_P = 1$, $\frac{1}{\sqrt{3}}$, and $\frac{2\sqrt{2}}{\sqrt{3}}$ for the π^0 , η_8 and η_1 , respectively [87]. The results for the η and η' transitions form factors are shown in Fig. 6. The calculations agree very well with available experimental data over a large range of Q^2 . The rapid growth of the large Q^2 data for the pion-photon transition form factor reported by the BaBar Collaboration is difficult to explain within the current

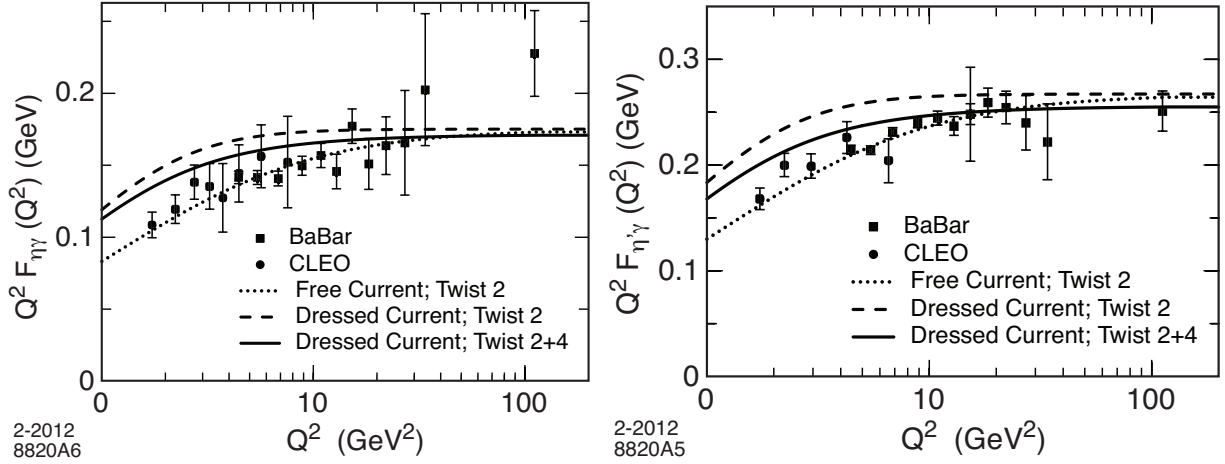


Figure 6: The $\gamma\gamma^* \rightarrow \eta$ transition form factor $Q^2 F_{\eta\gamma}(Q^2)$ (left). The dotted curve is the asymptotic result. The dashed and solid curves include the effects of using a confined EM current for twist-two plus twist-two plus twist-four respectively. Same for the $\gamma\gamma^* \rightarrow \eta'$ transition form factor $Q^2 F_{\eta'\gamma}(Q^2)$ (right). The data are from [89, 92, 93].

framework of QCD. The analysis presented here thus indicates the importance of additional measurements of the pion-photon transition form factor at large Q^2 .

5 Baryons in light-front holography

The study of the excitation spectrum of baryons is one of the most challenging aspects of particle physics. In fact, dedicated experimental programs are in place to determine the spectrum of nucleon excitations and its internal structure. Important computational efforts in lattice QCD aim to the reliable extraction of the excited nucleon eigenstates. Lattice calculations of the ground state light hadron masses agree with experimental values within 5% [47]. However, the excitation spectrum of the nucleon represents a formidable challenge to lattice QCD due to the enormous computational complexity required beyond the leading ground state configuration [118]. Moreover, a large basis of interpolating operators is required since excited nucleon states are classified according to irreducible representations of the lattice, not the total angular momentum.

As we shall discuss below, the analytical exploration of the baryon spectrum and nucleon form factors, using light-front gauge/gravity duality ideas, leads, in contrast, to simple formulas and rules which describe quite well the systematics of the established light-baryon

resonances and elastic and transition nucleon form factors, which can be tested against new experimental findings. The gauge/gravity duality can give us important insights into the strongly coupled dynamics of nucleons using simple analytical methods.

We can extend the holographic ideas to spin- $\frac{1}{2}$ hadrons by considering the propagation of spin- $\frac{1}{2}$ Dirac modes in AdS space [15]. The action for a Dirac field in AdS_{d+1} is

$$S_F = \int d^d x dz \sqrt{g} \left(\frac{i}{2} \bar{\Psi} e_A^M \Gamma^A D_M \Psi - \frac{i}{2} (D_M \bar{\Psi}) e_A^M \Gamma^A \Psi - \mu \bar{\Psi} \Psi \right), \quad (85)$$

where $\sqrt{g} = \left(\frac{R}{z}\right)^{d+1}$ and e_A^M is the inverse vielbein, $e_A^M = \left(\frac{z}{R}\right) \delta_A^M$. The covariant derivative of the spinor field is $D_M = \partial_M - \frac{i}{2} \omega_M^{AB} \Sigma_{AB}$ where Σ_{AB} are the generators of the Lorentz group in the spinor representation, $\Sigma_{AB} = \frac{i}{4} [\Gamma_A, \Gamma_B]$, and the tangent space Dirac matrices obey the usual anti-commutation relation $\{\Gamma^A, \Gamma^B\} = \eta^{AB}$. For d even we can choose the set of gamma matrices $\Gamma_A = (\Gamma_\mu, \Gamma_z)$ with $\Gamma_z = -\Gamma^z = \Gamma_0 \Gamma_1 \cdots \Gamma_{d-1}$. For $d = 4$ we have $\Gamma_A = (\gamma_\mu, -i\gamma_5)$, where γ_μ and γ_5 are the usual 4-dimensional Dirac matrices with $\gamma_5 = i\gamma_0\gamma_1\gamma_2\gamma_3$ and $\gamma_5^2 = +1$. The spin connection in AdS is $w_M^{AB} = (\eta^{Az} \delta_M^B - \eta^{Bz} \delta_M^A) / z$, thus the equation of motion $(ie_A^M \Gamma^A D_M - \mu) \Psi = 0$ leads to the Dirac equation in AdS space

$$\left[i \left(z \eta^{MN} \Gamma_M \partial_N + \frac{d}{2} \Gamma_z \right) - \mu R \right] \Psi = 0, \quad (86)$$

where the $d+1$ dimensional mass μ is a priori an arbitrary parameter.¹⁶

One can also take as starting point the construction of light-front wave equations in physical space-time for baryons by studying the LF transformation properties of spin 1/2 states [121]. The light-front wave equation describing baryons is a matrix eigenvalue equation $D_{LF} |\psi\rangle = \mathcal{M} |\psi\rangle$ with $H_{LF} = D_{LF}^2$. In a 2×2 spinor component representation

$$\begin{aligned} \frac{d}{d\zeta} \psi_+ + \frac{\nu + \frac{1}{2}}{\zeta} \psi_+ &= \mathcal{M} \psi_-, \\ -\frac{d}{d\zeta} \psi_- + \frac{\nu + \frac{1}{2}}{\zeta} \psi_- &= \mathcal{M} \psi_+. \end{aligned} \quad (87)$$

As shown below, we can identify ν with the orbital angular momentum L : $\nu = L + 1$.

Upon the substitution $z \rightarrow \zeta$ and

$$\Psi(x, z) = e^{-iP \cdot x} z^2 \psi(z) u(P), \quad (88)$$

¹⁶The spinor action (85) is often complemented by an additional surface term in the UV boundary [119] $\lim_{\epsilon \rightarrow 0} \int d^d x \sqrt{g_\epsilon} \bar{\Psi} \Psi$ where g_ϵ is the metric induced in the boundary surface by the metric g of AdS_{d+1} . The additional term is required to preserve the $O(d+1, 1)$ isometry group of AdS_{d+1} and to compute a two-point correlation function in the conformal boundary theory [120]. The equation of motion (86) is not modified by the surface term.

in (86) we recover for $d = 4$ its LF expression (87), provided that $|\mu R| = \nu + \frac{1}{2}$. The baryon invariant mass is $P_\mu P^\mu = \mathcal{M}^2$ and the spinor $u(P)$ is a four-dimensional spinor which obeys the Dirac equation $(\not{P} - \mathcal{M})u(P) = 0$. Thus the eigenvalue equation $H_{LF}\psi_\pm = \mathcal{M}^2\psi_\pm$ for the upper and lower components leads to the wave equation

$$\left(-\frac{d^2}{d\zeta^2} - \frac{1 - 4\nu^2}{4\zeta^2}\right)\psi_+(\zeta) = \mathcal{M}^2\psi_+(\zeta), \quad (89)$$

and

$$\left(-\frac{d^2}{d\zeta^2} - \frac{1 - 4(\nu + 1)^2}{4\zeta^2}\right)\psi_-(\zeta) = \mathcal{M}^2\psi_-(\zeta), \quad (90)$$

with solutions

$$\psi_+ \sim \sqrt{\zeta} J_\nu(\zeta \mathcal{M}), \quad \psi_- \sim \sqrt{\zeta} J_{\nu+1}(\zeta \mathcal{M}). \quad (91)$$

The solution of the spin- $\frac{3}{2}$ Rarita-Schwinger equation for the field Ψ_M in AdS space is more involved, but considerable simplification occurs in the $\Psi_z = 0$ gauge for physical polarization along Minkowski coordinates Ψ_μ , where it becomes similar to the spin- $\frac{1}{2}$ solution [122, 123].

5.1 A hard-wall model for baryons

The hermiticity of the LF Dirac operator D_{LF} in the eigenvalue equation $D_{LF}|\psi\rangle = \mathcal{M}|\psi\rangle$ implies that the surface term $\psi_+^*(\zeta)\psi_-(\zeta) - \psi_-^*(\zeta)\psi_+(\zeta)$ should vanish at the boundary. Thus in a truncated space holographic model, the light front modes ψ_+ or ψ_- should vanish at the boundary $\zeta = 0$ and $\zeta = \zeta_0$. This condition fixes the boundary conditions and determine the baryon spectrum in the truncated hard-wall model. A similar surface term arises when one computes the equation of motion from the action (85). In fact, integrating by parts (85) and using the equation of motion we find

$$S_F = -\lim_{\epsilon \rightarrow 0} \int \frac{d^d x}{2z^d} \left(\bar{\Psi}_+ \Psi_- - \bar{\Psi}_- \Psi_+ \right) \Big|_\epsilon^{z_0}, \quad (92)$$

where $\Psi_\pm = \frac{1}{2}(1 \pm \gamma_5)\Psi$, and R has units $R = 1$. The baryon mass spectrum thus follows from the LF “bag” boundary conditions $\psi_\pm(\zeta_0) = 0$ or the AdS boundary conditions $\Psi_\pm(z_0) = 0$ at the IR value, $z_0 = 1/\Lambda_{\text{QCD}}$, where the LF invariant impact variable ζ (19) is identified with the AdS holographic coordinate z , $z \rightarrow \zeta$. We find

$$\mathcal{M}^+ = \beta_{\nu,k} \Lambda_{\text{QCD}}, \quad \mathcal{M}^- = \beta_{\nu+1,k} \Lambda_{\text{QCD}}, \quad (93)$$

with a scale-independent mass ratio determined by the zeros of Bessel functions $\beta_{\nu,k}$.

In the usual AdS/CFT correspondence the baryon is an $SU(N_C)$ singlet bound state of N_C quarks in the large N_C limit. Since there are no quarks in this theory, quarks are introduced as external sources at the AdS asymptotic boundary [124, 125]. The baryon is constructed as an N_C baryon vertex located in the interior of AdS. In this top-down string approach baryons are usually described as solitons or Skyrmin-like objects [126, 127]. In contrast, the bottom-up light-front holographic approach described here is based on the precise mapping of AdS expressions to light-front QCD. Consequently, we construct baryons corresponding to $N_C = 3$ not $N_C \rightarrow \infty$. The corresponding interpolating operator for an $N_C = 3$ physical baryon $\mathcal{O}_{3+L} = \psi D_{\{\ell_1 \dots D_{\ell_q} \psi D_{\ell_{q+1}} \dots D_{\ell_m}\}} \psi$, $L = \sum_{i=1}^m \ell_i$, is a twist-3, dimension $9/2 + L$ with scaling behavior given by its twist-dimension $3 + L$. We thus require $\nu = L + 1$ to match the short distance scaling behavior. One can interpret L as the maximal value of $|L^z|$ in a given LF Fock state.

In the case of massless quarks, the nucleon eigenstate ($u_{\pm} = \frac{1}{2}(1 \pm \gamma_5)u$)

$$\begin{aligned} \psi(\zeta) &= \psi_+(\zeta)u_+ + \psi_-(\zeta)u_- \\ &= C\sqrt{\zeta}(J_\nu(\zeta\mathcal{M})u_+ + J_{\nu+1}(\zeta\mathcal{M})u_-), \end{aligned} \quad (94)$$

has components ψ_+ and ψ_- with different orbital angular momentum, $L^z = 0$ and $L^z = +1$, combined with spin components $S^z = +1/2$ and $S^z = -1/2$ respectively, but with equal probability¹⁷

$$\int d\zeta |\psi_+(\zeta)|^2 = \int d\zeta |\psi_-(\zeta)|^2, \quad (95)$$

a manifestation of the chiral invariance of the theory for massless quarks. Thus in light-front holography, the spin of the proton is carried by the quark orbital angular momentum: $J^z = \langle L^z \rangle = \pm 1/2$ since $\langle \sum S_q^z \rangle = 0$ [128], and not by its gluons.

An important feature of bound-state relativistic theories is that hadron eigenstates have in general Fock components with different L components. In the holographic example discussed above, the proton has S and P components with equal probability. In the case of QED, the ground state $1S$ state of the Dirac-Coulomb equation has both $L = 0$ and $L = 1$ components. By convention, in both light-front QCD and QED, one labels the eigenstate with its minimum value of L . For example, the symbol L in the light-front AdS/QCD spectral prediction for mesons (46) refers to the *minimum* L (which also corresponds to the leading twist) and S is the total internal spin of the hadron.

¹⁷For the truncated-space model, (95) follows from the identity $\int_0^1 x dx [J_\alpha^2(x\beta) - J_{\alpha+1}^2(x\beta)] = J_\alpha(\beta)J_{\alpha+1}(\beta)/\beta$, independently of the component wavefunction chosen to fix the boundary conditions at $\zeta = \zeta_0$.

Table 2: Classification of confirmed baryons listed by the PDG [49]. The labels L , S and n refer to the internal orbital angular momentum, internal spin and radial quantum number respectively. The even-parity baryons correspond to the **56** multiplet of $SU(6)$ and the odd-parity to the **70**.

L	S	n	Baryon State			
0	$\frac{1}{2}$	0	$N_{\frac{1}{2}}^{1+}(940)$			
0	$\frac{1}{2}$	1	$N_{\frac{1}{2}}^{1+}(1440)$			
0	$\frac{1}{2}$	2	$N_{\frac{1}{2}}^{1+}(1710)$			
0	$\frac{3}{2}$	0	$\Delta_{\frac{3}{2}}^{3+}(1232)$			
0	$\frac{3}{2}$	1	$\Delta_{\frac{3}{2}}^{3+}(1600)$			
1	$\frac{1}{2}$	0	$N_{\frac{1}{2}}^{1-}(1535) \quad N_{\frac{3}{2}}^{3-}(1520)$			
1	$\frac{3}{2}$	0	$N_{\frac{1}{2}}^{1-}(1650) \quad N_{\frac{3}{2}}^{3-}(1700) \quad N_{\frac{5}{2}}^{5-}(1675)$			
1	$\frac{1}{2}$	0	$\Delta_{\frac{1}{2}}^{1-}(1620) \quad \Delta_{\frac{3}{2}}^{3-}(1700)$			
2	$\frac{1}{2}$	0	$N_{\frac{3}{2}}^{3+}(1720) \quad N_{\frac{5}{2}}^{5+}(1680)$			
2	$\frac{1}{2}$	1	$N_{\frac{5}{2}}^{5+}(1900)$			
2	$\frac{3}{2}$	0	$\Delta_{\frac{1}{2}}^{1+}(1910)$	$\Delta_{\frac{3}{2}}^{3+}(1920)$	$\Delta_{\frac{5}{2}}^{5+}(1905)$	$\Delta_{\frac{7}{2}}^{7+}(1950)$
3	$\frac{1}{2}$	0	$N_{\frac{5}{2}}^{5-} \quad N_{\frac{7}{2}}^{7-}$			
3	$\frac{3}{2}$	0	$N_{\frac{3}{2}}^{3-}$	$N_{\frac{5}{2}}^{5-}$	$N_{\frac{7}{2}}^{7-}(2190)$	$N_{\frac{9}{2}}^{9-}(2250)$
3	$\frac{1}{2}$	0	$\Delta_{\frac{5}{2}}^{5-} \quad \Delta_{\frac{7}{2}}^{7-}$			
4	$\frac{1}{2}$	0	$N_{\frac{7}{2}}^{7+} \quad N_{\frac{9}{2}}^{9+}(2220)$			
4	$\frac{3}{2}$	0	$\Delta_{\frac{5}{2}}^{5+}$	$\Delta_{\frac{7}{2}}^{7+}$	$\Delta_{\frac{9}{2}}^{9+}$	$\Delta_{\frac{11}{2}}^{11+}(2420)$
5	$\frac{1}{2}$	0	$N_{\frac{9}{2}}^{9-} \quad N_{\frac{11}{2}}^{11-}$			
5	$\frac{3}{2}$	0	$N_{\frac{7}{2}}^{7-}$	$N_{\frac{9}{2}}^{9-}$	$N_{\frac{11}{2}}^{11-}(2600)$	$N_{\frac{13}{2}}^{13-}$

We list in Table 2 the confirmed (3-star and 4-star) baryon states from the updated Particle Data Group [49].¹⁸ To determine the internal spin, internal orbital angular momentum and radial quantum number assignment of the N and Δ excitation spectrum from the total angular momentum-parity PDG assignment, it is convenient to use the conventional $SU(6) \supset SU(3)_{\text{flavor}} \times SU(2)_{\text{spin}}$ multiplet structure, but other model choices are also possible [130].¹⁹

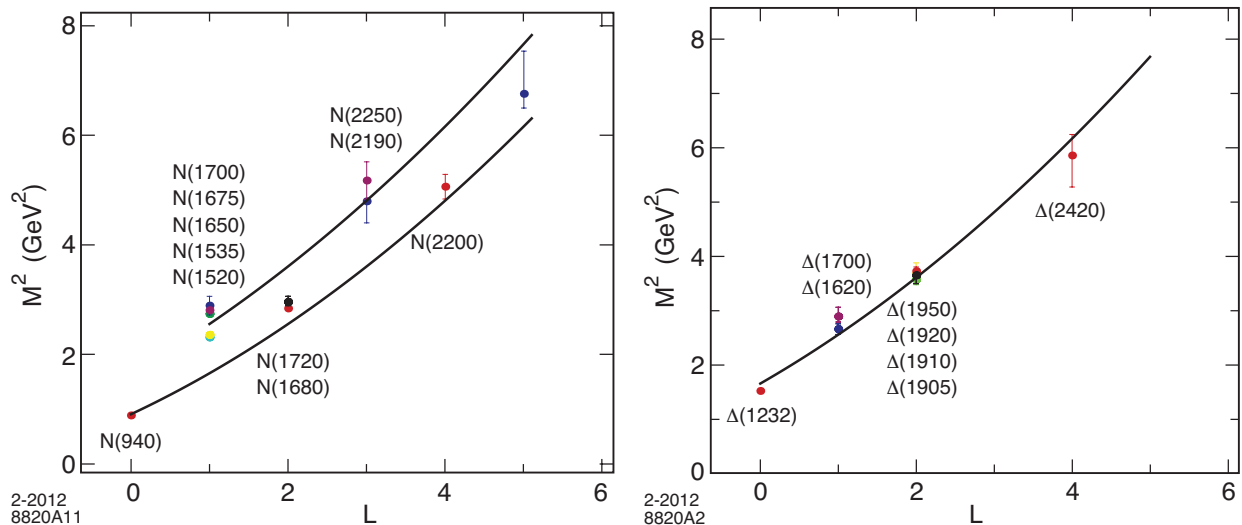


Figure 7: Light baryon orbital spectrum ($n = 0$) for $\Lambda_{\text{QCD}} = 0.25$ GeV. Predictions for the nucleons (left) and for the Δ trajectories (right).

We show in Fig. 7 the model predictions for the orbital excitation spectrum of baryons which follows from the boundary conditions $\psi_{\pm}(\zeta = 1/\Lambda_{\text{QCD}}) = 0$ in a truncated-space model in the infrared region [51].²⁰ The figure shows the predicted orbital spectrum of the nucleon and Δ orbital resonances for $n = 0$. The only parameter is the value of Λ_{QCD} which we take as 0.25 GeV. Orbital excitations are approximately aligned along two trajectories corresponding to even and odd parity states, with exception of the $\Delta_{\frac{1}{2}}^{-}(1620)$ and $\Delta_{\frac{3}{2}}^{-}(1700)$ states which are in the same trajectory. The spectrum shows a clustering of states with the same orbital L , consistent with a strongly suppressed spin-orbit force. This remarkable prediction for

¹⁸A recent exploration of the properties of baryon resonances derived from a multichannel partial wave analysis [129] report additional resonances not included in the Review of Particle Properties [49].

¹⁹In particular the $\Delta_{\frac{5}{2}}^{-}(1930)$ state (not shown in Table 2) has been given the non- $SU(6)$ assignment $S = 3/2$, $L = 1$, $n = 1$ in Ref. [130]. This assignment will be further discussed in the section below.

²⁰The results shown here in Fig. 7 give better results for the lower mass baryons as compared with Ref. [51] where naive conformal dimensions were used instead.

the baryons is not a peculiarity of the hard-wall model, but is an important property of light-front holographic models.

In the quark-diquark model of Jaffe and Wilczek [131], nucleon states with $S = 1/2$ in Fig. 7 (a) correspond to “good” diquarks, $S = 3/2$ nucleons and all the Δ states in Fig. 7 (b) to “bad” diquarks, with exception of the $\Delta(1930)$ which does not follow the simple $3q$ quark-diquark pattern. As for the case for mesons discussed in Sec. 3.1, the hard-wall model predicts $\mathcal{M} \sim 2n + L$, in contrast to the usual Regge behavior $\mathcal{M}^2 \sim n + L$ found in experiment [50]. The radial modes are also not well described in the truncated-space model. For example, the first AdS radial state has a mass 1.85 GeV, which is thus difficult to identify with the Roper $N(1440)$ resonance. This problem is not present in the soft wall model for baryons discussed below.

5.2 A soft-wall model for baryons

For fermion fields in AdS one cannot break conformality with the introduction of a dilaton in the action since it can be rotated away leaving the action conformally invariant.²¹ As a result, one must introduce an effective confining potential $V(z)$ in the action of a Dirac field propagating in AdS_{d+1} space to break the conformal invariance of the theory and generate a baryon spectrum

$$S_F = \int d^d x dz \sqrt{g} \left(\frac{i}{2} \bar{\Psi} e_A^M \Gamma^A D_M \Psi - \frac{i}{2} (D_M \bar{\Psi}) e_A^M \Gamma^A \Psi - \mu \bar{\Psi} \Psi - V(z) \bar{\Psi} \Psi \right). \quad (96)$$

The variation of the action (96) leads to the Dirac equation in AdS

$$\left[i \left(z \eta^{MN} \Gamma_M \partial_N + \frac{d}{2} \Gamma_z \right) - \mu R - R V(z) \right] \Psi = 0. \quad (97)$$

As in the case for the hard wall model described in the previous section, the corresponding light-front wave equation in physical space-time follows from identifying the transverse LF coordinate ζ with the AdS holographic variable z , $z \rightarrow \zeta$, and the substitution (88) in (97). For $d = 4$ we find the matrix eigenvalue equation in the 2×2 spinor component representation

$$\begin{aligned} \frac{d}{d\zeta} \psi_+ + \frac{\nu + \frac{1}{2}}{\zeta} \psi_+ + U(\zeta) \psi_+ &= \mathcal{M} \psi_-, \\ -\frac{d}{d\zeta} \psi_- + \frac{\nu + \frac{1}{2}}{\zeta} \psi_- + U(\zeta) \psi_- &= \mathcal{M} \psi_+, \end{aligned} \quad (98)$$

where $U(\zeta) = \frac{R}{\zeta} V(\zeta)$ is the effective confining potential in the light-front Dirac equation.

²¹This remarkable property was first pointed out in Ref. [132], and later derived independently in Ref. [133].

Instead of choosing a dilaton profile to reproduce linear Regge behavior, as described in Sec. 3.2 for the case of mesons, we choose the confining interaction V in (96) to reproduce linear Regge trajectories for the baryon mass spectrum \mathcal{M}^2 . This “soft-wall” model for baryons in a higher dimensional AdS space, has also a LF analogue; it corresponds to a Dirac equation in physical space-time in presence of an effective linear confining potential U defined at equal LF time. For the potential $U = \kappa^2 \zeta$ equation (98) is equivalent to the system of second order equations

$$\left(-\frac{d^2}{d\zeta^2} - \frac{1 - 4\nu^2}{4\zeta^2} + \kappa^4 \zeta^2 + 2(\nu + 1)\kappa^2 \right) \psi_+(\zeta) = \mathcal{M}^2 \psi_+(\zeta), \quad (99)$$

and

$$\left(-\frac{d^2}{d\zeta^2} - \frac{1 - 4(\nu + 1)^2}{4\zeta^2} + \kappa^4 \zeta^2 + 2\nu\kappa^2 \right) \psi_-(\zeta) = \mathcal{M}^2 \psi_-(\zeta). \quad (100)$$

As a consequence, when one squares the Dirac Equation with $U(\zeta)$, one generates a Klein-Gordon equation with the potential $\kappa^4 z^2$. This is consistent with the same confining potential which appears in the meson equations. The LF equation $H_{LF} \psi_{\pm} = \mathcal{M}^2 \psi_{\pm}$ has thus the two-component solution

$$\psi_+(\zeta) \sim \zeta^{\frac{1}{2}+\nu} e^{-\kappa^2 \zeta^2/2} L_n^\nu(\kappa^2 \zeta^2), \quad \psi_-(\zeta) \sim \zeta^{\frac{3}{2}+\nu} e^{-\kappa^2 \zeta^2/2} L_n^{\nu+1}(\kappa^2 \zeta^2), \quad (101)$$

with equal probability for the properly normalized components. The eigenvalues are

$$\mathcal{M}^2 = 4\kappa^2(n + \nu + 1), \quad (102)$$

identical for both plus and minus eigenfunctions. Note that, as expected, the potential $\kappa^4 \zeta^2$ in the second order equation matches the soft-wall potential for mesons discussed in Sec. 3.2. However, in contrast to the case for mesons, the dilaton modification of the action gives little guidance for finding an effective potential for baryons, since the dilaton can be scaled away by a field redefinition. Consequently the overall energy scale is left unspecified for the baryons [121]. The remarkable regularities observed in the nucleon spectrum and the analytical properties of the AdS/LF equations allows us, nonetheless, to built precise rules to describe the observed baryon spectrum and make predictions for, as yet undiscovered, new baryon excited states.

Before computing the baryon spectrum we must fix the overall mass scale and the parameter ν . Since our starting point for finding the bound state equation of motion for baryons is the light-front method, we shall require the mass scale to be identical for mesons and baryons

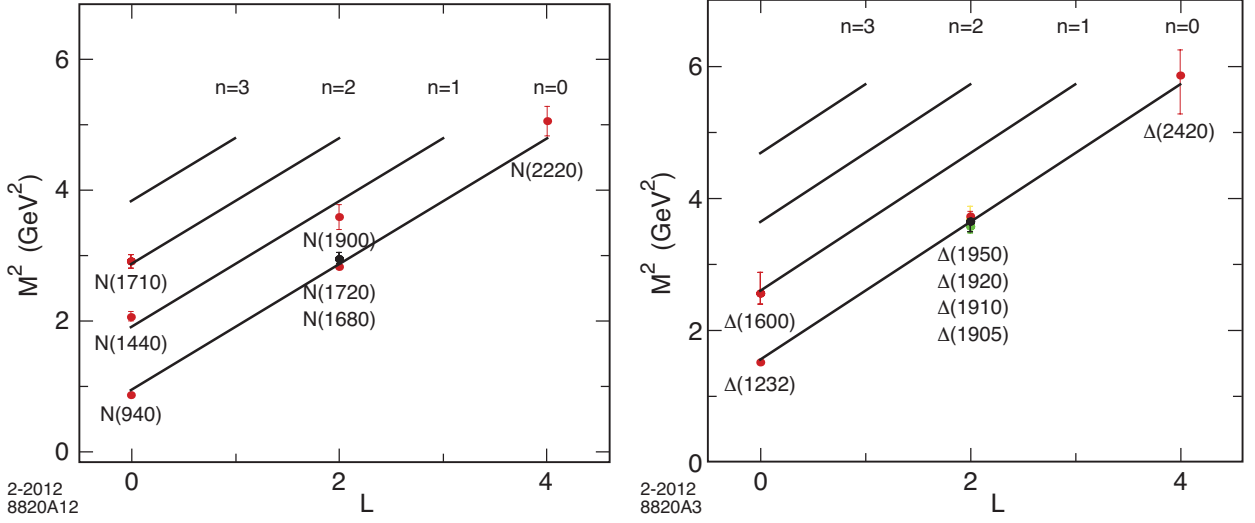


Figure 8: Orbital and radial baryon excitations for the positive-parity Regge trajectories for the N (left) and Δ (right) families for $\kappa = 0.49 - 0.51$ GeV.

while maintaining chiral symmetry for the pion [121] in the LF Hamiltonian equations. In practice, these constraints require a subtraction of $-4\kappa^2$ from (102).²²

As is the case for the truncated-space model, the value of ν is determined by the short distance scaling behavior, $\nu = L + 1$. Higher-spin fermionic modes $\Psi_{\mu_1 \dots \mu_{J-1/2}}$, $J > 1/2$, with all of its polarization indices along the $3 + 1$ coordinates follow by shifting dimensions for the fields as shown for the case of mesons in Ref. [54]²³. Therefore, as in the meson sector, the increase in the mass \mathcal{M}^2 for baryonic states for increased radial and orbital quantum numbers is $\Delta n = 4\kappa^2$, $\Delta L = 4\kappa^2$ and $\Delta S = 2\kappa^2$, relative to the lowest ground state, the proton; *i.e.*, the slope of the spectroscopic trajectories in n and L are identical. Thus for the positive-parity nucleon sector

$$\mathcal{M}_{n,L,S}^{2(+)} = 4\kappa^2 \left(n + L + \frac{S}{2} + \frac{3}{4} \right), \quad (103)$$

where the internal spin $S = \frac{1}{2}$ or $\frac{3}{2}$.

The resulting predictions for the spectroscopy of positive-parity light baryons are shown in Fig. 8. Only confirmed PDG [49] states are shown. The Roper state $N(1440)$ and

²²This subtraction to the mass scale may be understood as the displacement required to describe nucleons with $N_C = 3$ as a composite system with leading twist $3 + L$; *i.e.*, a quark-diquark bound state with a twist-2 composite diquark rather than an elementary twist-1 diquark.

²³The detailed study of higher fermionic spin wave equations in modified AdS spaces is based on our collaboration with Hans Guenter Dosch [32]. See also the discussion in Ref. [33].

the $N(1710)$ are well accounted for in this model as the first and second radial states of the proton. Likewise, the $\Delta(1660)$ corresponds to the first radial state of the $\Delta(1232)$ as shown in in Fig. 8. The model is successful in explaining the parity degeneracy observed in the light baryon spectrum, such as the $L = 2$, $N(1680) - N(1720)$ degenerate pair and the $L = 2$, $\Delta(1905)$, $\Delta(1910)$, $\Delta(1920)$, $\Delta(1950)$ states which are degenerate within error bars. The parity degeneracy of baryons shown in Fig. 8 is also a property of the hard-wall model described in the previous section, but in that case the radial states are not well described [51].

In order to have a comprehensive description of the baryon spectrum, we need to extend (103) to the negative-parity baryon sector. In the case of the hard-wall model, this was realized by choosing the boundary conditions for the plus or minus components of the AdS wave function Ψ^\pm . In practice, this amounts to allowing the negative-parity spin baryons to have a larger spatial extent, a point also raised in [134]. In the soft-wall model there are no boundary conditions to set in the infrared since the wave function vanishes exponentially for large values of z . We note, however, that setting boundary conditions on the wave functions, as done in Sec. 5.1, is equivalent to choosing the branch $\nu = \mu R - \frac{1}{2}$ for the negative-parity spin- $\frac{1}{2}$ baryons and $\nu = \mu R + \frac{1}{2}$ for the positive parity spin- $\frac{3}{2}$ baryons. This gives a factor $4\kappa^2$ between the lower-lying and the higher-lying nucleon trajectories as illustrated in Fig. 9, where we compare the lower nucleon trajectory corresponding to the $J = L + S$ spin- $\frac{1}{2}$ positive-parity nucleon family with the upper nucleon trajectory corresponding to the $J = L + S - 1$ spin- $\frac{3}{2}$ negative-parity nucleons. As is clearly shown in the figure, the gap is precisely the factor $4\kappa^2$.

If we apply the same spin-change rule previously discussed for the positive-parity nucleons, we would expect that the trajectory for the family of spin- $\frac{1}{2}$ negative-parity nucleons is lower by the factor $2\kappa^2$ compared to the spin- $\frac{3}{2}$ minus-parity nucleons according to the spin-change rule previously discussed. Thus the formula for the negative-parity baryons

$$\mathcal{M}_{n,L,S}^{2(-)} = 4\kappa^2 \left(n + L + \frac{S}{2} + \frac{5}{4} \right), \quad (104)$$

where $S = \frac{1}{2}$ or $\frac{3}{2}$. It is important to recall that our formulas for the baryon spectrum are the result of an analytic inference, rather than formally derived.

The full baryon orbital excitation spectrum listed in Table 2 for $n = 0$ is shown in Fig. 10. We note that $\mathcal{M}_{n,L,S=\frac{3}{2}}^{2(+)} = \mathcal{M}_{n,L,S=\frac{1}{2}}^{2(-)}$ and consequently the positive and negative-parity Δ states lie in the same trajectory, consistent with the experimental results. Only the confirmed PDG [49] states listed in Table 2 are shown. Our results for the Δ states agree with those of Ref. [59]. “Chiral partners” as the $N(1535)$ and the $N(940)$ with different orbital angular

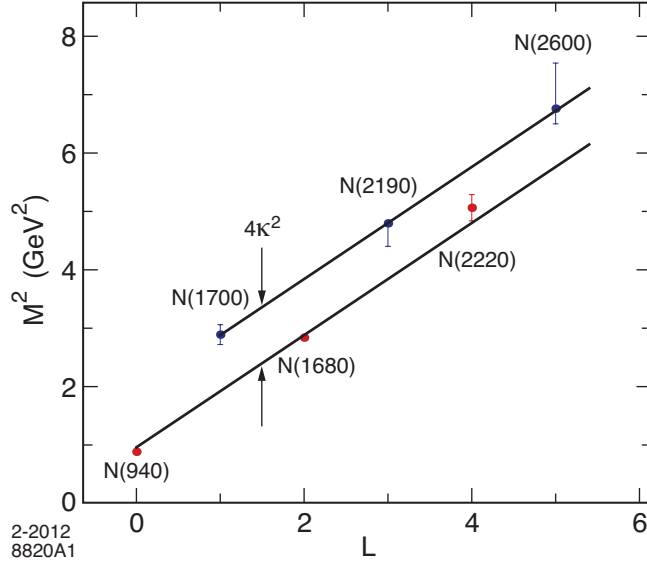


Figure 9: Spectrum gap between the negative-parity spin- $\frac{3}{2}$ nucleons and the spin- $\frac{1}{2}$ positive-parity nucleon families for $\kappa = 0.49$ GeV.

momentum are non-degenerate from the onset. Using (103) and (104) we find the relation

$$\frac{\mathcal{M}_{N(1535)}}{\mathcal{M}_{N(940)}} = \sqrt{\frac{5}{2}}, \quad (105)$$

which is consistent with experiment to a good accuracy. One can in fact also build the entire negative-parity excitation spectrum starting from the proton partner, the $J = 1/2$ negative-parity nucleon state $N(1535)$, using the same rules *e.g.*, an increase in mass \mathcal{M}^2 of $4\kappa^2$ for a unit change in the radial quantum number, $4\kappa^2$ for a change in one unit in the orbital quantum number and $2\kappa^2$ for a change of one unit of spin relative to the lowest negative-parity state, the $N(1535)$.

With the exception of the $\Delta(1930)$ state (which is not included in Table 2), all the confirmed baryon excitations are well described by formulas (103) and (104). If we follow the non- $SU(6)$ quantum number assignment for the $\Delta(1930)$ given in Ref. [130], namely $S = 3/2$, $L = 1$, $n = 1$ we find from (104) the value $\mathcal{M}_{\Delta(1930)} = 4\kappa \simeq 2$ GeV, consistent with the experimental result 1.96 GeV [49]. Expected results from new experiments are important to find out if new baryonic excitations follow the simple pattern described by Eqs. (103) and (104).

An important feature of light-front holography is that it predicts a similar multiplicity of states for mesons and baryons, consistent with what is observed experimentally [50]. This remarkable property could have a simple explanation in the cluster decomposition of the

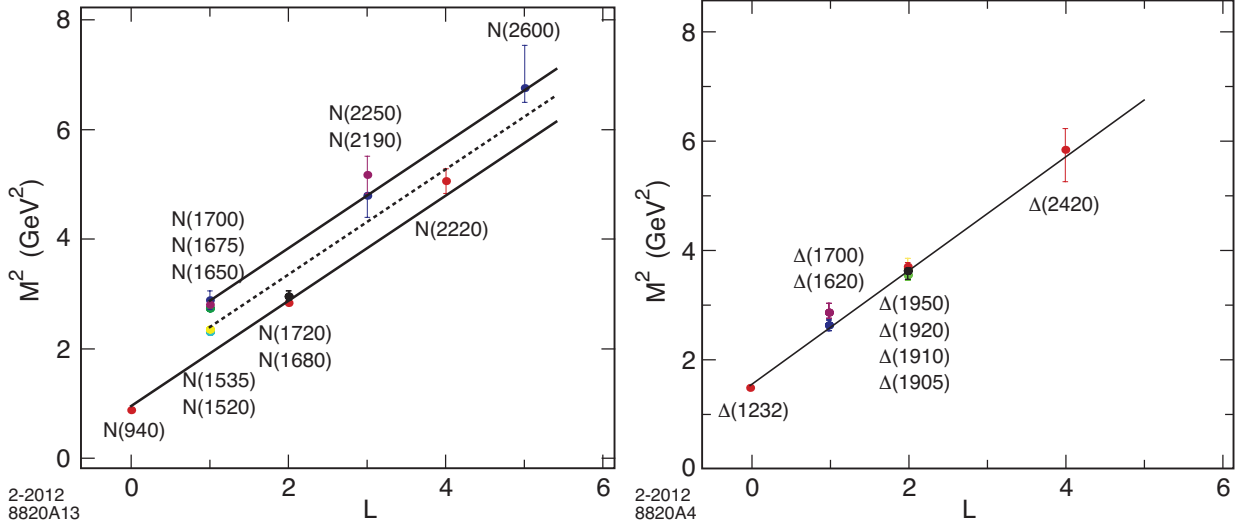


Figure 10: Baryon orbital trajectories for the N (left) and Δ families (right) for $n = 0$ and $\kappa = 0.49 - 0.51$ GeV. The lower and upper nucleon trajectories (left) correspond respectively to the the spin- $\frac{1}{2}$, positive-parity, and to the spin- $\frac{3}{2}$, negative-parity, families. The middle dotted trajectory (left) corresponds to spin- $\frac{1}{2}$ negative-parity nucleons. Plus and minus-parity states for the Δ states (right) are in the same Regge trajectory.

holographic variable, which labels a system of partons as an active quark plus a system of $n - 1$ spectators. From this perspective, a baryon with $n = 3$ looks in light-front holography as a quark-scalar-diquark system. It is also interesting to notice that in the hard wall model the proton mass is entirely due to the kinetic energy of the light quarks, whereas in the soft-wall model described here, half of the invariant mass squared \mathcal{M}^2 of the proton is due to the kinetic energy of the partons and half is due to the confinement potential.

6 Nucleon form factors

Proton and neutron electromagnetic form factors are among the most basic observables of the nucleon, and thus central for our understanding the nucleon's structure and dynamics. In general two form factors are required to describe the elastic scattering of electrons by spin- $\frac{1}{2}$ nucleons, the Dirac and Pauli form factors, F_1 and F_2

$$\langle P' | J^\mu(0) | P \rangle = u(P') \left[\gamma^\mu F_1(q^2) + \frac{i\sigma^{\mu\nu} q^\nu}{2\mathcal{M}} F_2(q^2) \right] u(P), \quad (106)$$

where $q = P' - P$. In the light-front formalism one can identify the Dirac and Pauli form factors from the LF spin-conserving and spin-flip current matrix elements of the J^+ cur-

rent [135].

On the higher dimensional gravity side the spin-non-flip amplitude for the EM transition corresponds to the non-local coupling of an external EM field $A^M(x, z)$ propagating in AdS with a fermionic mode $\Psi_P(x, z)$, given by the left-hand side of the equation below

$$\int d^4x dz \sqrt{g} \bar{\Psi}_{P'}(x, z) e_M^A \Gamma_A A^M(x, z) \Psi_P(x, z) \sim (2\pi)^4 \delta^4(P' - P - q) \epsilon_\mu u(P') \gamma^\mu F_1(q^2) u(P), \quad (107)$$

where $e_M^A = (\frac{R}{z}) \delta_M^A$ is the vielbein with curved space indices $M, N = 1, \dots, 5$ and tangent indices $A, B = 1, \dots, 5$. The expression on the right-hand side represents the Dirac EM form factor in physical space-time. It is the EM matrix element (106) of the local quark current $J^\mu = e_q \bar{q} \gamma^\mu q$ with local coupling to the constituents. In this case one can also show that a precise mapping of the J^+ elements can be carried out at fixed LF time, providing an exact correspondence between the holographic variable z and the LF impact variable ζ in ordinary space-time with the result [31]

$$G_\pm(Q^2) = g_\pm R^4 \int \frac{dz}{z^4} V(Q^2, z) \Psi_\pm^2(z), \quad (108)$$

for the components Ψ_+ and Ψ_- with angular momentum $L^z = 0$ and $L^z = +1$ respectively. The effective charges g_+ and g_- are determined from the spin-flavor structure of the theory.

A precise mapping for the Pauli form factor using light-front holographic methods has not been carried out. To study the spin-flip nucleon form factor F_2 using holographic methods, Abidin and Carlson [136] propose to introduce a non-minimal electromagnetic coupling with the ‘anomalous’ gauge invariant term

$$\int d^4x dz \sqrt{g} \bar{\Psi} e_M^A e_N^B [\Gamma_A, \Gamma_B] F^{MN} \Psi, \quad (109)$$

in the five-dimensional action, since the structure of (107) can only account for F_1 . Although this is a practical avenue, the overall strength of the new term has to be fixed by the static quantities and thus some predictivity is lost.

Light-front holographic QCD methods have also been used to obtain generalized parton distributions (GPDs) of the nucleon in the zero skewness limit in Refs. [137] and [138] for the soft and hard-wall models respectively. GPDs are nonperturbative, and thus holographic methods are well suited to explore their analytical structure.²⁴ In the sections below we discuss elastic and transition nucleon form factors using light-front holographic ideas.^{25 26}

²⁴See also the discussion in Ref. [139].

²⁵A study of the EM nucleon to Δ transition form factors has been carried out in the framework of the Sakai and Sugimoto model in Ref. [140].

²⁶LF holographic methods can also be used to study the flavor separation of the elastic nucleon form

6.1 Computing nucleon elastic form factors in light-front holographic QCD

In order to compute the individual features of the proton and neutron form factors one needs to incorporate the spin-flavor structure of the nucleons, properties which are absent in models of the gauge/gravity correspondence. The spin-isospin symmetry can be readily included in AdS/QCD by weighting the different Fock-state components by the charges and spin-projections of the quark constituents; e.g., as given by the $SU(6)$ spin-flavor symmetry. We label by $N_{q\uparrow}$ and $N_{q\downarrow}$ the probability to find the constituent q in a nucleon with spin up or down respectively. For the $SU(6)$ wave function we have

$$N_{u\uparrow} = \frac{5}{3}, \quad N_{u\downarrow} = \frac{1}{3}, \quad N_{d\uparrow} = \frac{1}{3}, \quad N_{d\downarrow} = \frac{2}{3}, \quad (110)$$

for the proton and

$$N_{u\uparrow} = \frac{1}{3}, \quad N_{u\downarrow} = \frac{2}{3}, \quad N_{d\uparrow} = \frac{5}{3}, \quad N_{d\downarrow} = \frac{1}{3}, \quad (111)$$

for the neutron. The effective charges g_+ and g_- in (108) are computed by the sum of the charges of the struck quark composed by the corresponding probability for the $L^z = 0$ and $L^z = +1$ components Ψ_+ and Ψ_- respectively. We find $g_p^+ = 1$, $g_p^- = 0$, $g_+^n = -\frac{1}{3}$ and $g_-^n = \frac{1}{3}$. The nucleon Dirac form factors in the $SU(6)$ limit are thus given by

$$F_1^p(Q^2) = R^4 \int \frac{dz}{z^4} V(Q^2, z) \Psi_+^2(z), \quad (112)$$

$$F_1^n(Q^2) = -\frac{1}{3} R^4 \int \frac{dz}{z^4} V(Q^2, z) [\Psi_+^2(z) - \Psi_-^2(z)], \quad (113)$$

where $F_1^p(0) = 1$ and $F_1^n(0) = 0$.

In the soft-wall model the plus and minus components of the twist-3 nucleon wave function are

$$\Psi_+(z) = \frac{\sqrt{2}\kappa^2}{R^2} z^{7/2} e^{-\kappa^2 z^2/2}, \quad \Psi_-(z) = \frac{\kappa^3}{R^2} z^{9/2} e^{-\kappa^2 z^2/2}, \quad (114)$$

and $V(Q^2, z)$ is given by (60). The results for $F_1^{p,n}$ follow from the analytic form (63) for any twist τ . We find

$$F_1^p(Q^2) = F_+(Q^2), \quad (115)$$

and

$$F_1^n(Q^2) = -\frac{1}{3} (F_+(Q^2) - F_-(Q^2)), \quad (116)$$

factors which have been determined recently up to $Q^2 = 3.4 \text{ GeV}^2$ [141]. This will be described elsewhere. See also Ref. [142].

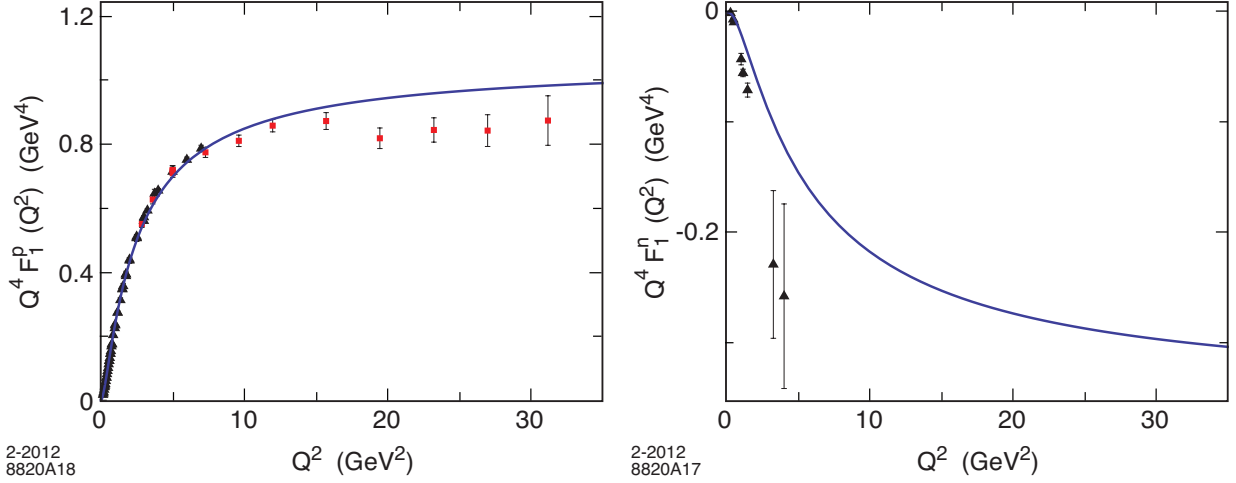


Figure 11: Predictions for $Q^4 F_1^p(Q^2)$ (left) and $Q^4 F_1^n(Q^2)$ (right) in the soft wall model. Data compilation from Diehl [143].

where we have, for convenience, defined the twist-2 and twist-3 form factors

$$F_+(Q^2) = \frac{1}{\left(1 + \frac{Q^2}{\mathcal{M}_\rho^2}\right)\left(1 + \frac{Q^2}{\mathcal{M}_{\rho'}^2}\right)}, \quad (117)$$

and

$$F_-(Q^2) = \frac{1}{\left(1 + \frac{Q^2}{\mathcal{M}_\rho^2}\right)\left(1 + \frac{Q^2}{\mathcal{M}_{\rho'}^2}\right)\left(1 + \frac{Q^2}{\mathcal{M}_{\rho''}^2}\right)}. \quad (118)$$

As discussed in Sec. 4.2, the multiple pole structure in (117) and (118) is derived from the dressed EM current propagating in AdS space.

The results for $Q^4 F_1^p(Q^2)$ and $Q^4 F_1^n(Q^2)$ are shown in Fig. 11. To compare with physical data we have shifted the poles in expression (63) to their physical values located at $M^2 = 4\kappa^2(n + 1/2)$ following the discussion in Sec. 4.4. The value $\kappa = 0.545$ GeV is determined from the ρ mass.

The expression for the elastic nucleon form factor $F_2^{p,n}$ follows from (106) and (109).

$$F_2^{p,n}(Q^2) \sim \int \frac{dz}{z^3} \Psi_+(z) V(Q^2, z) \Psi_-(z). \quad (119)$$

Using the twist-3 and twist-4 AdS soft-wall wavefunctions Ψ_+ and Ψ_- (114) we find

$$F_2^{p,n}(Q^2) = \chi_{p,n} F_-(Q^2), \quad (120)$$

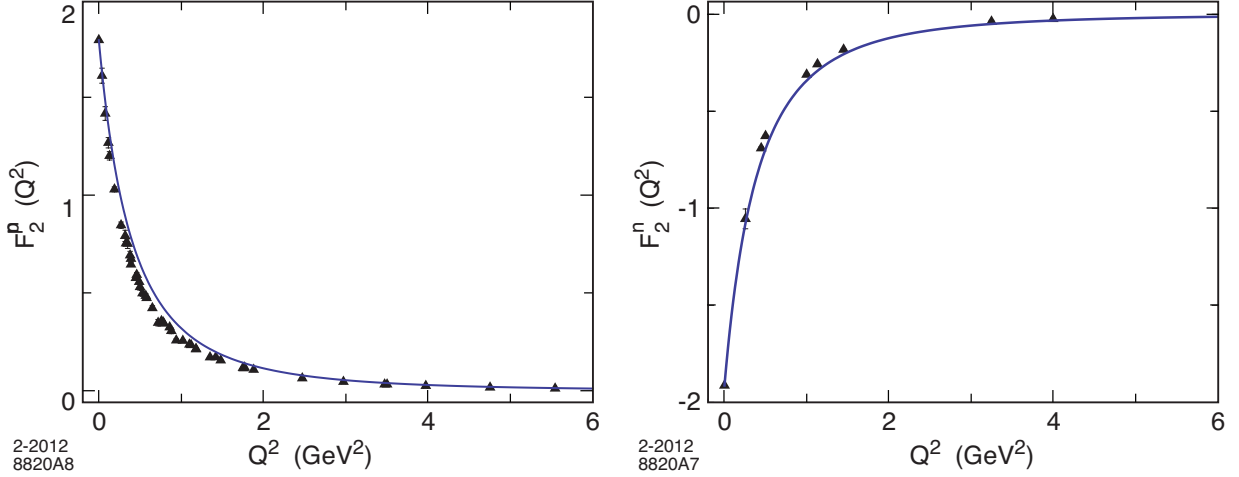


Figure 12: Predictions for $F_2^p(Q^2)$ (left) and $F_2^n(Q^2)$ (right) in the soft wall model. Data compilation from Diehl [143].

where the amplitude (119) has been normalized to the static quantities χ_p and χ_n and $F_-(Q^2)$ is given by (118). The experimental values $\chi_p = 1.793$ and $\chi_n = -1.913$ are consistent with the $SU(6)$ prediction [144] $\mu_P/\mu_N = -3/2$. In fact $(\mu_P/\mu_N)_{\text{exp}} = -1.46$ where $\mu_P = 1 + \chi_p$ and $\mu_N = \chi_n$. The results for $F_2^p(Q^2)$ and $F_2^n(Q^2)$ for $\kappa = 0.545$ GeV are shown in Fig. 12.

We compute the charge and magnetic root-mean-square (rms) radius from the usual electric and magnetic nucleon form factors

$$G_E(q^2) = F_1(q^2) + \frac{q^2}{4\mathcal{M}^2} F_2(q^2) \quad (121)$$

and

$$G_M(q^2) = F_1(q^2) + F_2(q^2). \quad (122)$$

Using the definition

$$\langle r^2 \rangle = -\frac{6}{F(0)} \frac{dF(Q^2)}{dQ^2} \Big|_{Q^2=0}, \quad (123)$$

we find the values $\sqrt{\langle r_E \rangle_p} = 0.802$ fm, $\sqrt{\langle r_M^2 \rangle_p} = 0.758$ fm, $\langle r_E^2 \rangle_n = -0.10$ fm² and $\sqrt{\langle r_M^2 \rangle_n} = 0.768$ fm, compared with the experimental values $\sqrt{\langle r_E \rangle_p} = (0.877 \pm 0.007)$ fm, $\sqrt{\langle r_M^2 \rangle_p} = (0.777 \pm 0.016)$ fm, $\langle r_E^2 \rangle_n = (-0.1161 \pm 0.0022)$ fm² and $\sqrt{\langle r_M^2 \rangle_n} = (0.862 \pm 0.009)$ fm from electron-proton scattering experiments [49].²⁷ The muonic hydrogen measurement gives $\sqrt{\langle r_E \rangle_p} = 0.84184(67)$ fm from Lamb-shift measurements [145].²⁸

²⁷The neutron charge radius is defined by $\langle r_E^2 \rangle_n = -6 \frac{dG_E(Q^2)}{dQ^2} \Big|_{Q^2=0}$.

²⁸Other soft and hard-wall model predictions of the nucleon rms radius are given in Refs. [136, 137, 138].

Chiral effective theory predicts that the slopes are singular for zero pion mass. For example, the slope of the Pauli form factor of the proton at $q^2 = 0$ computed by Beg and Zepeda diverges as $1/m_\pi$ [146]. This comes from the simple triangle diagram $\gamma^* \rightarrow \pi^+ \pi^- \rightarrow p \bar{p}$. One can also argue from dispersion theory that the singular behavior of the form factors as a function of the pion mass comes from the two-pion cut. Lattice theory computations of nucleon form factors require in fact the strong dependence at small pion mass to extrapolate the predictions to the physical pion mass [147]. The two-pion calculation [146] is a Born computation which probably does not exhibit vector dominance. To make a reliable computation in the hadronic basis of intermediate states one evidently has to include an infinite number of states. On the other hand, chiral divergences do not appear in AdS/QCD when we use the dressed current since, as shown in Sec. 4.2, the holographic analysis with a dressed EM current in AdS generates instead a nonperturbative multi-vector meson pole structure.²⁹

6.2 Computing nucleon transition form factors in light-front holographic QCD

As an illustrative example we consider in this section the form factor for the $\gamma^* p \rightarrow N(1440)P_{11}$ transition measured recently at JLab. We shall weight the different Fock-state components by the charges and spin-projections of the quark constituents using the $SU(6)$ spin-flavor symmetry as in the previous section. The expression for the spin non-flip proton form factors for the transition $n, L \rightarrow n' L$ is [31]

$$F_{1n,L \rightarrow n',L}^p(Q^2) = R^4 \int \frac{dz}{z^4} \Psi_+^{n',L}(z) V(Q^2, z) \Psi_+^{n,L}(z), \quad (124)$$

where we have factored out the plane wave dependence of the AdS fields

$$\Psi_+(z) = \frac{\kappa^{2+L}}{R^2} \sqrt{\frac{2n!}{(n+L+1)!}} z^{7/2+L} L_n^{L+1}(\kappa^2 z^2) e^{-\kappa^2 z^2/2}. \quad (125)$$

The orthonormality of the Laguerre polynomials in (125) implies that the nucleon form factor at $Q^2 = 0$ is one if $n = n'$ and zero otherwise. Using the integral representation of the bulk-to-boundary propagator $V(Q^2, z)$ given by (62) we find the twist-3 spin non-flip

²⁹In the limit of a free propagating current in AdS, we obtain logarithmic divergent results: $\langle r_p^2 \rangle_{F_1} = 3 \ln \left(\frac{4\kappa^2}{Q^2} \right) \Big|_{Q^2 \rightarrow 0}$ and $\langle r_p^2 \rangle_{F_2} = \frac{9}{2} \ln \left(\frac{4\kappa^2}{Q^2} \right) \Big|_{Q^2 \rightarrow 0}$.

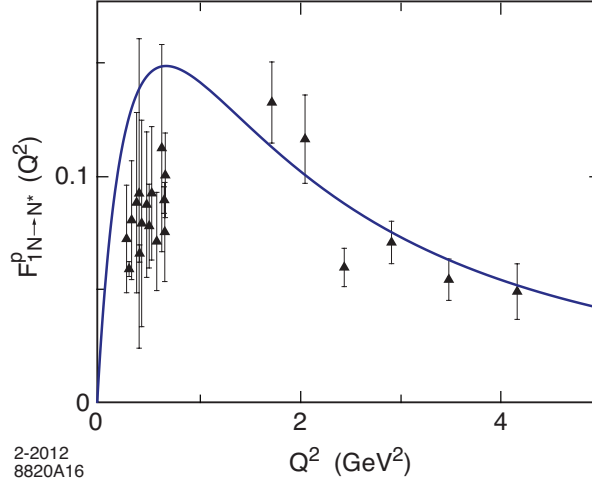


Figure 13: Proton transition form factor $F_{1N \rightarrow N^*}^p(Q^2)$ to the first radial excited state. Data from JLAB [148].

transition form factor

$$F_{1N \rightarrow N^*}^p(Q^2) = \frac{\sqrt{2}}{3} \frac{\frac{Q^2}{\mathcal{M}_\rho^2}}{\left(1 + \frac{Q^2}{\mathcal{M}_\rho^2}\right) \left(1 + \frac{Q^2}{\mathcal{M}_{\rho'}^2}\right) \left(1 + \frac{Q^2}{\mathcal{M}_{\rho''}^2}\right)}. \quad (126)$$

The result (126), compared with available data in Fig. 13, correspond to the valence approximation. The transition form factor (126) is expressed in terms of the mass of the ρ vector meson and its first two radial excited states, with no additional parameters. The results in Fig. 13 are in good agreement with experimental data. The transition to the $N(1440)P_{11}$ state corresponds to the first radial excitation of the three-quark ground state of the nucleon. In fact, the Roper resonance $N(1440)P_{11}$ and the $N(1710)P_{11}$ are well accounted in the light-front holographic framework as the first and second radial states of the nucleon family as shown in Sec. 5.2 (See Fig. 8). It is certainly worth to extend the simple computations described here and perform a systematic study of the different transition form factors measured at JLab. This study will help to discriminate among models and compare with the new results expected from the JLab 12 GeV Upgrade Project, in particular at photon virtualities $Q^2 > 5 \text{ GeV}^2$, which correspond to the experimental coverage of the CLAS12 detector at JLab [149].

7 Higher Fock components in light-front holographic QCD

The light-front Hamiltonian eigenvalue equation (7) is a matrix in Fock space which represents an infinite number of coupled integral equations for the Fock components $\psi_n = \langle n | \psi \rangle$. The resulting potential in quantum field theory can be considered as an instantaneous four-point effective interaction in LF time, similar to the instantaneous gluon exchange in the light-cone gauge $A^+ = 0$, which leads to $qq \rightarrow qq$, $q\bar{q} \rightarrow q\bar{q}$, $q \rightarrow qq\bar{q}$ and $\bar{q} \rightarrow \bar{q}q\bar{q}$ as in QCD(1+1). Higher Fock states can have any number of extra $q\bar{q}$ pairs, but surprisingly no dynamical gluons. Thus in holographic QCD, gluons are absent in the confinement potential.³⁰ This unusual property of AdS/QCD may explain the dominance of quark interchange [152] over quark annihilation or gluon exchange contributions in large angle elastic scattering [153].³¹

In order to illustrate the relevance of higher Fock states and the absence of dynamical gluons at the hadronic scale, we will discuss a simple semi-phenomenological model of the elastic form factor of the pion where we include the first two components in a Fock expansion of the pion wave function $|\pi\rangle = \psi_{q\bar{q}/\pi}|q\bar{q}\rangle_{\tau=2} + \psi_{q\bar{q}q\bar{q}}|q\bar{q}q\bar{q}\rangle_{\tau=4} + \dots$, where the $J^{PC} = 0^{-+}$ twist-two and twist-4 states $|q\bar{q}\rangle$ and $|q\bar{q}q\bar{q}\rangle$ are created by the interpolating operators $\bar{q}\gamma^+\gamma_5 q$ and $\bar{q}\gamma^+\gamma_5 q\bar{q}q$ respectively.

Since the charge form factor is a diagonal operator, the final expression for the form factor corresponding to the truncation up to twist four is the sum of two terms, a monopole and a three-pole term. In the strongly coupled semiclassical gauge/gravity limit hadrons have zero widths and are stable. One can nonetheless modify the formula (63) by introducing a finite width: $q^2 \rightarrow q^2 + \sqrt{2}i\mathcal{M}\Gamma$. We choose the values $\Gamma_\rho = 140$ MeV, $\Gamma_{\rho'} = 360$ MeV and $\Gamma_{\rho''} = 120$ MeV. The results for the pion form factor with twist two and four Fock states are shown in Fig. 14. The results correspond to $P_{q\bar{q}q\bar{q}} = 13$ %, the admixture of the $|q\bar{q}q\bar{q}\rangle$ state. The value of $P_{q\bar{q}q\bar{q}}$ (and the widths) are input in the model. The value of κ is determined from the ρ mass and the masses of the radial excitations follow from setting the poles at their physical locations, $\mathcal{M}^2 \rightarrow 4\kappa^2(n + 1/2)$, as discussed in Sec. 4.4. The time-like structure of the pion form factor displays a rich pole structure with constructive

³⁰This result is consistent with the flux-tube interpretation of QCD [150] where soft gluons interact so strongly that they are sublimated into a color confinement potential for quarks. The absence of constituent glue in hadronic physics has been invoked also in Ref. [151], where the role of the confining potential is attributed to an instanton induced interaction.

³¹In Ref. [154] we discuss a number of experimental results in hadron physics which support this picture.

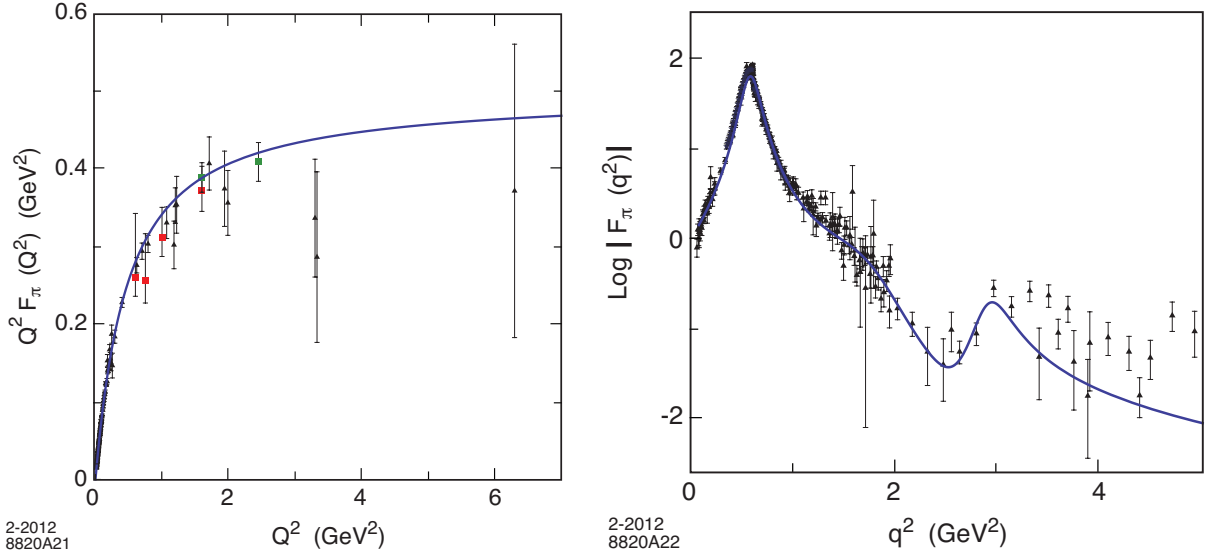


Figure 14: Structure of the space-like (left) and time-like (right) pion form factor in light-front holography for a truncation of the pion wave function up to twist four. Triangles are the data compilation from Baldini *et al.* [77], squares are JLAB data [78].

and destructive interfering phases; this is incompatible with the admixture of the twist-three state $|q\bar{q}g\rangle$ containing a dynamical gluon since the interference in this case is opposite in sign.

8 Conclusions

As we have shown, the exact light-front Hamiltonian $H_{LF}|\psi\rangle = \mathcal{M}^2|\psi\rangle$ for QCD can be systematically reduced to a relativistic frame-independent semiclassical wave equation [12]

$$\left(-\frac{d^2}{d\zeta^2} - \frac{1-4L^2}{4\zeta^2} + U(\zeta)\right)\phi(\zeta) = \mathcal{M}^2\phi(\zeta), \quad (127)$$

for the valence Fock state of mesons. The unmodified AdS equations correspond to the kinetic energy terms of the massless constituent quarks with relative orbital angular momentum $L = L^z$. The effective potential $U(\zeta)$ corresponds to the color-confining potential and follows from the truncation of AdS space, in a modified effective AdS action, and light-front holography. The variable ζ is the invariant separation of the constituents. This frame-independent light-front wave equation is comparable in simplicity to Schrödinger theory in atomic physics which is formulated at equal instant time. We have also derived an analogous light-front

Dirac equation for holographic QCD which describes light-quark baryons with finite color $N_C = 3$.

Remarkably, these light-front equations are equivalent to the equations of motion in a higher dimensional warped space asymptotic to AdS space. The mapping of the gravity theory to the boundary quantum field theory, quantized at fixed light-front time, thus gives a precise relation between holographic wave functions and the light-front wave functions which describe the internal structure of the hadrons and their electromagnetic couplings. This mapping provides the basis for a profound connection between physical QCD quantized in the light-front and the physics of hadronic modes in a higher dimensional AdS space. However, the derivation of the effective color-confining potential $U(\zeta)$ directly from QCD, remains an open question.

Despite some limitations of AdS/QCD [155], the light-front holographic approach to the gauge/gravity duality, *Light-Front Holography*, has already provided significant physical insight into the strongly-coupled nature and internal structure of hadrons; in fact, it is one of the few tools available. As we have seen, the resulting model provides a simple and successful framework for describing nonperturbative hadron dynamics: the systematics of the excitation spectrum of hadrons: the mass eigenspectrum, observed multiplicities and degeneracies. It also provides powerful new analytical tools for computing hadronic transition amplitudes, incorporating the scaling behavior and the transition from the hard-scattering perturbative domain, where quark and gluons are the relevant degrees of freedom, to the long range confining hadronic region.

The dressed current in AdS includes the nonperturbative pole structure. Consequently, the approach incorporates both the long-range confining hadronic domain and the constituent conformal short-distance quark particle limit in a single framework. The results display a simple analytical structure which allows us to explore dynamical properties in Minkowski space-time; in many cases these studies are not amenable to Euclidean lattice gauge theory computations. In particular, the excitation dynamics of nucleon resonances encoded in the nucleon transition form factors can provide fundamental insight into the strong-coupling dynamics of QCD. New theoretical tools are thus of primary interest for the interpretation of the results expected at the new mass scale and kinematic regions accessible to the JLab 12 GeV Upgrade Project.

The semiclassical approximation to light-front QCD described in this article is expected to break down at short distances where gluons become dynamical degrees of freedom and hard gluon exchange and quantum corrections become important. One can systematically improve the semiclassical approximation, for example, by introducing nonzero quark masses

and short-range Coulomb-like gluonic corrections, thus extending the predictions of the model to the dynamics and spectra of heavy and heavy-light quark systems. The model can also be improved by applying Lippmann-Schwinger methods to systematically improve the light-front Hamiltonian of the semiclassical holographic approximation. One can also use the holographic LFWFs as basis functions for diagonalizing the full light-front QCD Hamiltonian[156] as well as the input boundary functions to study the evolution of structure functions and distribution amplitudes at a low energy scale.

Acknowledgements

Invited lectures presented by GdT at the Niccolò Cabeo International School of Hadronic Physics, Ferrara, Italy, May 2011. GdT is grateful to the organizers and especially to Paola Ferretti Dalpiaz for her outstanding hospitality. We thank E. Klempt, V. E. Lyubovitskij and S. D. Glazek for helpful comments. We are grateful to F.-G. Cao, A. Deur, H. G. Dosch and J. Erlich for collaborations. This research was supported by the Department of Energy contract DE-AC02-76SF00515.

Appendices

A AdS boundary conditions and interpolating operators

The formal statement of the duality between a gravity theory on $(d + 1)$ -dimensional Anti-de Sitter AdS_{d+1} space and the strong coupling limit of a conformal field theory (CFT) on the d -dimensional asymptotic boundary of AdS_{d+1} at $z = 0$ is expressed in terms of the $d + 1$ partition function for a field $\Phi(x, z)$ propagating in the bulk

$$Z_{grav}[\Phi] = e^{iS_{eff}[\Phi]} = \int \mathcal{D}[\Phi] e^{iS[\Phi]}, \quad (128)$$

where S_{eff} is the effective action of the AdS_{d+1} theory, and the d -dimensional generating functional of correlation functions of the conformal field theory in presence of an external source $\Phi_0(x^\mu)$

$$Z_{CFT}[\Phi_0] = e^{iW_{CFT}[\Phi_0]} = \left\langle \exp \left(i \int d^d x \Phi_0(x) \mathcal{O}(x) \right) \right\rangle. \quad (129)$$

The functional W_{CFT} is the generator of connected Green's functions of the boundary theory and \mathcal{O} is a QCD local interpolating operator.

According to the AdS/CFT correspondence, to every operator in the conformal field theory there corresponds an AdS field. We use the isometries of AdS space to map the scaling dimensions of the local interpolating operators defined at the AdS boundary into the modes propagating inside AdS space. The precise relation of the gravity theory on AdS space to the conformal field theory at its boundary is [7]

$$Z_{grav}[\Phi(x, z)|_{z=0} = \Phi_0(x)] = Z_{CFT}[\Phi_0], \quad (130)$$

where the partition function (128) on AdS_{d+1} is integrated over all possible configurations Φ in the bulk which approach its boundary value Φ_0 . If we neglect the contributions from quantum fluctuations to the gravity partition function, then the generator W_{CFT} of connected Green's functions of the four-dimensional gauge theory (129) is precisely equal to the classical (on-shell) gravity action (128)

$$W_{CFT}[\phi_0] = S_{eff}[\Phi(x, z)|_{z=0} = \Phi_0(x)]_{\text{on-shell}}, \quad (131)$$

evaluated in terms of the classical solution to the bulk equation of motion. This defines the semiclassical approximation to the conformal field theory. In the bottom-up phenomenological approach, the effective action in the bulk is usually modified for large values of z to incorporate confinement and is truncated at the quadratic level.

In the limit $z \rightarrow 0$, the independent solutions behave as

$$\Phi(x, z) \rightarrow z^\tau \Phi_+(x) + z^{d-\tau} \Phi_-(x), \quad (132)$$

where τ is the scaling dimension. The non-normalizable solution Φ_- has the leading boundary behavior and is the boundary value of the bulk field Φ which couples to a QCD gauge invariant operator \mathcal{O} in the $z \rightarrow 0$ asymptotic boundary, thus $\Phi_- = \Phi_0$. The normalizable solution Φ_+ is the response function and corresponds to the physical states [157]. The interpolating operators \mathcal{O} of the boundary conformal theory are constructed from local gauge-invariant products of quark and gluon fields and their covariant derivatives, taken at the same point in four-dimensional space-time in the $x^2 \rightarrow 0$ limit. According to (129) the scaling dimensions of \mathcal{O} are matched to the conformal scaling behavior of the AdS fields in the limit $z \rightarrow 0$ and are thus encoded into the propagation of the modes inside AdS space.

Integrating by parts, and using the equation of motion for the field in AdS, the bulk contribution to the action vanishes, and one is left with a non-vanishing surface term in the ultraviolet boundary

$$S = R^{d-1} \lim_{z \rightarrow 0} \int d^d x \frac{1}{z^{d-1}} \Phi \partial_z \Phi, \quad (133)$$

which can be identified with the boundary QFT functional W_{CFT} . Substituting the leading dependence (132) of Φ near $z = 0$ in the ultraviolet surface action (133) and using the functional relation

$$\frac{\delta W_{CFT}}{\delta \Phi_0} = \frac{\delta S_{\text{eff}}}{\delta \Phi_0}, \quad (134)$$

one finds that $\Phi_+(x)$ is related to the expectation values of \mathcal{O} in the presence of the source Φ_0 [157]

$$\langle 0 | \mathcal{O}(x) | 0 \rangle_{\Phi_0} \sim \Phi_+(x). \quad (135)$$

The exact relation depends on the normalization of the fields chosen [158]. The field Φ_+ thus acts as a classical field, and it is the boundary limit of the normalizable string solution which propagates in the bulk.

References

- [1] K. G. Wilson, “Confinement of quarks,” *Phys. Rev. D* **10**, 2445 (1974).
- [2] J. M. Cornwall, “Dynamical mass generation in continuum QCD,” *Phys. Rev. D* **26**, 1453 (1982).
- [3] P. A. M. Dirac, “Forms of relativistic dynamics,” *Rev. Mod. Phys.* **21**, 392 (1949).
- [4] S. J. Brodsky, H. C. Pauli and S. S. Pinsky, “Quantum chromodynamics and other field theories on the light cone,” *Phys. Rept.* **301**, 299 (1998) [[arXiv:hep-ph/9705477](#)].
- [5] M. Burkardt, “Light front quantization,” *Adv. Nucl. Phys.* **23**, 1 (1996) [[arXiv:hep-ph/9505259](#)].
- [6] J. M. Maldacena, “The large N limit of superconformal field theories and supergravity,” *Int. J. Theor. Phys.* **38**, 1113 (1999) [[arXiv:hep-th/9711200](#)].
- [7] S. S. Gubser, I. R. Klebanov and A. M. Polyakov, “Gauge theory correlators from non-critical string theory,” *Phys. Lett. B* **428**, 105 (1998) [[arXiv:hep-th/9802109](#)].
- [8] E. Witten, “Anti-de Sitter space and holography,” *Adv. Theor. Math. Phys.* **2**, 253 (1998) [[arXiv:hep-th/9802150](#)].
- [9] J. Polchinski and M. J. Strassler, “Hard scattering and gauge/string duality,” *Phys. Rev. Lett.* **88**, 031601 (2002) [[arXiv:hep-th/0109174](#)].
- [10] S. J. Brodsky and G. R. Farrar, “Scaling laws at large transverse momentum,” *Phys. Rev. Lett.* **31**, 1153 (1973).
- [11] V. A. Matveev, R. M. Muradian and A. N. Tavkhelidze, “Automodellism in the large-angle elastic scattering and structure of hadrons,” *Lett. Nuovo Cim.* **7**, 719 (1973).
- [12] G. F. de Teramond and S. J. Brodsky, “Light-front holography: a first approximation to QCD,” *Phys. Rev. Lett.* **102**, 081601 (2009) [[arXiv:0809.4899](#) [[hep-ph](#)]].
- [13] S. J. Brodsky and G. F. de Teramond, “Hadronic spectra and light-front wavefunctions in holographic QCD,” *Phys. Rev. Lett.* **96**, 201601 (2006) [[arXiv:hep-ph/0602252](#)].
- [14] S. J. Brodsky and G. F. de Teramond, “Light-front dynamics and AdS/QCD correspondence: the pion form factor in the space- and time-like regions,” *Phys. Rev. D* **77**, 056007 (2008) [[arXiv:0707.3859](#) [[hep-ph](#)]].

- [15] J. Polchinski and M. J. Strassler, “Deep inelastic scattering and gauge/string duality,” *JHEP* **0305**, 012 (2003) [[arXiv:hep-th/0209211](#)].
- [16] S. D. Drell and T. M. Yan, “Connection of elastic electromagnetic nucleon form-factors at large Q^2 and deep inelastic structure functions near threshold,” *Phys. Rev. Lett.* **24**, 181 (1970).
- [17] G. B. West, “Phenomenological model for the electromagnetic structure of the proton,” *Phys. Rev. Lett.* **24**, 1206 (1970).
- [18] S. J. Brodsky and G. F. de Teramond, “Light-front dynamics and AdS/QCD correspondence: gravitational form factors of composite hadrons,” *Phys. Rev. D* **78**, 025032 (2008) [[arXiv:0804.0452](#) [[hep-ph](#)]].
- [19] Z. Abidin and C. E. Carlson, “Gravitational form factors of vector mesons in an AdS/QCD model,” *Phys. Rev. D* **77**, 095007 (2008) [[arXiv:0801.3839](#) [[hep-ph](#)]].
- [20] J. Erlich, E. Katz, D. T. Son and M. A. Stephanov, “QCD and a holographic model of hadrons,” *Phys. Rev. Lett.* **95**, 261602 (2005) [[arXiv:hep-ph/0501128](#)].
- [21] L. Da Rold and A. Pomarol, “Chiral symmetry breaking from five dimensional spaces,” *Nucl. Phys. B* **721**, 79 (2005) [[arXiv:hep-ph/0501218](#)].
- [22] S. J. Brodsky and G. F. de Teramond, “Light-front hadron dynamics and AdS/CFT correspondence,” *Phys. Lett. B* **582**, 211 (2004) [[arXiv:hep-th/0310227](#)].
- [23] A. Karch, E. Katz, D. T. Son and M. A. Stephanov, “Linear confinement and AdS/QCD,” *Phys. Rev. D* **74**, 015005 (2006) [[arXiv:hep-ph/0602229](#)].
- [24] M. Shifman, “Highly excited hadrons in QCD and beyond,” [arXiv:hep-ph/0507246](#).
- [25] S. D. Glazek and M. Schaden, “Gluon condensate induced confinement in mesons and baryons,” *Phys. Lett. B* **198**, 42 (1987).
- [26] S. J. Brodsky and R. Shrock, “Maximum wavelength of confined quarks and gluons and properties of quantum chromodynamics,” *Phys. Lett. B* **666**, 95 (2008) [[arXiv:0806.1535](#) [[hep-th](#)]].
- [27] H. C. Pauli, “On the effective Hamiltonian for QCD: An overview and status report,” *Nucl. Phys. Proc. Suppl.* **108**, 273 (2002) [[arXiv:hep-ph/0202179](#)].

- [28] G. 't Hooft, “A two-dimensional model for mesons,” *Nucl. Phys. B* **75**, 461 (1974).
- [29] E. Katz and T. Okui, “The 't Hooft model as a hologram,” *JHEP* **0901**, 113 (2009) [[arXiv:0710.3402](#) [[hep-th](#)]].
- [30] G. Parisi, “Conformal invariance in perturbation theory,” *Phys. Lett. B* **39**, 643 (1972).
- [31] S. J. Brodsky and G. F. de Teramond, “AdS/CFT and light-front QCD,” *World Scientific Subnuclear Series*, **45**, 139 (2007) [[arXiv:0802.0514](#) [[hep-ph](#)]].
- [32] S. J. Brodsky, H. G. Dosch and G. F. de Teramond *in preparation*.
- [33] T. Gutsche, V. E. Lyubovitskij, I. Schmidt, A. Vega, “Dilaton in a soft-wall holographic approach to mesons and baryons,” [arXiv:1108.0346](#) [[hep-ph](#)] (To appear in *Phys. Rev. D*).
- [34] C. Fronsdal, “Singletons and massless, integral spin fields on de Sitter space,” *Phys. Rev. D* **20**, 848 (1979).
- [35] E. S. Fradkin, M. A. Vasiliev, “Cubic interaction in extended theories of massless higher spin fields,” *Nucl. Phys. B* **291**, 141 (1987).
- [36] R. R. Metsaev, “Shadows, currents and AdS,” *Phys. Rev. D* **78**, 106010 (2008) [[arXiv:0805.3472](#) [[hep-th](#)]]; “Gauge invariant two-point vertices of shadow fields, AdS/CFT, and conformal fields,” *Phys. Rev. D* **81**, 106002 (2010) [[arXiv:0907.4678](#) [[hep-th](#)]]; “Gauge invariant approach to low-spin anomalous conformal currents and shadow fields,” *Phys. Rev. D* **83**, 106004 (2011) [[arXiv:1011.4261](#) [[hep-th](#)]].
- [37] G. F. de Teramond and S. J. Brodsky, “Gauge/Gravity duality and hadron physics at the light-front,” *AIP Conf. Proc.* **1296**, 128 (2010) [[arXiv:1006.2431](#) [[hep-ph](#)]].
- [38] J. Sonnenschein, “Stringy confining Wilson loops,” [arXiv:hep-th/0009146](#).
- [39] S. S. Afonin, “No-wall holographic model for QCD,” *Int. J. Mod. Phys. A* **26**, 3615 (2011) [[arXiv:1012.5065](#) [[hep-ph](#)]].
- [40] C. Csaki and M. Reece, “Toward a systematic holographic QCD: a braneless approach,” *JHEP* **0705**, 062 (2007) [[hep-ph/0608266](#)].

- [41] U. Gursoy, E. Kiritsis and F. Nitti, “Exploring improved holographic theories for QCD: Part II,” *JHEP* **0802**, 019 (2008) [[arXiv:0707.1349](#) [[hep-th](#)]].
- [42] W. de Paula, T. Frederico, H. Forkel and M. Beyer, “Dynamical AdS/QCD with area-law confinement and linear Regge trajectories,” *Phys. Rev. D* **79**, 075019 (2009) [[arXiv:0806.3830](#) [[hep-ph](#)]].
- [43] T. Gherghetta, J. I. Kapusta and T. M. Kelley, “Chiral symmetry breaking in the soft-wall AdS/QCD model,” *Phys. Rev. D* **79**, 076003 (2009) [[arXiv:0902.1998](#) [[hep-ph](#)]].
- [44] Z. Abidin, H. J. Kwee and J. A. Tan, “Asymptotic freedom in holographic QCD,” *JHEP* **1112**, 026 (2011) [[arXiv:1110.2037](#) [[hep-ph](#)]].
- [45] L. D. Landau and E. M. Lifshitz, *Quantum Mechanics*, Pergamon, New York, 1958, Sec. 35.
- [46] P. Breitenlohner and D. Z. Freedman, “Stability in gauged extended supergravity,” *Annals Phys.* **144**, 249 (1982).
- [47] See, for example: J. J. Dudek, R. G. Edwards, K. Orginos and D. G. Richards, “Lattice QCD and the Jefferson Lab program,” *J. Phys. Conf. Ser.* **299**, 012007 (2011).
- [48] A. Chodos, R. L. Jaffe, K. Johnson, C. B. Thorn and V. F. Weisskopf, “A new extended model of hadrons,” *Phys. Rev. D* **9**, 3471 (1974).
- [49] K. Nakamura *et al.* [Particle Data Group Collaboration], “Review of particle physics,” *J. Phys. GG* **37**, 075021 (2010).
- [50] E. Klempt and A. Zaitsev, “Glueballs, hybrids, multiquarks. Experimental facts versus QCD inspired concepts,” *Phys. Rept.* **454**, 1 (2007) [[arXiv:0708.4016](#) [[hep-ph](#)]].
- [51] G. F. de Teramond, S. J. Brodsky, “Hadronic spectrum of a holographic dual of QCD,” *Phys. Rev. Lett.* **94**, 201601 (2005) [[hep-th/0501022](#)].
- [52] I. R. Klebanov and J. M. Maldacena, “Solving quantum field theories via curved space-times,” *Phys. Today* **62**, 28 (2009).
- [53] O. Andreev, “ $1/q^2$ corrections and gauge/string duality,” *Phys. Rev. D* **73**, 107901 (2006) [[hep-th/0603170](#)]; O. Andreev and V. I. Zakharov, “Heavy-quark potentials and AdS/QCD,” *Phys. Rev. D* **74**, 025023 (2006) [[arXiv:hep-ph/0604204](#)].

- [54] G. F. de Teramond and S. J. Brodsky, “Light-front holography and gauge/gravity duality: the light meson and baryon spectra,” *Nucl. Phys. B, Proc. Suppl.* **199**, 89 (2010) [[arXiv:0909.3900](#) [[hep-ph](#)]]
- [55] H. Boschi-Filho, N. R. F. Braga and H. L. Carrion, “Glueball Regge trajectories from gauge/string duality and the Pomeron,” *Phys. Rev. D* **73**, 047901 (2006) [[arXiv:hep-th/0507063](#)].
- [56] N. Evans and A. Tedder, “Perfecting the ultra-violet of holographic descriptions of QCD,” *Phys. Lett. B* **642**, 546 (2006) [[arXiv:hep-ph/0609112](#)].
- [57] D. K. Hong, T. Inami and H. U. Yee, “Baryons in AdS/QCD,” *Phys. Lett. B* **646**, 165 (2007) [[arXiv:hep-ph/0609270](#)].
- [58] P. Colangelo, F. De Fazio, F. Jugeau and S. Nicotri, “On the light glueball spectrum in a holographic description of QCD,” *Phys. Lett. B* **652**, 73 (2007) [[arXiv:hep-ph/0703316](#)].
- [59] H. Forkel, M. Beyer, T. Frederico, “Linear square-mass trajectories of radially and orbitally excited hadrons in holographic QCD,” *JHEP* **0707**, 077 (2007) [[arXiv:0705.1857](#) [[hep-ph](#)]].
- [60] H. Forkel, “Holographic glueball structure,” *Phys. Rev. D* **78**, 025001 (2008) [[arXiv:0711.1179](#) [[hep-ph](#)]].
- [61] A. Vega and I. Schmidt, “Scalar hadrons in $AdS_5 \times S^5$,” *Phys. Rev. D* **78**, 017703 (2008) [[arXiv:0806.2267](#) [[hep-ph](#)]].
- [62] K. Nawa, H. Suganuma and T. Kojo, “Baryons with holography,” *Mod. Phys. Lett. A* **23**, 2364 (2008) [[arXiv:0806.3040](#) [[hep-th](#)]].
- [63] P. Colangelo, F. De Fazio, F. Giannuzzi, F. Jugeau and S. Nicotri, “Light scalar mesons in the soft-wall model of AdS/QCD,” *Phys. Rev. D* **78**, 055009 (2008) [[arXiv:0807.1054](#) [[hep-ph](#)]].
- [64] H. Forkel and E. Klempt, “Diquark correlations in baryon spectroscopy and holographic QCD,” *Phys. Lett. B* **679**, 77 (2009) [[arXiv:0810.2959](#) [[hep-ph](#)]].
- [65] H. C. Ahn, D. K. Hong, C. Park and S. Siwach, “Spin 3/2 baryons and form factors in AdS/QCD,” *Phys. Rev. D* **80**, 054001 (2009) [[arXiv:0904.3731](#) [[hep-ph](#)]].

- [66] Y. -Q. Sui, Y. -L. Wu, Z. -F. Xie and Y. -B. Yang, “Prediction for the mass spectra of resonance mesons in the soft-wall AdS/QCD with a modified 5D metric,” *Phys. Rev. D* **81**, 014024 (2010) [[arXiv:0909.3887 \[hep-ph\]](#)].
- [67] J. I. Kapusta and T. Springer, “Potentials for soft wall AdS/QCD,” *Phys. Rev. D* **81**, 086009 (2010) [[arXiv:1001.4799 \[hep-ph\]](#)].
- [68] P. Zhang, “Improving the excited nucleon spectrum in hard-wall AdS/QCD,” *Phys. Rev. D* **81**, 114029 (2010) [[arXiv:1002.4352 \[hep-ph\]](#)]; “Mesons and nucleons in soft-wall AdS/QCD,” *Phys. Rev. D* **82**, 094013 (2010) [[arXiv:1007.2163 \[hep-ph\]](#)].
- [69] I. Iatrakis, E. Kiritsis and A. Paredes, “An AdS/QCD model from Sen’s tachyon action,” *Phys. Rev. D* **81**, 115004 (2010) [[arXiv:1003.2377 \[hep-ph\]](#)].
- [70] T. Branz, T. Gutsche, V. E. Lyubovitskij, I. Schmidt and A. Vega, “Light and heavy mesons in a soft-wall holographic approach,” *Phys. Rev. D* **82**, 074022 (2010) [[arXiv:1008.0268 \[hep-ph\]](#)].
- [71] M. Kirchbach, C. B. Compean, “Conformal symmetry and light flavor baryon spectra,” *Phys. Rev. D* **82**, 034008 (2010) [[arXiv:1003.1747 \[hep-ph\]](#)].
- [72] Y. -Q. Sui, Y. -L. Wu and Y. -B. Yang, “Predictive AdS/QCD model for mass spectra of mesons with three flavors,” *Phys. Rev. D* **83**, 065030 (2011) [[arXiv:1012.3518 \[hep-ph\]](#)].
- [73] J. Erlich, “How well does AdS/QCD describe QCD?,” *Int. J. Mod. Phys. A* **25**, 411 (2010) [[arXiv:0908.0312 \[hep-ph\]](#)].
- [74] Y. Kim and D. Yi, “Holography at work for nuclear and hadron physics,” *Adv. High Energy Phys.* **2011**, 259025 (2011) [[arXiv:1107.0155 \[hep-ph\]](#)].
- [75] D. E. Soper, “The parton model and the Bethe-Salpeter wave function,” *Phys. Rev. D* **15**, 1141 (1977).
- [76] G. F. de Teramond, S. J. Brodsky, “Light-front quantization and AdS/QCD: an overview,” *J. Phys. Conf. Ser.* **287**, 012007 (2011) [[arXiv:1103.1100 \[hep-ph\]](#)].
- [77] R. Baldini *et al.*, “Nucleon time-like form factors below the N anti-N threshold,” *Eur. Phys. J. C* **11**, 709 (1999).

- [78] V. Tadevosyan *et al.*, [Jefferson Lab F_π Collaboration], “Determination of the pion charge form factor for $Q^2=0.60\text{--}1.60$ GeV²,” *Phys. Rev. C* **75**, 055205 (2007) [[arXiv:nucl-ex/0607007](#)]; T. Horn *et al.*, [Jefferson Lab F_π Collaboration], “Determination of the charged pion form factor at $Q^2 = 1.60$ and 2.45 (GeV/c)²,” *Phys. Rev. Lett.* **97**, 192001 (2006) [[arXiv:nucl-ex/0607005](#)].
- [79] H. R. Grigoryan, A. V. Radyushkin, “Structure of vector mesons in holographic model with linear confinement,” *Phys. Rev. D* **76**, 095007 (2007) [[arXiv:0706.1543](#) [[hep-ph](#)]].
- [80] H. J. Kwee and R. F. Lebed, “Pion form-factors in holographic QCD,” *JHEP* **0801**, 027 (2008) [[arXiv:0708.4054](#) [[hep-ph](#)]]. See also: H. J. Kwee and R. F. Lebed, “Pion form factor in improved holographic QCD backgrounds,” *Phys. Rev. D* **77**, 115007 (2008) [[arXiv:0712.1811](#) [[hep-ph](#)]].
- [81] H. R. Grigoryan and A. V. Radyushkin, “Pion form-factor in chiral limit of hard-wall AdS/QCD model,” *Phys. Rev. D* **76**, 115007 (2007) [[arXiv:0709.0500](#) [[hep-ph](#)]].
- [82] F. Zuo, “Improved soft-wall model with a negative dilaton,” *Phys. Rev. D* **82**, 086011 (2010) [[arXiv:0909.4240](#) [[hep-ph](#)]].
- [83] S. Nicotri, “Phenomenology of the holographic soft-wall model of QCD with ‘reversed’ dilaton,” *AIP Conf. Proc.* **1317**, 322 (2011) [[arXiv:1009.4829](#) [[hep-ph](#)]].
- [84] A. Karch, E. Katz, D. T. Son and M. A. Stephanov, “On the sign of the dilaton in the soft wall models,” *JHEP* **1104**, 066 (2011) [[arXiv:1012.4813](#) [[hep-ph](#)]].
- [85] G. F. de Teramond and S. J. Brodsky, “Excited baryons in holographic QCD,” [arXiv:1108.0965](#) [[hep-ph](#)].
- [86] S. J. Brodsky, F.-G. Cao and G. F. de Teramond, “Evolved QCD predictions for the meson-photon transition form factors,” *Phys. Rev. D* **84**, 033001 (2011) [[arXiv:1104.3364](#) [[hep-ph](#)]].
- [87] S. J. Brodsky, F.-G. Cao and G. F. de Teramond, “Meson transition form factors in light-front holographic QCD,” *Phys. Rev. D* **84**, 075012 (2011) [[arXiv:1105.3999](#) [[hep-ph](#)]].
- [88] G. P. Lepage and S. J. Brodsky, “Exclusive processes in perturbative quantum chromodynamics,” *Phys. Rev. D* **22**, 2157 (1980).

- [89] B. Aubert *et al.* [The BABAR Collaboration], “Measurement of the $\gamma\gamma^* \rightarrow \pi^0$ transition form factor,” *Phys. Rev.* **D80**, 052002 (2009) [[arXiv:0905.4778 \[hep-ex\]](#)].
- [90] P. A. Sanchez *et al.* [The BABAR Collaboration], “Measurement of the $\gamma\gamma^* \rightarrow \eta$ and $\gamma\gamma^* \rightarrow \eta'$ transition form factors,” [arXiv:1101.1142 \[hep-ex\]](#).
- [91] V. P. Druzhinin *et al.* [The BABAR Collaboration], “Recent BABAR results on two-photon physics,” *PoS ICHEP*, 144 (2010) [[arXiv:1011.6159 \[hep-ex\]](#)].
- [92] H.-J. Behrend *et al.* [CELLO Collaboration], “A measurement of the π^0 , η and η' electromagnetic form-factors,” *Z. Phys. C* **49**, 401 (1991).
- [93] J. Gronberg *et al.* [CLEO Collaboration], “Measurements of the meson-photon transition form factors of light pseudoscalar mesons at large momentum transfer,” *Phys. Rev. D* **57**, 33 (1998) [[arXiv:hep-ex/9707031](#)].
- [94] H.-N. Li and S. Mishima, “Pion transition form factor in k_T factorization,” *Phys. Rev. D* **80**, 074024 (2009) [[arXiv:0907.0166 \[hep-ph\]](#)].
- [95] S. V. Mikhailov and N. G. Stefanis, “Pion transition form factor at the two-loop level vis-a-vis experimental data,” *Mod. Phys. Lett. A* **24**, 2858 (2009) [[arXiv:0910.3498 \[hep-ph\]](#)].
- [96] X.-G. Wu and T. Huang, “An implication on the pion distribution amplitude from the pion-photon transition form factor with the new BABAR data,” *Phys. Rev. D* **82**, 034024 (2010) [[arXiv:1005.3359 \[hep-ph\]](#)].
- [97] H. L. L. Roberts, C. D. Roberts, A. Bashir, L. X. Gutierrez-Guerrero, and P. C. Tandy, “Abelian anomaly and neutral pion production,” *Phys. Rev. C* **82**, 065202 (2010) [[arXiv:1009.0067 \[nucl-th\]](#)].
- [98] W. Broniowski and E. R. Arriola, “Pion transition form factor in the Regge approach,” *PoS LC2010*, 062 (2010) [[arXiv:1008.2317 \[hep-ph\]](#)].
- [99] P. Kroll, “The form factors for the photon to pseudoscalar meson transitions - an update” [arXiv:1012.3542 \[hep-ph\]](#).
- [100] M. Gorchtein, P. Guo, and A. P. Szczepaniak, “Pion form factors” [arXiv:1102.5558 \[nucl-th\]](#).

- [101] A. E. Dorokhov, “Photon-pion transition form factor: BABAR puzzle is cracked,” [arXiv:1003.4693 \[hep-ph\]](#); “Photon-pion transition form factor at high photon virtualities within the nonlocal chiral quark model,” *JETP Lett.* **92** 707 (2010).
- [102] S. S. Agaev, V. M. Braun, N. Offen, and F. A. Porkert, “Light cone sum rules for the $\pi^0\gamma^*\gamma$ form factor revisited,” *Phys. Rev. D* **83**, 054020 (2011) [[arXiv:1012.4671 \[hep-ph\]](#)].
- [103] A. P. Bakulev, S. V. Mikhailov, A. V. Pimikov, and N. G. Stefanis “Pion-photon transition – the new QCD frontier,” *Phys. Rev. D* **84**, 034014 (2011) [[arXiv:1105.2753 \[hep-ph\]](#)].
- [104] Y. N. Klopot, A. G. Oganesian and O. V. Teryaev, “Axial anomaly and mixing: from real to highly virtual photons,” *Phys. Rev. D* **84**, 051901 (2011) [[arXiv:1106.3855 \[hep-ph\]](#)].
- [105] X. -G. Wu and T. Huang, “Constraints on the light pseudoscalar meson distribution amplitudes from their meson-photon transition form factors,” *Phys. Rev. D* **84**, 074011 (2011) [[arXiv:1106.4365 \[hep-ph\]](#)].
- [106] S. Noguera and S. Scopetta, “Eta-photon transition form factor,” *Phys. Rev. D* **85**, 054004 (2012) [[arXiv:1110.6402 \[hep-ph\]](#)].
- [107] I. Balakireva, W. Lucha and D. Melikhov, “Pion elastic and $(\pi^0, \eta, \eta') \rightarrow \gamma\gamma^*$ transition form factors in a broad range of momentum transfers,” *Phys. Rev. D* **85**, 036006 (2012) [[arXiv:1110.6904 \[hep-ph\]](#)]; “Elastic and transition form factors of light pseudoscalar mesons from QCD sum rules,” [arXiv:1203.2599 \[hep-ph\]](#).
- [108] D. McKeen, M. Pospelov and J. M. Roney, “Pion-photon transition form factor and new physics in the τ sector,” *Phys. Rev. D* **85**, 053002 (2012) [[arXiv:1112.2207 \[hep-ph\]](#)].
- [109] C. -C. Lih and C. -Q. Geng, “ $\pi^0 \rightarrow \gamma^*\gamma$ transition form factor within the light-front quark model,” *Phys. Rev. C* **85**, 018201 (2012) [[arXiv:1201.2220 \[hep-ph\]](#)].
- [110] H. Czyz, S. Ivashyn, A. Korchin and O. Shekhovtsova, “Two-photon form factors of the π^0, η and η' mesons in the chiral theory with resonances,” [arXiv:1202.1171 \[hep-ph\]](#).
- [111] A. Pomarol, A. Wulzer, “Baryon physics in holographic QCD,” *Nucl. Phys.* **B809**, 347-361 (2009) [[arXiv:0807.0316 \[hep-ph\]](#)].

- [112] H. R. Grigoryan, A. V. Radyushkin, “Anomalous form factor of the neutral pion in extended AdS/QCD model with Chern-Simons term,” *Phys. Rev.* **D77**, 115024 (2008) [[arXiv:0803.1143](#) [[hep-ph](#)]].
- [113] H. R. Grigoryan and A. V. Radyushkin, “Pion in the Holographic Model with 5D Yang-Mills Fields,” *Phys. Rev. D* **78**, 115008 (2008) [[arXiv:0808.1243](#) [[hep-ph](#)]].
- [114] F. Zuo, Y. Jia, T. Huang, “ $\gamma^* \rho^0 \rightarrow \pi^0$ transition form factor in extended AdS/QCD models,” *Eur. Phys. J.* **C67**, 253-261 (2010) [[arXiv:0910.3990](#) [[hep-ph](#)]].
- [115] T. Sakai, S. Sugimoto, “More on a holographic dual of QCD,” *Prog. Theor. Phys.* **114**, 1083-1118 (2005) [[arXiv:hep-th/0507073](#)].
- [116] C. T. Hill, C. K. Zachos, “Dimensional deconstruction and Wess-Zumino-Witten terms,” *Phys. Rev.* **D71**, 046002 (2005) [[arXiv:hep-th/0411157](#)].
- [117] I. V. Musatov, A. V. Radyushkin, “Transverse momentum and Sudakov effects in exclusive QCD processes: $\gamma^* \gamma \pi^0$ form factor,” *Phys. Rev.* **D56**, 2713 (1997) [[arXiv:hep-ph/9702443](#)].
- [118] See, for example: R. G. Edwards, J. J. Dudek, D. G. Richards and S. J. Wallace, “Excited state baryon spectroscopy from lattice QCD,” *Phys. Rev. D* **84**, 074508 (2011) [[arXiv:1104.5152](#) [[hep-ph](#)]].
- [119] M. Henningson and K. Sfetsos, “Spinors and the AdS / CFT correspondence,” *Phys. Lett. B* **431**, 63 (1998) [[arXiv:hep-th/9803251](#)].
- [120] W. Mueck and K. S. Viswanathan, “Conformal field theory correlators from classical field theory on anti-de Sitter space. 2. Vector and spinor fields,” *Phys. Rev. D* **58**, 106006 (1998) [[arXiv:hep-th/9805145](#)].
- [121] G. F. de Teramond, S. J. Brodsky, “Light-front quantization approach to the gauge-gravity correspondence and hadron spectroscopy,” *AIP Conf. Proc.* **1257**, 59 (2010) [[arXiv:1001.5193](#) [[hep-ph](#)]]; S. J. Brodsky and G. F. de Teramond, “AdS/CFT and light-front QCD,” *World Scientific Subnuclear Series*, **45**, 139 (2007) [[arXiv:0802.0514](#) [[hep-ph](#)]].
- [122] A. Volovich, “Rarita-Schwinger field in the AdS / CFT correspondence,” *JHEP* **9809**, 022 (1998) [[arXiv:hep-th/9809009](#)].

- [123] P. Matlock and K. S. Viswanathan, “The AdS / CFT correspondence for the massive Rarita-Schwinger field,” *Phys. Rev. D* **61**, 026002 (2000) [[arXiv:hep-th/9906077](#)].
- [124] E. Witten, “Baryons and branes in anti-de Sitter space,” *JHEP* **9807**, 006 (1998) [[arXiv:hep-th/9805112](#)].
- [125] D. J. Gross and H. Ooguri, “Aspects of large N gauge theory dynamics as seen by string theory,” *Phys. Rev. D* **58**, 106002 (1998) [[arXiv:hep-th/9805129](#)].
- [126] D. K. Hong, M. Rho, H. -U. Yee and P. Yi, “Chiral dynamics of baryons from string theory,” *Phys. Rev. D* **76**, 061901 (2007) [[arXiv:hep-th/0701276](#)].
- [127] H. Hata, T. Sakai, S. Sugimoto and S. Yamato, “Baryons from instantons in holographic QCD,” *Prog. Theor. Phys.* **117**, 1157 (2007) [[arXiv:hep-th/0701280](#)].
- [128] S. J. Brodsky and G. F. de Teramond, “Applications of AdS/QCD and light-front holography to baryon physics,” *AIP Conf. Proc.* **1388**, 22 (2011) [[arXiv:1103.1186](#) [[hep-ph](#)]].
- [129] A. V. Anisovich, R. Beck, E. Klempt, V. A. Nikonov, A. V. Sarantsev and U. Thoma, “Properties of baryon resonances from a multichannel partial wave analysis,” [arXiv:1112.4937](#) [[hep-ph](#)].
- [130] E. Klempt and J. M. Richard, “Baryon spectroscopy,” *Rev. Mod. Phys.* **82**, 1095 (2010) [[arXiv:0901.205](#) [[hep-ph](#)]].
- [131] F. Wilczek, “Diquarks as inspiration and as objects,” [arXiv:hep-ph/0409168](#); A. Selem and F. Wilczek, “Hadron systematics and emergent diquarks,” [arXiv:hep-ph/0602128](#).
- [132] I. Kirsch, “Spectroscopy of fermionic operators in AdS/CFT,” *JHEP* **0609**, 052 (2006) [[arXiv:hep-th/0607205](#)].
- [133] H. G. Dosch, “A practical guide to AdS/CFT,” Lectures given at the School of Physics and Technology, Wuhan University, March-April (2009), <http://www.thphys.uni-heidelberg.de/~dosch/wuhantot.pdf>.
- [134] E. Klempt, “Is chiral symmetry broken and or restored in high-mass light baryons?,” [arXiv:1011.3644](#) [[hep-ph](#)].

- [135] S. J. Brodsky and S. D. Drell, “The anomalous magnetic moment and limits on fermion substructure,” *Phys. Rev. D* **22**, 2236 (1980).
- [136] Z. Abidin, C. E. Carlson, “Nucleon electromagnetic and gravitational form factors from holography,” *Phys. Rev. D* **79**, 115003 (2009) [[arXiv:0903.4818 \[hep-ph\]](#)].
- [137] A. Vega, I. Schmidt, T. Gutsche, V. E. Lyubovitskij, “Generalized parton distributions in AdS/QCD,” *Phys. Rev. D* **83**, 036001 (2011) [[arXiv:1010.2815 \[hep-ph\]](#)].
- [138] A. Vega, I. Schmidt, T. Gutsche and V. E. Lyubovitskij, “Generalized parton distributions in an AdS/QCD hard-wall model,” [arXiv:1202.4806 \[hep-ph\]](#).
- [139] R. Nishio, T. Watari, “Investigating generalized parton distribution in gravity dual,” [arXiv:1105.2907 \[hep-ph\]](#).
- [140] H. R. Grigoryan, T.-S. H. Lee, H.-U. Yee, “Electromagnetic nucleon-to-delta transition in holographic QCD,” *Phys. Rev. D* **80**, 055006 (2009) [[arXiv:0904.3710 \[hep-ph\]](#)].
- [141] G. D. Cates, C. W. de Jager, S. Riordan and B. Wojtsekhowski, “Flavor decomposition of the elastic nucleon electromagnetic form factors,” *Phys. Rev. Lett.* **106**, 252003 (2011) [[arXiv:1103.1808 \[nucl-ex\]](#)].
- [142] M. Rohrmoser, K. -S. Choi and W. Plessas, “Flavor analysis of nucleon electromagnetic form factors,” [arXiv:1110.3665 \[hep-ph\]](#).
- [143] M. Diehl, “Generalized parton distributions from form factors,” *Nucl. Phys. Proc. Suppl.* **161**, 49 (2006) [[arXiv:hep-ph/0510221](#)].
- [144] M. A. B. Beg, B. W. Lee and A. Pais, “SU(6) and electromagnetic interactions,” *Phys. Rev. Lett.* **13**, 514 (1964).
- [145] R. Pohl, A. Antognini, F. Nez *et al.*, “The size of the proton,” *Nature* **466**, 213 (2010).
- [146] M. A. B. Beg and A. Zepeda, “Pion radius and isovector nucleon radii in the limit of small pion mass,” *Phys. Rev. D* **6**, 2912 (1972).
- [147] S. Collins, M. Gockeler, P. Hagler *et al.*, “Dirac and Pauli form factors from lattice QCD,” *Phys. Rev. D* **84**, 074507 (2011) [[arXiv:1106.3580 \[hep-lat\]](#)].
- [148] I. G. Aznauryan *et al.* [CLAS Collaboration], “Electroexcitation of nucleon resonances from CLAS data on single pion electroproduction,” *Phys. Rev. C* **80**, 055203 (2009) [[arXiv:0909.2349 \[nucl-ex\]](#)].

- [149] I. G. Aznauryan and V. D. Burkert, “Electroexcitation of nucleon resonances,” *Prog. Part. Nucl. Phys.* **67**, 1 (2012) [[arXiv:1109.1720 \[hep-ph\]](#)].
- [150] N. Isgur and J. E. Paton, “A flux tube model for hadrons in QCD,” *Phys. Rev. D* **31**, 2910 (1985).
- [151] E. Klempt, “Hadron spectroscopy without constituent glue,” *Int. J. Mod. Phys. A* **20**, 1720 (2005) [[arXiv:hep-ph/0409164](#)].
- [152] J. F. Gunion, S. J. Brodsky, R. Blankenbecler, “Composite theory of inclusive scattering at large transverse momenta,” *Phys. Rev.* **D6**, 2652 (1972).
- [153] B. R. Baller, G. C. Blazey, H. Courant *et al.*, “Comparison of exclusive reactions at Large t ,” *Phys. Rev. Lett.* **60**, 1118 (1988).
- [154] S. J. Brodsky and G. F. de Teramond, “AdS/QCD, Light-Front Holography, and Sublimated Gluons,” *PoS QCD -TNT-II*, 008 (2011) [[arXiv:1112.4212 \[hep-th\]](#)].
- [155] C. Csaki, M. Reece and J. Terning, “The AdS/QCD correspondence: still undelivered,” *JHEP* **0905**, 067 (2009) [[arXiv:0811.3001 \[hep-ph\]](#)].
- [156] J. P. Vary, H. Honkanen, J. Li, P. Maris, S. J. Brodsky, A. Harindranath, G. F. de Teramond, P. Sternberg *et al.*, “Hamiltonian light-front field theory in a basis function approach,” *Phys. Rev. C* **81**, 035205 (2010) [[arXiv:0905.1411 \[nucl-th\]](#)].
- [157] V. Balasubramanian, P. Kraus and A. E. Lawrence, “Bulk vs. boundary dynamics in anti-de Sitter spacetime,” *Phys. Rev. D* **59**, 046003 (1999) [[arXiv:hep-th/9805171](#)].
- [158] I. R. Klebanov and E. Witten, “AdS/CFT correspondence and symmetry breaking,” *Nucl. Phys. B* **556**, 89 (1999) [[arXiv:hep-th/9905104](#)].